GEOSPATIAL TECHNOLOGIES IN EVALUATING MORPHOTECTONIC FEATURES IN SUB-HIMALAYAN REGION, INDIA

Ph.D. THESIS

by

GAURAV SINGH

DEPARTMENT OF EARTH SCIENCES
INDIAN INSTITUTE OF TECHNOLOGY ROORKEE
ROORKEE-247 667 (INDIA)
APRIL, 2019

GEOSPATIAL TECHNOLOGIES IN EVALUATING MORPHOTECTONIC FEATURES IN SUB-HIMALAYAN REGION, INDIA

A THESIS

Submitted in partial fulfilment of the requirements for the award of the degree

of

DOCTOR OF PHILOSOPHY

in

EARTH SCIENCES

by

GAURAV SINGH

DEPARTMENT OF EARTH SCIENCES
INDIAN INSTITUTE OF TECHNOLOGY ROORKEE
ROORKEE-247 667 (INDIA)
APRIL, 2019

INDIAN INSTITUTE OF TECHNOLOGY ROORKEE
ROORKEE

CANDIDATE'S DECLARATION

I hereby certify that the work which is being presented in this thesis entitled "**GEOSPATIAL TECHNOLOGIES IN EVALUATING MORPHOTECTONIC FEATURES IN SUB-HIMALAYAN REGION, INDIA**" in partial fulfilment of the requirements for the award of the Degree of Doctor of Philosophy and submitted in the Department of Earth Sciences of the Indian Institute of Technology Roorkee, Roorkee is an authentic record of my own work carried out during the period from January, 2013 to April, 2019 under the supervision of Dr. Arun K. Saraf, Professor, Department of Earth Sciences and Dr. Josodhir Das, Associate Professor, Department of Earthquake Engineering, Indian Institute of Technology Roorkee, Roorkee.

The matter presented in the thesis has not been submitted by me for the award of any other degree of this or any other Institute.

(GAURAV SINGH)

This is to certify that the above statement made by the candidate is correct to the best of our knowledge.

(Dr. Arun K. Saraf)
Supervisor

(Dr. Josodhir Das)
Supervisor

The Ph.D. Viva-Voce Examination of **Mr. Gaurav Singh**, Research Scholar, has been held on **September 16th, 2019**.

Chairman, SRC **Signature of External Examiner**

This is to certify that the student has made all the corrections in the thesis.

Signature of supervisors **Head of the Department**

ABSTRACT

The Himalaya is young mountain range with an extension of about 2400 kilometres from west to east having arc shape occurs along the northern edge of Indian sub-continent. It is the classic example of collision-type orogenic belt and it consists mostly of uplifted sedimentary and metamorphic rocks (Gansser, 1964; Dhital, 2015; Chakrabarti, 2016). The Himalaya was originated as a result of collision between the northward moving Indian continental mass with the Asian landmass. Due to continued moving and pushing of the Indian plate beneath the Eurasian plate several complex structures have developed in and around Himalayan region. Ongoing tectonic activity in the region is well indicated by moderate to large magnitude earthquakes, as well as prominent tectonically controlled geomorphic indicators. For this reason, it has attracted the attention of geoscientists for several decades. The northward movement of Indian plate resulted in crustal shortening in north which is accommodated by south-verging thrusts (Thakur, 2004). The major longitudinal tectonic features present are Indus-Tsangpo Suture Zone (ITSZ), Main Central Thrust (MCT), Main Boundary Thrust (MBT), and Himalayan Frontal Thrust (HFT). These thrusts show relatively young age and shallowing depth, suggesting that the main deformation front has shifted southward (Thakur, 2004). In the western Himalaya, large numbers of recesses are present in the deformation front. These recesses are described as re-entrants (Thakur and Rawat, 1992). Kangra re-entrant is the largest of these recesses. Karunakaran and Ranga Rao (1979) have attributed the formation of these re-entrants to the effect of basement wedges in the underlying Indian Plate. Himalayan belt is most seismo-tectonically active and youngest orogenic belt on the earth. Naturally occurring events such as earthquakes, cause sudden deformations inside the earth as well as on the surface. The HFT developing along the southernmost boundary of the Siwaliks belongs to the latest active region of the Himalaya. Some of the most destructive earthquakes have occurred historically in India took place within the Himalayan region. This research work is focused on the study of morphotectonic features based on morphometric indices, drainage anomaly etc. The study will also help in identifying occurrence of existing tectonic fault and terrain modification.

As indicated by Gansser (1964) the Himalaya might be subdivided into five geological divisions from north to south in their longitudinal structure, by a progression of a parallel structural zones. The Sub-or Outer-Himalaya framing the foot-slope zone known as Siwaliks are delimited in the south by the Ganges alluvial plains, though the northern edge has an

obviously illustrated structural component - the MBT. Between the MBT in the south and the MCT in the north lies the stretch of the Lesser Himalaya. Farther north, beyond MCT the zone is the Central Crystalline of Higher Himalaya.

Present study area comprising Kangra re-entrant, Nahan salient and Dehradun re-entrant is located in Sub-Himalaya (actively deforming front of the Himalaya) and is bounded by HFT in south and MBT in north in Himachal Pradesh and Uttarakhand. It extends for about 350 km in length and average width of about 75 km. The Doon valley is bounded to the northeast by MBT that separates the Precambrian rocks of the Krol belt of the Lesser Himalaya to the Cenozoic sediments of the outer Himalaya (Thakur, 1992). The relief suddenly rises in the south in the form of Siwalik Hills (Mohand ridge) which is separated from the recent alluvial sediments by the Himalayan Frontal Thrust (HFT), commonly known as Mohand thrust. In the west the Mohand ridge is bounded by the Yamuna Fault and in the east, by the Ganga fault. The detailed and careful inspection of geomorphic features and geomorphic indices such as the Valley width, river sinuosity index, the river gradient index, and drainage pattern can help in the understanding of overall evolution of landform and its ongoing tectonic movement. Therefore, an integrated approach of Remote Sensing and Geographic Information Systems (GIS) is used in the present study.

The north-western edge of Kangra re-entrant in the NW Himalaya witness of 1905 great Kangra earthquake.. It is bounded by Himalayan Frontal Thrust (HFT) in south and Main Boundary Thrust (MBT) in north in Himachal Pradesh. Ongoing tectonic activity in the region is well indicated by moderate to large magnitude earthquakes, as well as prominent tectonically controlled geomorphic indicators. Identification of morphotectonic features, analysis of drainage network and finding out its relation to tectonics are the main objective of the present study. It has been observed that due to the Kangra re-entrant structure, large number of landforms has developed which are marked by NW-SE trending linear ridges. Extensive river network also have formed in the area and rivers have crossed the ridges at several places. The longitudinal profile of the Beas River clearly shows the HFT, Jwalamukhi thrust and MBT. Among these, Jwalamukhi thrust and MBT are very prominent. River becomes braided within the Kangra valley after entering Jaisingpur and near Jwalamukhi thrust. The sinuosity of the river increases and deep valley can be seen formed before the thrust.

Hypsometric curve and hypsometric integral are used for watershed health indicator. In a tectonically active region, the basin topography is generally dynamic and its evolution responds

to the stress regime of the region. The basin topography is also highly affected by the extent of erosional activities ongoing in the region. In Himalayan system, which is a highly active orogeny, the fluvial erosion plays a significant role in modifying the morphology. The quantification of this interplay of the tectonic uplift and subsequent erosion can be done in the form of a geomorphic index (Weissel et al., 1994). Based on the very same understanding of this interaction, several researchers have carried out hypsometric analysis to study the tectono-geomorphic evolution of different regions (Pandey et al., 2004; Singh et al., 2008a; Singh et al., 2008b; Sharma and Seth 2010 and Sharma et al., 2011). The basins can be classified by analysing the shape of hypsometric curves. These curves may be convex upward, S-shaped (concave upwards at high elevations and convex downwards at low elevations) or concave upward implying the youth, mature and peneplain stage of the basin, respectively (Strahler, 1952). The hypsometric integral value has applications for soil and water conservation measures also as it can be used to assess the erosion status of watershed (Singh et al. 2008). The present work involves study of role of active tectonics in channel modification and watershed geometry over Mohand anticline using morphometric tools.

Hypsometric analysis of the study area also shows significant changes in sub-basins of all major rivers comes under study area that are Beas, Sutlej, Yamuna and Ganga. Hypsometric analysis of watershed demonstrates the complexity of denudation processes and the rate of morphological changes. Therefore, it is useful to comprehend the erosion status of watersheds and prioritize them for undertaking soil and water conservation measures. With the hypsometric integral and hypsometric profile, we can identify and predict the geological stages of all watersheds. According to the hypsometric curves of watersheds, it is observed that Khajnaur Rao and Mohan Rao watersheds are having more influence of tectonic activity. According to hypsometric integral values of the entire watersheds lie on the Mohand Anticline showing different geological stages. Hypsometric integral (HI) of Khajnaur Rao and Mohand Rao watersheds are having values 0.41 and 0.44 respectively. This also indicates that Mohand Rao and Khajnaur Rao watershed are more prone to erosion in comparison to other watersheds adjacent to it.

The most important confirmation for fault identification has been given by the dislocation and displacement of mountain ridges and valleys, clearly recognizable lineaments, and drainage offsets observed in the true colour composite image of the area. Also, the morphometric

analysis and shaded relief models (SRMs) created from DEM, further substantiates the presence of such features in the study area.

Significant and unique tectonic feature depicting re-entrant and salient have formed comprising both the curved and northwest-southeast trending linear ridges. The folded rocks forming linear ridges are the result of fault propagation operated in these regions under the influence of prevailed convergent tectonics. The present topography exhibit effect of extensive erosion carving out several erosional features in the area. These ridges also reveal effect of faulting through dislocations at many places. The nature of folded rocks in the re-entrant areas indicate the area were subjected to slow and low intensity deformation.

Acknowledgement

First of all my eternal bow in reverence and gratitude is to **"Almighty God"** whose gracious blessing enabled me to complete my work in time. Words cannot express the depth of my gratitude for all those who directly or indirectly helped me in my endeavour.

I wish to take this opportunity to express my heartfelt deep sense of gratitude to my supervisor, **Prof. Arun Kumar Saraf** and **Dr Josodhir Das** for their constant, and benevolent guidance, sustained encouragement, unlimited patience, endless advices, keen interest, judicious planning of the project, and the continual support that inspired and fuelled my research engine over the year and made me to bring this work to a successful completion. Words seem inadequate to articulate my indebtedness to them for moulding me with the cologne of strong scientific lust. I am very much grateful to them for their appreciation, suggestions and constructive criticism. Their overly enthusiasm, integral view on research has made an everlasting impression on me. It is matter of pride to get a unique opportunity of working with an affectionate, courageous and great professor.

I would like to thank the Heads of the Department of Earth Sciences, IIT Roorkee, during the tenure of my research, namely: **Prof. A. K. Saraf, Prof. D. C. Srivastava** and **S. Bajpai** for their academic help and encouragement.

I express my sincere thanks, to all Student Research Committee members namely **Prof A Joshi, Dr. S.P. Pradhan, Dr. G.J. Chakrapani and Dr. S.K Jain** and Staff of Earth Sciences Department for their co-operation and support. Especially, I would like to acknowledge **Dr. Ajanta Goswami** for his moral support and extending a helping hand throughout my research work. I also wish to thank **Dr. V.C. Goel** for his generous help and invaluable suggestions during evaluations of my research works.

I wish to sincerely acknowledgement the continuous financial support by **University Grant Commission (UGC)** and Ministry of **Human Resources and Development** (MHRD), New Delhi supporting me as **Research fellow** without which it would have become difficult to take up this work.

I convey my heartfelt and esteemed sense of gratitude for my lab mates **Mr. Mrinmoy Das**, **Mrs**. **Kanika Sharma**, **Suman Sourav Baral** and **Susanta Borgohain** for their helping hand during my period of research work. I am also grateful to **Zia, Eirin** for their immense

help and cooperation at each and every step of my research. I extend my deep sense of appreciation to my loving juniors **Arun Ojha, Debasmita Maharana,** and others for their respect, affection, and wholehearted cooperation and for keeping my morale high.

I would like to thanks **Dr. Susanta Borgohain** and **Dr Aditya Verma** for their generous help (personal/academic) during my stay in Roorkee. They definitely make my stay in Roorkee memorable. Especial thanks to **Dr. Susanta Borgohain, Mrs. Rinki Moni Kunwar** and **Avantika Kunwar Borgohain** during my stay at Himgiri Apartment.

I would like to thank **Nair Ji**, and **Mohd. Aslam Ji** for their open-hearted support and administrative help during the course of my stay at Roorkee. I also wish to thank the members of non-teaching staff at Department of Earth Sciences and James Thomson Building, IIT Roorkee for their administrative help during the course of research. A special place holds for **Late Mohd. Rahil** for his constant lab supports during the initial period of my research.

I also wish to thank my friends **Mr. Suman Kumar Padhee** , **Mr. Raj Kumar Yadav** and **Mohd. Shahbaz Khan** for their continuous moral support. Especially, I want to thank Mr. **Mr. Suman Kumar Padhee** for his generous help (personal/academic) during my stay in Roorkee.

I feel a sense of unique pleasure to pen down my feelings for my loving **Mummy and Papa** whose ineffable love, selfless sacrifice, moral support, loving inspiration and faith in me, has always made things simpler and life more worthy to live.

I am truly thankful to the almighty for having my all siblings who have always supported me and stood beside me at all the times for their affectionate supports and encouragements. I am also thankful to my all relatives for their encouragement.

Last but not the least I would like to express my heartfelt thanks to my beloved wife **Mrs. Shweta Singh** for her selfless love, sacrifice, moral support and encouragement in every phase of life. Without her help and co-operation I would never have reached this mile-stone.

Round out the picture I thank all those who have helped me directly or indirectly at various stages of this work.

Table of Contents

Table of Contents

List of Figures:

List of Tables:

Chapter 1
Introduction

1. 1. Preamble:

The arc shaped Himalaya is young mountain range with an extension of about 2400 km from west to east sprawling along the northern edge of Indian sub-continent. It consists mostly of uplifted sedimentary and metamorphic rocks. The Himalaya was formed as a result of a collision between the northward-moving Indian continental mass with the Asian landmass. Due to continued drifting and pushing of the Indian plate beneath the Eurasian plate, several complex structures have developed in and around Himalayan belt. The Himalaya is one of the most tectonically active regions of the world and remained responsible for generating major Earthquakes in this region. Historically, some of the most destructive Earthquakes have occurred within the Himalayan region. Ongoing tectonic activities within the region are well indicated by medium to high magnitude earthquakes and geomorphic markers. The northward movement of Indian plate resulted in crustal shortening in the north which is accommodated by south-verging thrusts (Thakur, 2004). The major longitudinal tectonic features existing are Indus-Tsangpo Suture Zone (ITSZ), Main Central Thrust (MCT), Main Boundary Thrust (MBT) and Himalayan Frontal Thrust (HFT). These thrusts are relatively young in age and having shallow depth, suggesting that the main deformation front has shifted southward (Thakur, 2004). In the Western Himalaya, large numbers of recesses are present in the deformation front. These recesses are termed as re-entrants (Thakur and Rawat, 1992). Kangra re-entrant is the largest of these recesses (Karunakaran and Ranga Rao, 1979). Formation of these re-entrants has been attributed to the effect of basement wedges in the underlying Indian Plate.

This study is focused on morphotectonic analysis for the evolution of tectonic activity in the region, drainage and terrain anomaly study for detecting a possible tectonic fault, Earthquake distribution analysis for association of Earthquake with major tectonic grains or active/neotectonic faults. Satellite images are capable of displaying prominent morphotectonic features on the Earth especially when these have large spatial extents.

Present study area is located in Sub-Himalayan region bounded by HFT and MBT in Himachal Pradesh and Uttarakhand states, India. Interactions between active tectonics and erosion processes have resulted in this complex geomorphology of the landscapes. However,

geodynamics of the region is not yet completely understood. Detailed study of geomorphic markers of the region, such as river terraces, sinuosity index, drainage pattern etc. have helped in understanding the evolution processes of the landforms within the region. An integrated approach of Remote Sensing and Geographic Information Systems (GIS) has been employed in the present study for identification and delineation of geomorphic markers located within the study area. Analysis of morphotectonic features and finding out their relations to active tectonics of the region are the main objective of the present work. In order to carry out the present study, satellite images of different years and DEMs have been collected. Several operations to process those using ArcGIS and ERDAS Imagine are performed. The processed data have been analysed to identify the morphotectonic features in order to get knowledge about the tectonic evolution of the region.

The ever developing techniques of remote sensing have the perspective to contribute and support human research in assessing natural processes and events occurring frequently on the Earth's surface. Remote sensing provides synoptic and repetitive coverage, unbiased recording of the Earth's surface and events, cost-effective technique, takes very less time and produces multi-spectral data. GIS provides proficient analysis of Earth features, natural hazard effects, tracing emergency areas, assisting in rehabilitation etc. Apart from identifying damaged areas, remote sensing also allows monitoring of the Earth on a real-time basis for impending signs of a disaster (Gupta, 2000; Tronin, 1996 and 2006). The changes in Earth's topography can unfold many unidentified natural processes related to Earthquakes happening due to tectonic/fault movements. Any deformation occurring on the land surface in a tectonically active region can be observed regularly as a manifestation of Earthquakes.

As Earthquake studies have improved progressively, remote sensing has become an integral part of Earthquake disaster management. Till now, some major factors like non-availability of good resolution data for the damaged area, cost of high-resolution data, temporal resolution (revisit cycle of a satellite), lack of knowledge in this field viz., the complexity of the phenomenon called ‘Earthquake' were the hindrances to such studies.

Now, remote sensing is the most widely used technique to study natural and Earth's surface processes. In this field, we can utilize two or more data sources together to get more environmental information rather than extracting from separate data sources individually (Cracknell, 1997, 1998). Several researchers (Mansor, et al., 1994; Krishna, 1996; Tripathi, et

al., 2000; Tripathi & Singh, 2000; Krishna, 2005; Pati, 2005; Jasrotia, et al., 2007; Pati et al., 2008; Chaudhary & Aggarwal, 2009; Maiti & Bhattacharya, 2009; Pirasteh et al. 2009 and 2010) have used geospatial techniques for similar studies worldwide. Sensors on-board satellites having sensing capabilities in different bands of electromagnetic spectrum permit the user to interpret various Earth objects and physical phenomena with high accuracy and reliability. Studies using various remote sensing techniques have found many directions and have proven its utility in different realms of life and property. In disaster management, optical remote sensing has been widely used.

Basins along HFT and other major thrust have been selected for accessing the tectonic activity in the region. To comprehend the geometrical property of the landforms; different morphometric parameters such as mountain front sinuosity, longitudinal river profile, valley floor width to valley height ratio used to characterize the degree and nature of tectonic activity while the drainage orientation studies help in reconstructing the sequence of recent tectonic activities in the area. These morphometric indices inferred the study area as active except for the basin located in westernmost of the study area which shows very less activity.

1. 2. Morphotectonics:

Morphotectonics describes the study of short and long-term surficial pieces of evidence of tectonic activity. The Earth's endogenous mechanisms resulting out of the active tectonics are always associated with relative movements, such as uplifting and/or subsidence and/or translation of parts of the Earth’s crust. Present day landforms are the result of interactions between active tectonics and the weathering-erosion processes occurred in the past. Combination of geometry and tectonic activity describe landforms primarily at continental, sub-continental as well as local scales, whereas structural geomorphology which deliberates the passive influence of geological structure on landforms is known as morphotectonic. It bring out the influence of Earth movements on landform evolution. It comprises of the study of the origin of mountains, drainage patterns, erosion surfaces, and sediments on land and offshore. These types of existing and newly developed morphotectonic features can be evaluated by using Geoinformatics comprising multi-sensor images, topographic maps, field data, and multi-date remotely sensed data, DEMs, GIS, visual interpretation and advanced digital image processing techniques.

In tectonically active regions, significant topographical change can be directly observed from direct field observation. However, the regions where the rate of tectonism is mild or very slow can be well studied by analysing the morphometric indices. Streams and drainages are able to record even negligible tectonic deformation. Tectonic activities are often demonstrated by characteristic geomorphic markers such as erosional surfaces, slope-breaks, linear valleys, ridgelines etc. Analysis of optical and microwave remote sensing data with DEM by means of quantitative geomorphology helps in recognizing lineaments, faults and characterizing the tectonics of an area. Morphometric parameters like drainage basin asymmetry, river sinuosity, slope gradient index, hypsometry, stream length gradient index etc. are key indicators of neotectonic activities prevailing in a region (Singh, 2008).

The relationship between geomorphology and tectonics is the basis to comprehend the landscape evolution for the morphotectonic study. The associated tectonic features can be well studied by the interpretation of various surface expressions. These observations compare the morphological structure of geomorphic markers such as drainage systems, courses of the river, landscapes and mass movements with joint orientations along with fault movements. These are the major indicators of neotectonic changes.

Remote sensing can be a very useful tool in the evaluation of various morphotectonic parameters. A synoptic view is provided by the satellite images and proficient of producing information regarding the areas which are inaccessible during field surveys due to rugged topography, climatic conditions, and dense vegetation. Availability of high-resolution satellite images bestowing even different minor topographies; distinctly give the opportunity to look into details of occurred modification, if any. Image interpretation based on its elements such as tone, texture, pattern, shape, size etc., and correlation with geotechnical elements such as vegetation, land use, land cover, drainage gives useful idea of prevailed geomorphology of a region. Remote sensing techniques provide us different data product and implementing GIS techniques makes it extremely effective. Hence, these two techniques are complementary to each other. By using GIS, several maps like geomorphological, geological, structural, drainage etc. can be easily prepared for morphometric and morphotectonic evaluation of any region. GIS technology is digital, spatial and generic. Further, GIS provides a platform to handle all the information effectively which are georeferenced (having latitude/longitude information). The GIS technique has the unique capability by means of overlaying and superimposing different layers of images in a single map and therefore, it becomes easy to analyse the impact of one

parameter on another. For example, river morphology and drainage pattern are very sensitive to neo-tectonic activities, and both can be easily extracted by remote sensing and GIS approach.

The temporal and spatial distribution of large Earthquakes in the Western Himalaya region shows a non-uniform distribution pattern. The Earthquake distribution concentrates in the area between MCT and MBT. HFT has witnessed very few Earthquakes which raise the risk of occurring higher magnitude Earthquake in the near future (Srivastava et al., 2015).

The India-Asia collision and convergence of both the continents are being controlled by strong northward drift of the Indian plate and anti-clockwise rotation of India pinned in the western syntaxes (Catherine, 2004; Gupta and Gahalaut, 2012; Paul et al., 2001; Singh et al., 2012). The collision resulted in a highly deformed continental margin of India, building up the Himalaya with a characteristic arc shape (Gahalaut and Kundu, 2012). The Western Himalaya lies within a seismotectonically complex area that is undergoing rapid and intense ground deformation since last 50Ma (Paul et al., 2001). The area plays a vital role in the kinematic processes of the Indian Plate. In this region, Earthquakes are more frequent and generally occur along a narrow well-defined zone (Mahesh et al., 2012). Highest seismic activities in the Himalaya currently occur in the north-western part that includes the HFT, MBT and MCT zones.

The Kangra re-entrant in the NW Himalaya is one of the most seismically active regions in the Himalaya. It is bounded by HFT in south and MBT in the north in Himachal Pradesh. Identification of morphotectonic features, analysis of drainage network and finding out its relation to tectonics is the main objective of the present study. Therefore, an integrated approach of remote sensing and GIS is used to identify significant morphotectonic features in the area. It is observed that due to the Kangra re-entrant structures, a large number of landforms have developed which are marked by NW-SE trending linear ridges. Extensive river network has formed in the area and rivers have crossed these ridges at several places. High-density drainage developed in the central part of the re-entrant. The longitudinal profile of the Beas River clearly shows the HFT, Jwalamukhi thrust, and MBT. Among these, Jwalamukhi thrust and MBT are very prominent. The river becomes braided within the Kangra valley after entering Jaisingpur and near Jwalamukhi thrust the sinuosity of the river increases and deep gorges can be seen before the thrust.

1. 2. 1. Drainage and Topographic profile anomaly:

Drainage system attains a specific drainage pattern as time passes. A setup of stream channels and tributaries are developed and is determined by local geological factors. The developments of landscapes in tectonically active regions result from a complex integration of the effects of vertical and/or horizontal motions of crustal rocks and erosional processes (Burbank and Anderson, 2001). In tectonically active regions especially in folded mountains, qualitative and quantitative analyses of drainage systems are useful to evaluate the impact of the active tectonics on geomorphic processes and landscape development (Ramsey et al., 2008). Drainage analysis generally provides clues to structures and lithology. The underlying concept is that rivers necessarily flow from high to low elevations parallel to the maximum regional slope. Any deviation from a flow direction oblique to the regional topographic gradient termed as "misfit stream" (Deffontaines et al., 1992), is considered as drainage anomaly related either to structural or lithological discontinuity. Some type of drainage anomaly indicates towards the sub-surface faulting/activity or abrupt changes in bedrock or topography. The linear arrangement of lakes, sinkholes or drainage line indicates the presence of a fault, fracture or less resistant linear rock outcrop as the stream tends to flow along the weak path. Anomalous curves or turns of a stream indicate the presence of surface or near-surface structures across the path of the stream. For example, acute or obtuse elbow turn indicates a fault, round turn around an area indicates sub-surface high. Abrupt and localized meander in streams represents an interruption related to a subtle upstream reduction in stream gradient and indicates the occurrence of an active zone of uplift. Squeezed, compressed and incised meanders may be due to the occurrence of a fault, fold or dome structure across the stream. A linear segment of streams when the regional drainage pattern is other than rectangular or trellis, indicates that the stream is flowing along a fault, fracture or easily erodible vein or dike.

As tectonic deformation changes the relief of a region, topography gives a first and vital indication of the distribution and arrangement of morphological structures. Three-dimensional (3D) visualization is therefore crucial for the structures. The visualization of a 3D structure from a 2D map is greatly complicated by topographic relief. The analysis of the topography is done by either DEM or Digital Terrain Models (DTM). DEMs provide an opportunity to quantify land surface geometry in terms of elevation and its derivatives. The basic geometric properties that characterize the terrain surface at a point are elevation, inflection points, break-lines, ridges and valley lines. The relationship between geometric point attributes and tectonic structures such as slope-breaks and fractures is often straightforward (Jordan et al., 2005).

Steep slopes of uniform aspect over an area may be the result of faulting. Linear valleys, ridgelines, and slope-breaks are commonly associated with faults (Prost, 1994). Complex structures, such as folds and curving fault lines, are difficult to capture by geometric analysis.

1. 2. 2. Hypsometry:

Hypsometry of a river basin describes cumulative distribution of elevations with respect to area (Singh, 2008). Hypsometric curves can reveal significant information on geomorphic condition of a catchment. Sediment yield and maturity of a river basin can be directly interpreted from hypsometric curve of the basin. Hypsometric curves for different catchments of the study area have been derived from ASTER-GDEM. From the Beas, Sutlej, Yamuna and Ganga River basins 54 catchment areas have been selected. And from south-western slope of the Mohand ridge 10 stream catchments are selected. Hypsometric analysis have been carried out for all the catchments and further analysis have done with the help of hypsometric curves, which shows significantly changes in all the basins.

1. 2. 3. Lineaments:

Lineaments have been defined as extended mappable linear features on the Earth's surface, whose parts are aligned in a rectilinear or slightly curvilinear relationship. A lineament differs distinctly from the pattern of the adjacent features and presumably reflects a subsurface fold, fracture or fault (Sabins, 2007). Lineaments are straight linear elements visible at the Earth's surface as a significant "lines of the landscape" (Abdullah et al., 2010). Lineaments are primarily indications of discontinuities on the Earth's surface caused by geological or geomorphic processes. Geological features that might appear as lineaments include faults, ridges, shear zones, fractures, veins, bedding planes, stratigraphic contacts etc. Lineaments help to locate faults, joints, lithologic boundaries, and major structural features.

Remote sensing data i.e. satellite images of an area are useful to map lineaments. For better interpretation of lineaments in the study area, satellite images are digitally processed using image processing software. Geologic contact designates linear contacts between surficial materials with different reflectivity (the contrast between two geologic contacts is relatively high). Tonal anomaly designates a linear feature that cannot be clearly recognized as a member of any of the previous categories. The feature may be a composite physiographic feature that

becomes evident because several geomorphic elements, such as scarps and stream courses, combine to produce a discernible pattern on the satellite image (Prost, 1994).

1. 3. Objectives:

The Major objectives of the present study are outlined as below:

1. Understanding the geological, tectonic and seismic set up of the study area.
2. To identify various morphotectonic features associated with the fault/thrust using satellite images and DEM data.
3. Analysis of drainage network and its relation to tectonics.
4. Morphometric analysis of the study area.

1. 4. Methodology and Overview:

Satellite data of previous 20 years have been collected and performed several image processing techniques to enhance the quality of the images and also the features. From the satellite data, False Colour Composites (FCCs) and mosaic are prepared for all the years for better visualization and getting more information about the area. Also collected DEM acquired through ASTER-GDEM to get a 3-D view of the region. From DEM data, river channel network, drainage density and topographical cross-section are extracted so that the possible changes that took place over the time could be found out. Also prepared shaded relief model to get more information about an area. Seismotectonic Atlas of India has been referred to distinguish about the tectonic evolution of the study area. Toposheets and images of different times have been cropped and compared for analysis purpose. Processing and analysis of the Landsat data were done using ArcGIS 10.1 and ERDAS Imagine 14 software.

1. 5. Study Area:

The states of Uttarakhand and Himachal Pradesh extend from 29°37' N latitude, 79°40' E longitude to 29°10' N latitude, 80°18' E latitudes and 31°30' N latitude , 76°55' E longitude to 32°11' N latitude 76°23' E longitude respectively. The region is surrounding by Nepal in the east, Tibetan region in the northeast, Jammu & Kashmir in the northwest, Haryana and Punjab in south and southwest, and U.P. in the south and southeast. Uttarakhand spread geographically

over an area of 53483 km^2 whereas the Himachal Pradesh has 55,673 km^2. The study area is located in Sub-Himalaya which is bounded by HFT in southwest and MBT in the northeast in Himachal Pradesh. It extends about 115 km in length and an average width of about 75 km(figure 1.1). In the Doon valley the MBT separates the Precambrian rocks of the Krol belt of the Lesser Himalaya to the Cenozoic sediments of the outer Himalaya (Thakur, 1992). The relief suddenly rises in the south in the form of Siwalik hills (known as Mohand ridge) which is separated from the recent alluvial sediments by the HFT, commonly known as Mohand thrust. The Mohand ridge is bounded by the Yamuna Fault and Ganga fault towards northwest and southeast respectively.

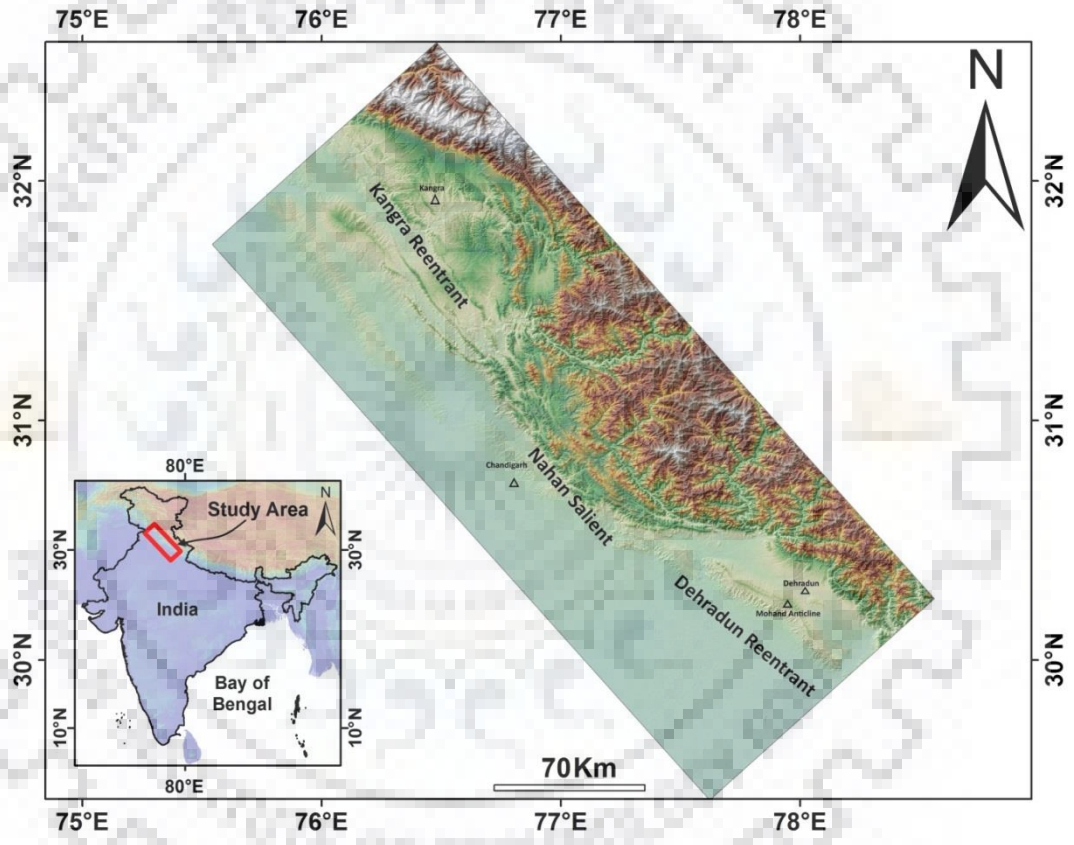

Figure 1.1. Study area showing Kangra reentrant, Nahan salient and Dehradun reentrant on shaded relief model of ASTER-GDEM (30m).

1. 6. Major Rivers within the Study Area:

Rivers are significantly influenced by valley floor structures and slopes. Hence, any tectonic activity bringing change into the valley floor slope and structure can change the nature and morphology of the river. Tectonic uplift of a river valley can make the river rejuvenate and form incised valley. Slow tectonic deformation affect channel stability and can be a threat to development and planning. Quantitative analysis of drainage basin is a useful tool to know the influence of active tectonics on a river channel. The major rivers viz., Beas, Sutlej, Yamuna and Ganga along with overall stream network of the area is shown in figure 1.2 and similarly figure 1.3 shows these same rivers superimposing on the tectonic features and satellite image of the study area.

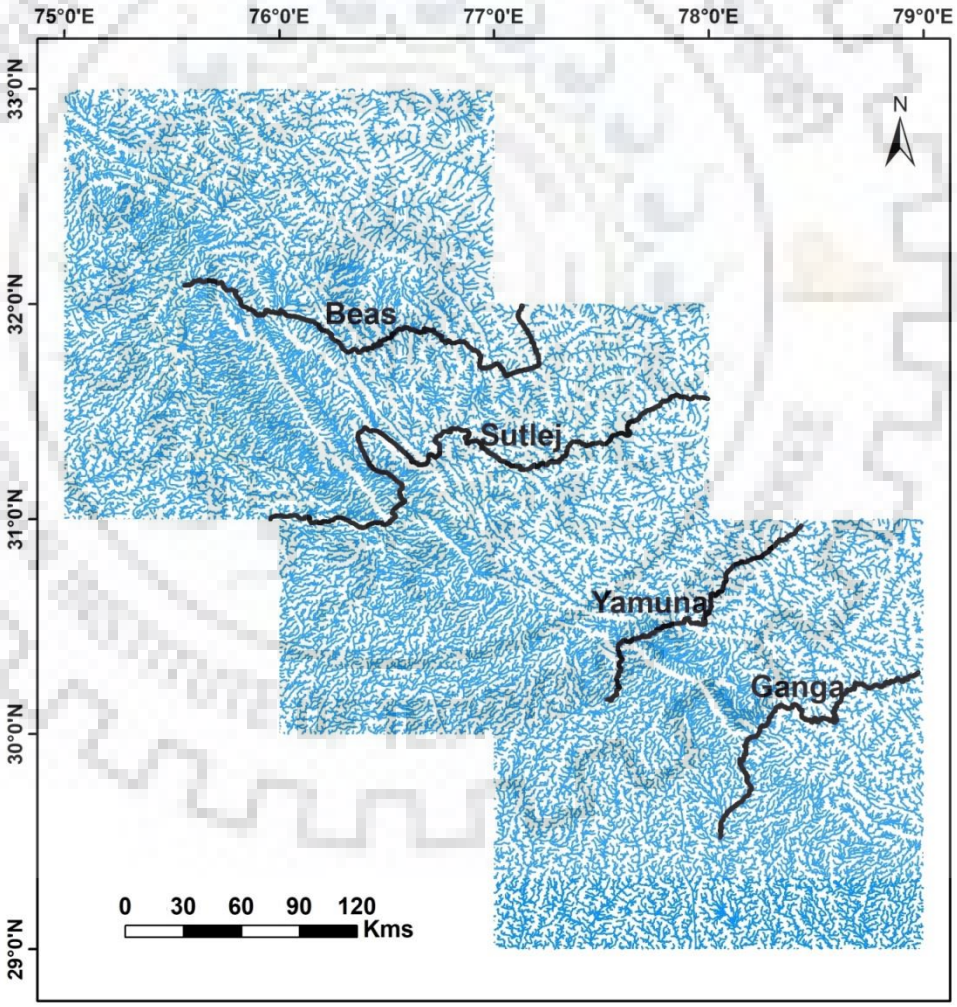

Figure 1.2. Four major river of the study area along with streams channels derived from ASTER GDEM with spatial resolution of 30m.

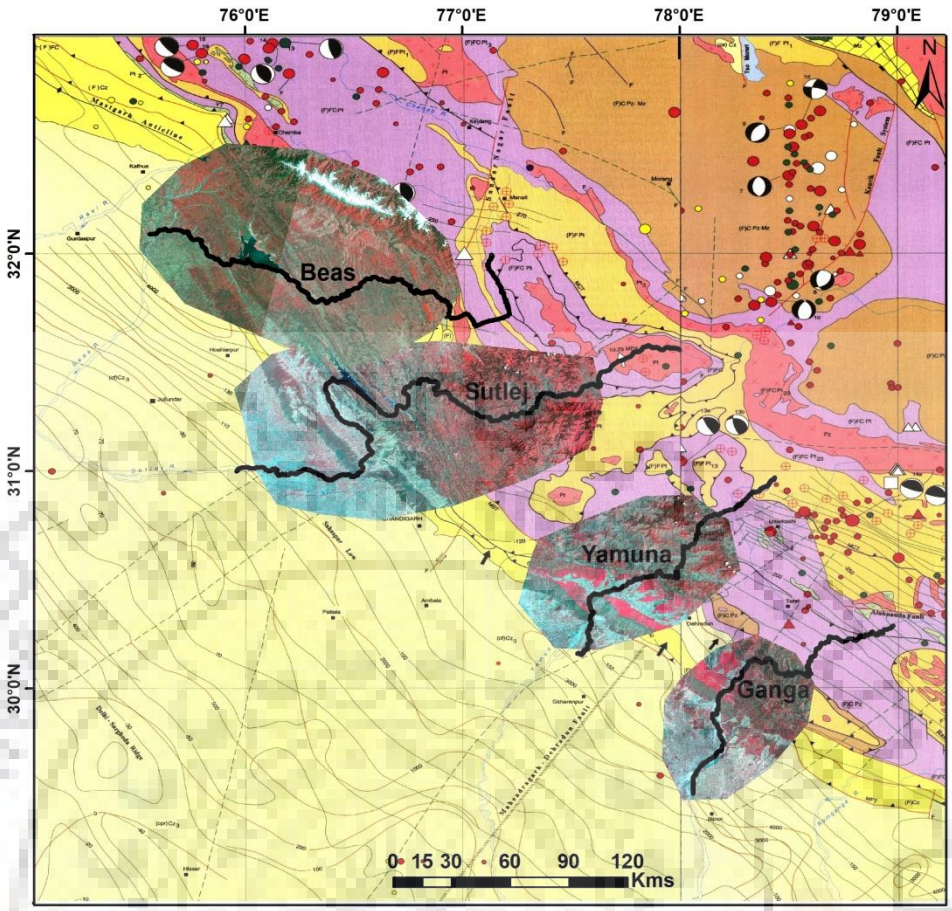

Figure 1.3 Study area along with major rivers flowing from the Himalaya. In the background satellite data of Landsat 8 has been shown. These rivers flow across some of the major thrusts for example HFT, MBT and MCT (Dasgupta et al., 2000).

1. 7. Organization of Chapters:

The thesis has been organized in eight chapters including this chapter of introduction. Basic purposes of each chapter have been discussed below:

Chapter 1: Contains general introduction to Himalaya and seismotectonic relations. The chapter also discusses various remote sensing and GIS tools that have been used for such studies. Objectives of the research work and details of the study area have also been discussed in this chapter.

Chapter 2: Gives details of data and methodology used in the present study.

Chapter 3: Discusses geology, tectonics of Himalaya and seismicity of the region.

Chapter 4: Discusses morphology of the rivers and morphometric analysis of the drainage systems. Drainage and streams network anomalies have also been discussed in this chapter.

Chapter 5: Contains discussions on results obtained from morphometric analysis, image interpretation, DEM analysis and their relations to active tectonics.

Chapter 6: This is the final chapter which includes conclusion of the study.

Chapter 2

Data Used and Methodology

Now-a-days satellite images are available in diverse spatial, spectral and temporal, resolutions due to the advent of diverse remote sensing techniques and successive improvements in remote sensing systems, data communication and processing technologies. Different applications involve remote sensing data with particular resolution at which the scientific studies can be carried out. Hence the essential aspect is to lay less importance upon the image resolution than the application or to place no importance on one specific resolution and accept relatively medium or high spatial resolution satellite images. The purpose of this study is to analyze different features and neotectonic activities in study area engaging various remote sensing data sets followed by estimation of earthquake induced ground deformation using geomorphometric study and ground truthing/field validation.

2. 1. Data Used:

A dataset is the prime requirement for collection of various data and information for carrying out any study in geology. With the help of remote sensing technique, various types of information about a very vast area can be congregated quickly. For all these purposes, satellite images provide very useful data because of their synoptic coverage and multispectral approach. A larger and clear view with much different perspective can be obtained from satellite images which are not only very difficult but also very time consuming in case of point ground observations for investigating various geological features. Integrated approach of Remote Sensing and GIS forms very powerful tool for integration of data, its analysis and interpretation. Various data used in the present study are discussed below.

For understanding the structures and features of study area with the neo-tectonic activity from the morphometric study, remote sensing data have been used extensively. However the other data products used in this research are as follows:

a) Maps (Topographic, Geological and Seismotectonic)

b) Landsat-7 and 8 datasets (from USGS)

c) Google Earth satellite images (from Google Earth)

d) Digital Elevation Model (DEM) (from CGIAR-CSI, USGS and JAXA website)

Toposheets: Survey of India topographic maps (1:50000 scale and 1:25000) have been used for the present study. The topographic maps for the study area were first georeferenced. These have provided with the information on locations of several places (town/villages) which served as an important guide.

Geological Map: The geological map acquired from Geological survey of India (GSI) and then was georeferenced. The Geological map 1:50,000 have been used to understand the geology of the area, rock units and geologic strata where the attributes are shown by colour or symbols to indicate where they are exposed at the surface.

Seismotectonic Atlas of India: Tectonic features of the study area are from Seismotectonic Atlas of India and its Environs (Dasgupta et al., 2000). SEISAT-8, 9 and 12 maps were scanned, georeferenced and mosaiced similarly as the toposheets. The maps for the study area were georeferenced using ArcGIS version 10.2 and the major faults, minor and major lineaments were digitized.

Seismic Data: The seismic data from 1905 to 2018 has been collected from the webpages of United States Geological Survey (USGS).

Landsat Images: Landsat program is a cooperative attempt of the NASA and USGS. The first Landsat satellite was launched on 23rd July, 1972. Continuous image coverage of the Earth's surface has been provided by Landsat satellites. NASA has been developing sensors, spacecraft and launching the satellites including their performance validation. On the contrary, USGS has been developing the ground systems and operating the satellites, as well as management of data reception, archiving and distribution. The Landsat-7 enhanced thematic mapper (ETM) is available which has almost similar characteristics as that of Landsat-8. Since late 2008, Landsat-8 data is available for public free of cost. Carefully calibrated Landsat images provide consistent inventory of the Earth's surface globally. The most current Landsat-

8 was launched on 11th February, 2013. In this work, Landsat-8 datasets were acquired from the USGS (http://earthexplorer.usgs.gov). Landsat satellite has two instruments: Operational Land Imager (OLI) and Thermal Infrared Sensor (TIRS). Approximate scene size of Landsat-8 is 170 km N-S by 183 km E-W (http://landsat.usgs.gov/landsat8.php).

Landsat-8 technical detail: In different frequency ranges of the electromagnetic spectrum, Landsat-8 senses the Earth's surface representing a colour. However, all frequency ranges are not visible to human eyes. These ranges are known as bands and Landsat-8 is capable of sensing in11 bands. Details of different bands and their resolutions are given in table 2.1 and 2.2.

Table 2.1 List of Landsat-8 satellite bands (Source: USGS).

Band number	Band name	Wavelength (μm)	Spatial Resolution (m)
Band-1	Coastal	0.43-0.45	30
Band-2	Blue	0.45-0.51	30
Band-3	Green	0.53-0.59	30
Band 4	Red	0.64-0.67	30
Band-5	NIR	085-0.88	30
Band-6	SWIR1	1.57-1.65	30
Band-7	SWIR2	2.11-2.29	30
Band-8	Panchromatic	0.50-0.68	15
Band-9	Cirrus	1.36-1.38	30
Band -10	TIR1	10.68-11.10	100(30)
Band-11	TIR2	11.50-12.51	100(30)

Table 2.2. Details of Landsat images used in this study with bands and resolution (USGS).

Satellite/Sensor/Spatial Resolution	Path/Raw	Band number	Wavelength (µm)
Landsat 5/TM/30m	146/38, 146/39, 147/38, 147/39, 148/38, 148/39, 149/38, 149/39, 157/38, 157/39, 158/38, 158/59, 159/38, 159/39	Band 2 Band 3 Band 4	0.52 - 0.60 0.63 - 0.70 0.76 - 0.90
Landsat 7/ETM+/30m	146/38, 146/39,147/38, 147/39, 148/38, 148/39, 149/38, 149/39, 157/38, 157/39, 158/38, 158/59, 159/38, 159/39	Band 2 Band 3 Band 4	0.52 - 0.60 0.63 - 0.69 0.77 - 0.90
Landsat 8/OLI/30m	146/38, 146/39,147/38, 147/39, 148/38, 148/39, 149/38, 149/39, 157/38, 157/39, 158/38, 158/59, 159/38, 159/39	Band 3 Band 4 Band 5	0.53 - 0.59 0.64 - 0.67 0.85 - 0.88
Landsat 7/OLI/15m	146/38, 146/39,147/38, 147/39, 148/38, 148/39, 149/38, 149/39, 157/38, 157/39, 158/38, 158/59, 159/38, 159/39	Band 8	0.50 - 0.68

Google Earth Datasets: On 11th June, 2001 Google Earth was launched. It is a virtual globe map and a custom designed geographical information program. Originally the program was called Earth Viewer. The view of the Earth is generated by superimposition of satellite images and aerial photographs over Shuttle Radar Topographic Mission (SRTM) DEMs using geographic information systems (GIS) onto a 3D globe. Satellites images belonging to different time periods are provided by Google Earth (https://earthengine.google.com/datasets/).

Digital Elevation Model (DEM): Digital Elevation Model (DEM) provides enormous information of various topography characteristics. Any study done in a highly rugged terrain a DEM becomes indispensable e.g. Himalaya, Alps etc. A DEM is a 3-D representation of terrain surface in a two dimensional matrix form. This model is usually created by using terrain elevation data. The elevation data can be acquired through stereo pairs, In-SAR, Lidar, GPS,

and topographic maps etc. Now different types of global DEMs are available at different spatial resolutions (public domain). For example: SRTM DEM with 30m and 90m resolutions (http://srtm.csi.cgiar.org/), Advanced Space-borne Thermal Emission and Reflection Radiometer (ASTER) Global DEM at 30m spatial resolution that cover almost the entire globe (USGS). ALOS PALSAR DEM of resolution 12.5 m and 30 m derived from ALOS PALSAR SAR and Prism images respectively has been used at various stages of present work. DEM of the study area were acquired from USGS Earth Explorer site.

SRTM DEM: Shuttle Radar Topography Mission (SRTM) data of NASA provides comprehensive map of approximately 80% of the surface of the earth with a resolution of 30 meters globally. It covers from 56° S to 60° N latitudes. DEM of the study area were acquired from USGS Earth Explorer site. The Shuttle Radar Topographic Mission (SRTM) was 11days (11-22 Feb., 2000) space shuttle program for elevation mapping of the Earth's surface. The mission covered almost 80% of the Earth's surface. As the sensor system was based on RADAR technology, resulted datasets are associated with shadow effect, especially the regions with very high ruggedness, like Himalaya, Alps etc. Moreover, the used frequency is unable to penetrate tree covers. Thus the elevation values given by SRTM-DEM always represent the tree tops, not the barren ground. 1-arc Second (spatial resolution 30m) SRTM data are freely available in USGS Earth Explorer site since late 2014. Vertical errors of SRTM-DEM may increase to 15m in highly rugged terrains. However, for flat regions it is less than 5m (Rodriguez, et al., 2005).

ASTER GDEM: Advanced Spaceborne Thermal Emission and Reflection Radiometer (ASTER) Global DEM is another DEM data used extensively in this work. The DEM covers almost 99% of the Earth's surface being the most extensive DEM of the Earth with spatial resolution of 30m. It covers from 83° N to 83° S. It is joint operation between NASA & Japan METI. ASTER-GDEM is derived from stereo-pairs which gives more accurate information of hilly terrains in comparison to SRTM-DEM, as it is devoid of shadow effects. On the other hand, flat/plain regions are associated with serious errors. ASTER-GDEM gives very erroneous values over plains (Baral et al., 2016). Therefore, ASTER-GDEM was used only for the hilly regions. Morphotectonic analyses of the river basins were done using ASTER-GDEM data.

High Resolution ESRI World Imagery: ESRI provides access to imagery in several different ways for different projects. The most popular ones are:

1. ArcGIS Online World Imagery Base-map

2. ArcGIS Online Image Services

3. Data Appliance for ArcGIS.

World imagery provides high resolution (1 meter) satellite imagery and aerial photographs for various parts of the globe. We used this to rectify the streams orders and for comparison purposes.

Toposheets: Scanned 1:50,000 scaled toposheets of the study area were purchased from SOI. Those were georeferenced using the same software and projection system as 1:250k toposheets. Toposheets numbers 53F/10 53F/11 53 F/12 53 F/15 53 F/16 53J/3 53J/4 53J/8 53K/1 53 K/5 43 P/16 44 M/13 44 M/14 52 D/4 53 A/1 A/2 A/3 A/6 A/7 A/8 A/11 A/12 A/15 A/16 53 B/9 B/13 B 14 53 E/4 53 F/1 F/2 F/3 F/5 F/6 F/7 F/10 were mosaicked together to make a single map of the study area. Rivers, streams, lineaments and morphotectonic features of the study area were digitized from these toposheets. Numbers of old streams could be identified from these toposheets.

Earthquake data: Earthquake data of the study area were obtained from USGS Earthquake Archives. CSV (Comma-separated values) files of epicentral locations/details were downloaded and converted to point-vector files in ArcGIS. Epicentral locations were plotted over tectonic map to study seismotectonic scenario of the valley. The Upper Assam valley which has been reported as "Seismic gap" by many authors has experienced a few moderate earthquake epicentered within the valley itself.

2. 2. Data Processing:

The pre-processing of satellite images and satellite based DEM applied were: registration of satellite images, contrast stretching, filling of voids of the ASTER GDEM, SRTM DEM and data fusion of satellite for better image interpretation.

The initial datasets used for this study were the topographical map (published by Survey of India) to create the necessary vector data such as drainage network and drainage basin boundaries. The project deals with a number of different data sets, hence a common projection system and datum (Projection: UTM; Datum: WGS 84) has been used. Similarly ancillary data (seismotectonic atlas, geological maps and geomorphological maps) scanned and registered.

Linear contrast stretching were used to enhance the contrast of the images so that the stretched data values maintain the same relationship to each other as the original data by adjusting the values of brightness in the 0-255 grey level range of satellite imagery bands.

The SRTM DEMs were pre-processed to fill the hole using algorithms defined by (Jenson and Domingue, 1988), which is available in various GIS software (e.g. ArcGIS, PCI Geomatica). In this study the Fill & Sink analysis tool of ArcGIS 10.1 was used. This procedure can be particular useful within the valleys (by providing a more homogeneous dataset without depression and hole sinks).

The PAN image has high spatial resolution but poor spectral resolution, while the MS image has low spatial resolution but high spectral resolution. High resolution panchromatic imagery can be used to increase the spatial resolution of low resolution (multi-spectral imagery by spatial sharpening (data fusion) techniques. Different types of image fusion techniques exist for combining PAN and MS image, including Brovey Transform (BT), Intensity-Hue-Saturation (HIS), Principal Component Analysis (PCA), and Subtractive Resolution Merge (SRM). The SRM fusion method was chosen for this project because it adopts strategy to combining two image by image segmentation associated with a RGB colour analyses to group pixels into like categories.

2. 3. Softwares Used:

ArcVIEW GIS: ArcView is GIS software for visualizing, managing, generating, and analyzing geographic data. (http://www.esri.com/arcview). ArcView is a powerful tool which is easy to use that brings geographic information to the desktop. ArcView makes an environment to display and query the contents of a spatial database. It allows exploring the database, exhibiting all parts of its contents, questioning, displaying or saving results and pass information or graphics on to the other applications.

ArcGIS (version 10-10.6): ArcGIS is extensively used GIS software, developed by Environmental Science Research Institute (ESRI). A very wide range of GIS tools are provided by this software. Most of the GIS operations for this research work were performed in ArcGIS version 10.2. Different locations are digitized as line and polygon vector files from Landsat images. The ArcScene extension is used to create 3D prospective view by draping high resolution satellite images over DEM. Using the same software, all maps were prepared. A 30 user's licensed version of the software is available at Indian Institute of Technology, Roorkee which has been used for this research work.

Erdas Imagine version 14 and 15: This commercial software is available from Hexagon Geospatial agency. Erdas Imagine enable researchers to envision, experience and communicate geographic information. ERDAS IMAGINE offers true value, photogrammetry, consolidating remote sensing, basic vector analysis, LiDAR analysis and radar processing into a single product. Mosaicking, digitizing and classifying are executed using this software. A multi user licensed version of the software is available at Indian Institute of Technology, Roorkee which has been used for this research work.

2. 4. Methodology:

Major goals of this research work were achieved by numbers of steps and processes. Satellite data of previous 40 years have been downloaded from USGS. We performed several image processing techniques to enhance the quality of the images and also the features. From that satellite data we prepared FCC and Mosaic for all the years for better visualization and for getting more information about the area. All required datasets were collected from various sources mentioned above. Landsat images and DEMs were pre-registered, therefore did not require georeferencing. On the other hand, toposheets were georeferenced into the same projection system as the satellite images, i.e., UTM WGS 1984, Zone 43N, which provides with length/area calculations. 1:50,000 Survey of India toposheets surveyed during the period of 2000-2015 and 1:250,000 toposheets surveyed during the period of 1918-1920 were used for river channel studies.

Vector files were created for river channels, river catchments, and structural features like fault lineament etc. Same projection system (UTM WGS 1984, Zone 43N) for those vector files has also been used. Secondly, the toposheets were cropped to their map areas only to create a mosaic of toposheets. DEM and other satellite images were mosaiced together to create a continuous topographic map of the study area using the same software. From DEM data, we extracted river channel network, drainage density, and topographical cross-section so that we can find out the possible changes that took place over the time. Length and area calculations of the vector files were done in GIS environment using ArcGIS. Map making and Graphic operations were performed in the same software. Graphs were prepared from attribute tables of the vector files. The flowchart in figure 1.1 illustrates the steps/processes followed in this research work.

Morphometric analysis of the study area was performed using ASTER GDEM. Longitudinal profiles and hypsometric curves of the river basins were delineated in ArcGIS. Tectonic features of the study area were marked from seismotectonic atlas of India (Dasgupta et al., 2000). Earthquake data were collected from USGS Earthquake data catalogue. Finally all results obtained from these studies were correlated to identify role of active tectonics within the study area.

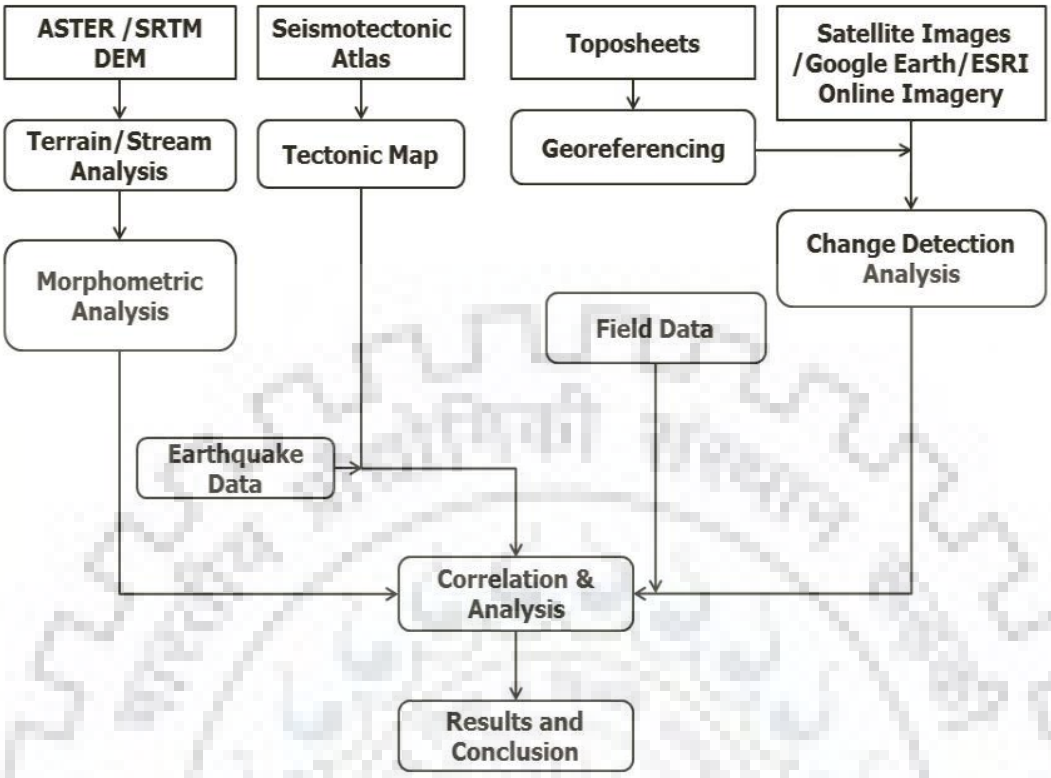

Figure 2.1. Flowchart enumerating the methodology of the research work.

Chapter 3

Geology and Tectonics of Himalaya

3. 1. Tectonics of the Himalaya:

The Himalaya ranges stretches over a 2400 km, from Arunachal in the east to Kashmir in the west. The mountain range can be grouped into four major litho-tectonic units, the Outer Himalaya, the Lesser Himalaya, the Greater Himalaya and the Tethyan Himalaya (Thakur, 2004, Guo and Wilson, 2012; figure 3.1). The Outer Himalaya comprises the Siwalik rocks deposited during the Miocene Epoch (23.03 to 5.3 Ma). It is located adjacent to the Indo-Gangetic alluvial plain marking southern limit of the orogen. The MFT separates the Outer Himalaya from the Indo-Gangetic alluvial plain. At many places Siwaliks are covered with thin deposits of Recent Alluvium. River terraces and U-shaped valleys are very common geomorphic markers over the entire Outer Himalaya range. The entire range is covered with very dense vegetation. Topographic slope of the Outer Himalaya range ranges between 0°-16°. The MBT separates the Outer Himalaya from the Lesser Himalaya.

The elevation of the Lesser Himalaya range ranges between 3,700 to 4,500 m reaching an average elevation of about 2000 m. The rocks comprise fossiliferous sediments covering a lateral sequence of thrust sheets that jumped from north to south in course of the great continent–continent collision. The entire range is highly dissected and less vegetated in comparison to Outer Himalaya range. V-shaped valleys are more common geomorphic markers within this range. River terraces are relatively rare within the Lesser Himalaya range. Topographic slope of the range ranges between 15°-30°. The MCT separates the Lesser Himalaya from the Greater Himalaya.

The Greater Himalaya is the highest mountain range reaching an elevation up to 8800 m. The Mount Everest with an elevation of 8848 m located within this range. Most of the rock type within this range is crystalline rocks. Mountain peaks, deep gorges, canyons and V-shaped valleys are major geomorphic features within this range. The entire region is lack of river terraces. The Outer Himalaya range is scarcely vegetated and mostly covered with snow and glaciers. The Tethyan Himalaya range comprises mostly fossiliferous sediments of Precambrian to Cretaceous age. Ophiolite and mélange of the India Eurasia suture lies adjacent to this range. The entire range is totally devoid of vegetation. Average elevation of

this range is relatively lower than that of the higher Himalaya range. The region further north is referred as the Trans-Himalaya.

The general understanding is that initially, during the Mesozoic-Early Tertiary period oceanic Indian lithosphere subducted beneath the Tibetan continental lithosphere along the Indo-Tsangpo Suture Zone (ISZ). Subsequently, subduction ceased with the collision of India and Asia during Eocene, paving way for under thrusting of the Indian subcontinent along intercontinental thrusts during Middle Tertiary (Rao et al., 2006). The detachment surface below the Outer and the Lesser Himalaya coincides with the upper surface of the subducting Indian lithosphere. The MBT and MCT that dip steeply near the surface are believed to flatten out at depth, merging with this detachment plane, contemporarily hosting most of the earthquakes (Prasad et al., 2011).

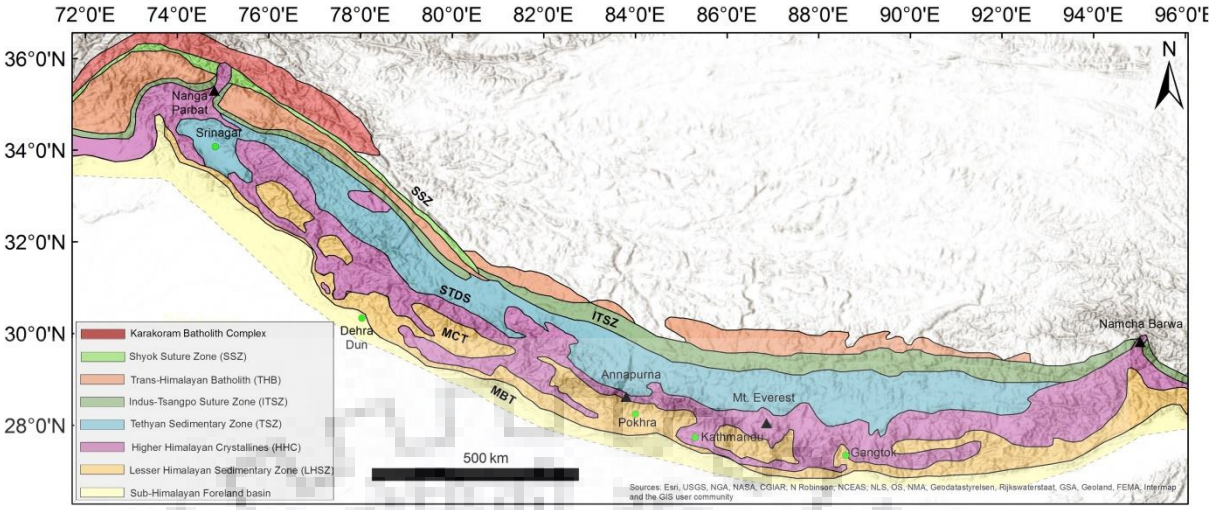

Figure 3.1 Regional geology of the Himalaya and major litho-tectonic units. SSZ–Shyok Suture Zone; ITSZ–Indus Tsangpo Suture Zone; THSZ/STDS–Trans Himadri Shear Zone/South Tibetan Detachment System (Singh, 2019; Thakur, 2004; Yin, 2006).

The Outer and Lesser Himalaya ranges are the most active zones of earthquake. Most of the major earthquakes affecting India have been epicentered within these zones. For example the Kangra earthquake of 1905 with a magnitude of M~7.8, the 1934 Bihar Nepal earthquake with a magnitude of M~8.3 etc. It is well known that the major mechanism of earthquake generation is the ongoing collision between the India and Eurasia plates. However, the exact nature of thrusting and convergence of various segments of the entire Himalaya are not well understood.

3. 2. Crustal deformation along plate boundaries:

The Himalayan orogen has developed around 55 Ma due to collision of Indian and Eurasian plates. The Indian plate is moving northeast at the rate of 50-55 mm/year (Paul et al., 2001). It has been observed that almost half of the plate motion is being accommodated by the numerous thrust systems lying within Himalaya only. Only half of the plate motion is being propagated to the Tibetan Plateau (Wang et al., 2008). The accommodated plate motion within the Himalaya has resulted active deformation within the mountain range (figure 3.2). As a result shortening has occurred within the entire Himalaya. However, it is suggested that at present the Himalayan Frontal Thrust is the major plane of shortening across the entire Himalaya (Yeats and Thakur, 2008). It has been observed that major earthquakes of the region have occurred near the MCT, MBT zones during the last few centuries (Kayal, 2007).

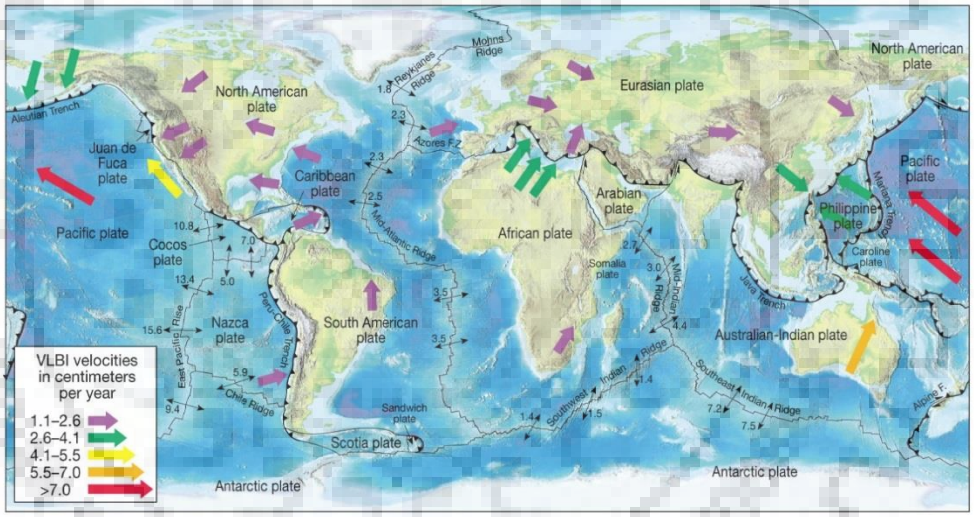

Figure 3.2. Tectonic plate boundaries of the World (Source: internet).

3. 3. Study Area and Geological Set-Up:

Study area is within the Sub-Himalaya region bounded by HFT and MBT. It is located in Himachal Pradesh and Uttarakhand states of India. It extends about 115 km in length and average width of about 75 km. Geological map Kangra reentrant, Nahan Salient and Dehradun are shown in figure 3.3. Himachal Pradesh and Uttarakhand are mountainous state which lies in the western Himalayas. There are a many recesses in the thrust zones in the western Himalaya, known as re-entrants (Thakur and Rawat, 1992). The Kangra re-entrant is the largest among these.

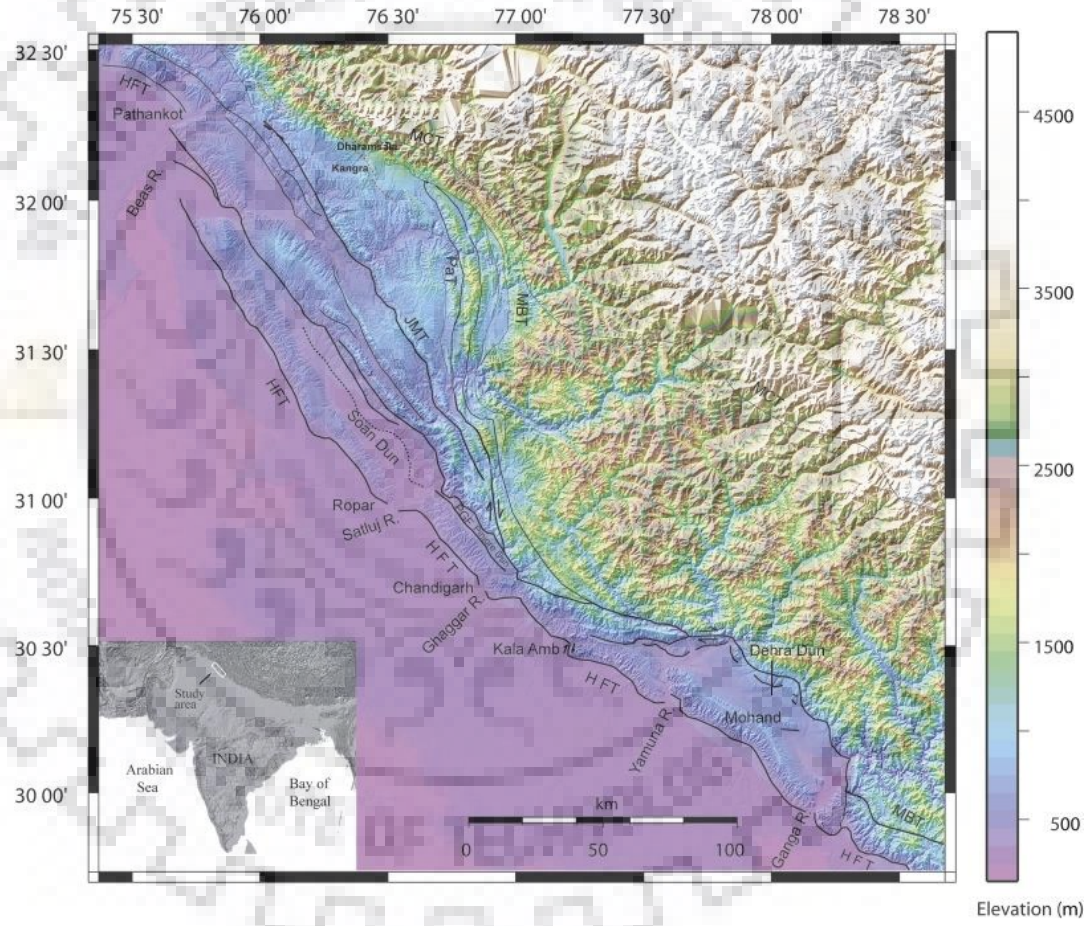

Figure 3.3. Shaded relief model of the study area. ASTER GDEM has been used for generating the shaded relief model. Major faults and thrusts are marked by black lines (Power et al., 1998). Location of the study area is shown in inset (white rectangle).

3. 3. 1. Vaikrita Thrust and Formation:

The Vaikrita Thrust demarcates the base of Joshimath Formation of the Vaikrita Group of high grade metamorphic rocks (Valdiya, 1973). The thrust is marked by sillimanite and kyanite at the bottom of the Vaikrita formations. From the Sutlej Valley it skirts around the northern boundary of the Rampur-Larji Window. The thrust swings towards north and possibly links up with the Panjal Thrust towards Karsog. Rocks of Chamba, Manjir, Katarigali, Salooni and Spiti Basin lie over the Vaikrita formation.

3. 3. 2. Jutogh Thrust and Formation:

Slates, phyllites, schists, meta-quartzites, limestone and gneisses are the major rock types of Jutogh Formation. In and around Shimla area it lies over the Jaunsar Group as a klippe. The structure of the Jutogh was interpreted as major recumbent anticline whose normal limbs have been eroded (Pilgrim and West, 1928). Lithology of the Jutogh Formation differ from those of the Vaikrita Group in their grade of metamorphism and the nature of the granitic bodies. They are predominantly of garnet grade.

3. 3. 3. Chail Thrust and Formation:

The lithology of the Chail Formation is predominantly talcose quartzite, quartz schist and phyllites (Pilgrim and West, 1928). Most of the rocks are regionally metamorphosed up to the grade of green schist facies. Sandstones are rare in this formation. Most of the sandstones are oligomictic, greywacke, and tuffaceous types. The volcano-sedimentary origin of the above rocks is proved by their extreme irregular granularity, the presence of well rounded, angular grains of quartz and plagioclase; fragments of micro-granular rocks of volcanic appearance; and a wide and common occurrence of albitization, characteristic of eugeosynclinal volcanic origin.

MBT in the study area shows major re-entrant which is known as Kangra re-entrant. Its trend in the North and South is NW-SE but N16E-S16W in the Centre (Dubey et al., 2004). The various lithological units present in the area are listed in table 3.2. Indo-Gangetic alluvium is the youngest unit which is exposed in the South. Alluvium and Siwalik molasse are separated by HFT. Siwalik molasse in the area are exposed near the foothills. The Siwalik rocks in the study area are deformed weakly but several large non cylindrical folds have been developed. Fault propagated folds are present near the exposers of the thrusts. On the other hand, buckle folds

can be noticed away from the thrust exposers (Raiverman, 2002). Both these folds have their hinge lines parallel to the HFT, but close to the ramp, they are somewhat curved.

Table 3.1. Litho tectonic units present in the region. (Dubey et.al. 2009).

Litho Stratigraphic Unit	**Age**	**Lithology**
Alluvium	Recent	Indo Gangetic Alluvium
Himalayan Frontal Thrust		
Siwalik Group	Middle Miocene to pleistocene	Upper Siwalik (Conglomerate, Sandstone) Middle Siwalik (Mainly Sandstone) Lower Siwalik (sandstone, Shale)
Dharamsala Group	Oligocene to Early Miocene	Upper Dharamsala (sandstone, few shale) Lower Dharamsala (Red Shale, Sandstone)
Subathu Group	Paleocene to Eocene	Green Nummulitic shale and limestone
Kakara Series	Paleocene	Green Grey and purple shale with siltstone intercalations, lenticular bands of limestone
Unconformity / Krol Thrust/ Main Boundary Thrust		
Tal Formation	Early Cambrian	Orthoquarzite and calc-arenite with pebble quartzite, shale; black phosphoritic and cherty layers
Krol Formation	Precambrian	Dolomitic limestone and shale alteration
Balini Formation		Slate and muddy quartzite, conglomerate, limestone
Nagthat Formation		Orthoquarzite (locally pebbliferous) and subordinate shale
Chandpur Formation		Olive green and grey phyllite with subordinate slate
Mandhali Formation		Arenaceous limestone gritty and slaty quartzite; Phyllite
Simla Group		Slate Sandstone and Quartzite
Shali Thrust		
Shali Formation		Cherty limestone and stromatoltic limestone
Chail Thrust		
Chail Formation		Low to medium grade metamorphic rocks
Jutogh Thrust		
Jutogh Formation		Medium to high grade metamorphic Rocks

Fault traces follow the major folding which gives an indication that they are formed during folding. But several back thrusts are also present which are formed at a later stage of thrusting (Ramsay and Huber, 1987). Presence of earlier tensional phase in the region is indicated by the basal decollement (Dubey et al., 2001). Subathu formation of Palaegene age is exposed only in the eastern part of the study area. Numerous imbricate thrust faults are exposed in the eastern part where Subathu formation, Dharamsala Group and Siwalik rocks meet. The dip of the MBT varies from 44° to 60° (Dubey and Misra, 1999). In the middle of the Kangra re-entrant there is

one extensional basin which contains Tertiary and subsidiary Siwalik rocks (figure 3.4). The time of formation of this basin is same as the time of thrusting at the frontal ramps. Due to lack of geochronological data, smaller size of the basin and thrusting at later stage makes it difficult to recognize the relationship between the younger formations. Deposition and basin development continued into the Pleistocene (Srivastava and Sah, 1993). Away from this basin, Siwalik rocks become straight and follow a general trend of NW-SE near the HFT. Hanging wall of MBT contains meta-sedimentary rocks of Lesser Himalaya. Numerous major Synclines occur near the MBT such as Shimla Syncline, Mussoorie Synclince etc. In the northwest direction of Shimla Syncline exposure of Shali formation is there along the Shali thrust. Chail thrust is also there which has similar curvature as the Shali thrust. Chail has low to medium grade metamorphic rocks whose grade decreases in the north-westerly direction. Chamba is surrounded by rocks known as Haimanta/Salkhala formation (Thakur and Rawat, 1992). Jutogh formation contains rocks of medium to high grade metamorphism that are equivalent to the Chail formation. Despite of large horizontal translation, Jutogh and Chail formation still remain in contact with their crystalline root in the Higher Himalaya. The seismotectonic map of the region was prepared by digitizing the Seismotectonic Alas of India and Its Environs, prepared by Narula et al., (2000).

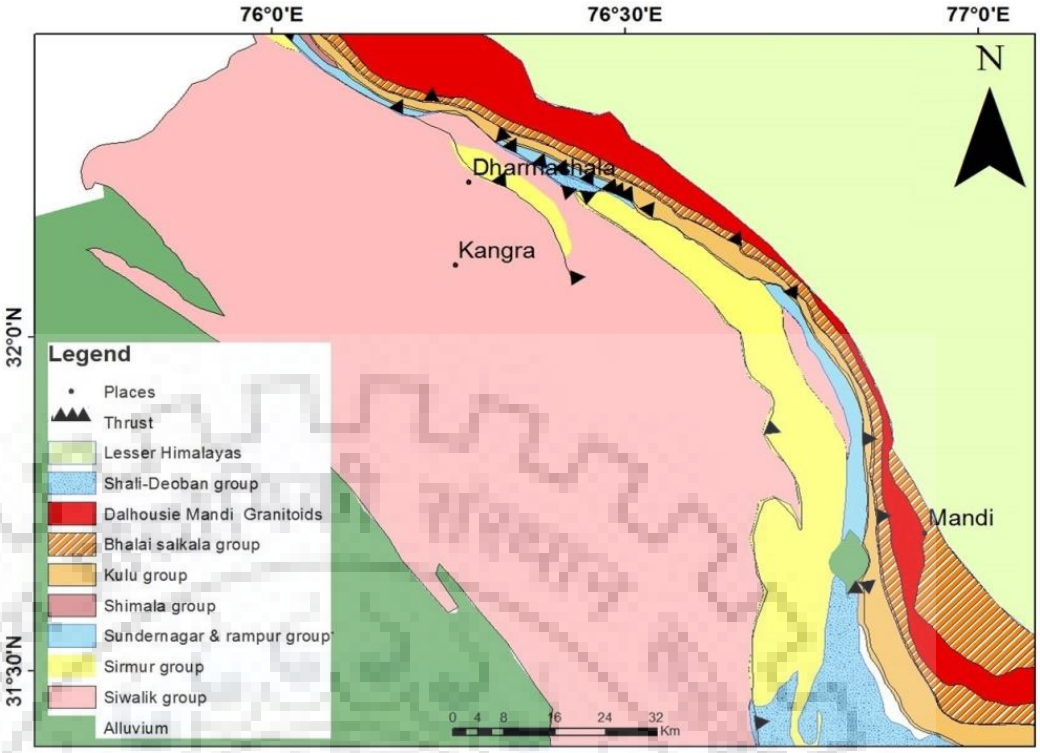

Figure 3.4. Geological map of the Kangra reentrant (Source: Srikantia and Bhargava, 1998).

3. 4. Kangra Reentrant:

The term Reentrant was privioulsy used as recess which means curve of an orogenic belt concave towards the craton (Billings, 1954). The term reentrant has been used by the others in the same sense. Himalaya is the result of convergence between the Indian and the Eurasian plates. Convergence gradually migrated to the south in a sequence motion forming linear zones of deformation like HFT, MBT and MCT respectively (figure 3.5). The HFT is the southernmost fault bounds with Siwalik rocks. In most of the region the HFT is a blind thrust. Thus strain released manifested as anticlinal folding (Yeat et al., 1991).

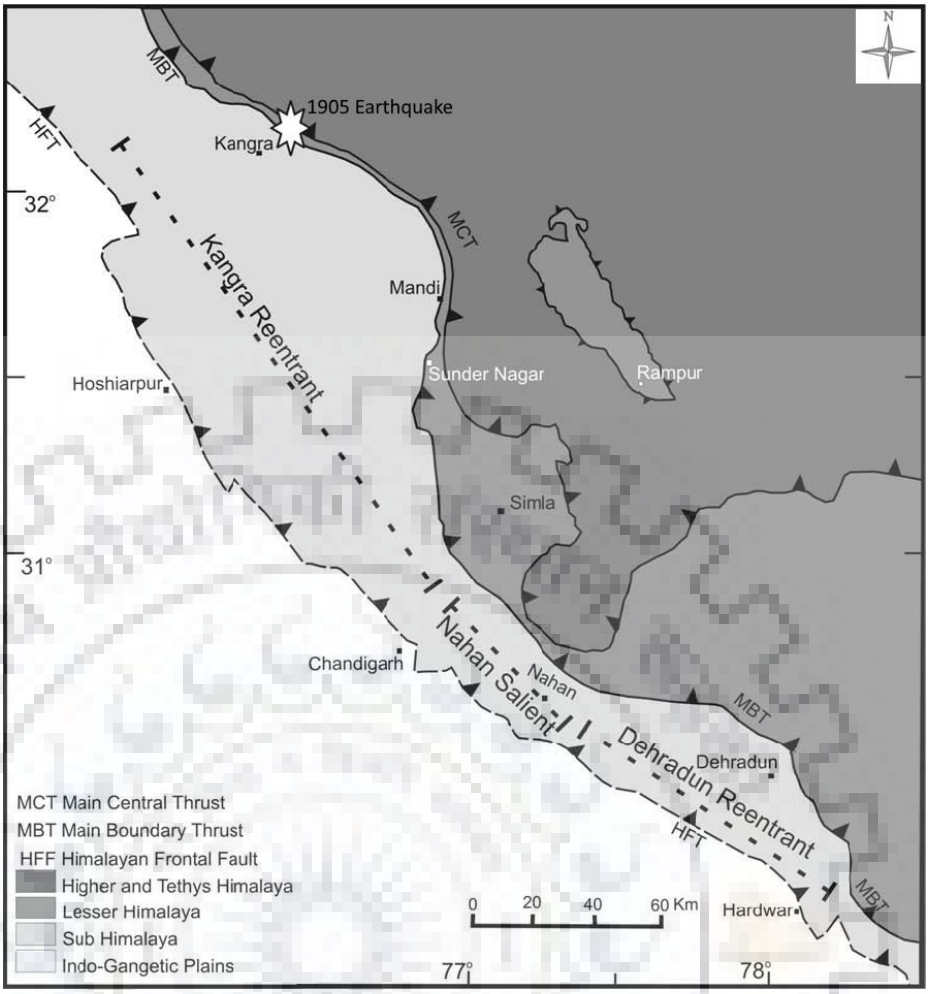

Figure 3.5. Litho-tectonic map of the Himalaya within the study area. Curved nature of the MBT has given rise to structural 'reentrants' and 'salients'. The Nahan Salient is bound towards west by the Kangra reentrant and towards east by the Dehradun re-entrant (Tejpal et al. 2011).

3. 5. Nahan Salient:

Regional Geology: The following is the succession of the rocks in the area-boulders, gravels, sand and clay Recent Holocene to Pleistocene. Boulders Conglomerate Upper Siwalik Pinjor, Tarot, Cromerian (Mid Pleistocene) Villafranchain (Lr. Pleistocene), Lower Siwaliks-Nahan Sandstone Middle to Upper Miocene (Power et el., 1998).

Dagshai Formation: The Subathus are overlain by the rocks of the Dagshai series. They comprise very hard, fine grained, grey or purplish brown quartzitic sandstones with intercalation of the res clays and shales. The clay predominates in the lower part whereas the sandstone gradually increases in the proportion in the upper part.

Kasauli Formation: Kasauli consist essentially of hard massive sandstones, grey to greenish in color with minor argillaceous bands. These argillaceous bands are gritty, greenish or brown and weather into angular splintery shales.

Nahan Sandstone: These consist essentially of a vast thickness of fluviatile sediments and show alterations of soft coarse grained, micaceous sandstones and pink or grey shales. Near the Nahan Thrust these rocks are considerably sheared. In the sections near Thaliga Lahan, Sen Ki Sair (Nahan, Himachal Pradesh) these rocks are characterized by alterations of orange clays and hard sandstones in the Upper part and grey clays and soft sandstones in the lower part.

Tatrot Stage: Tatrot stage with a variegated clay-sandstone sequesnce, trending North West to South East and dipping northerly. At places undulations are common in the beds. The sandstones are more friable massive, medium to coarse grained and grey in color, and show a tendency for pillar and /or spherical weathering. Being very soft and friable these offer least resistance to the action of water. Formations of gullies and potholes are common. The clays are variegated of red, purple, drab and green colors. At places they contain grits and have become hard. In general clays and soft and offer least resistance to cation of water. They occurs as intercalation with sandstones, are as much as 55 meters in thickness at places.

3. 6. Dehradun Reentrant:

The Dehradun valley lies between the Ganga and Yamuna rivers in the south-western part of Uttarakhand, India. Deposition of Recent sediments in a synclinal trough within the Siwaliks ranges have resulted formation the Dehradun valley. Recent sediments primarily supplied by Song-Nun river systems lies over the Siwaliks within the valley. However, Siwalik rocks are exposed at many locations within the valley. Pre-Tertiary formations of lesser Himalaya lie between Siwaliks and Recent sediments towards the northern boundary of the valley (Misra et al., 1988).

Major rivers within the valley, the Ganga and the Yamuna exhibit perennial flow along their entire course. Active flow can be seen only during and after Monsoonal rain in other tributaries of Ganga and Yamuna. When the rivers debouch into the plains Dehradun, elevation of the riverbed drops suddenly leading deposition of the carried sediments along with. This phenomenon makes the rivers highly braided within the Dehradun valley. The synclinal Dehradun valley has developed by folding of the Siwalik formations of the Upper Tertiary age.

The MBT boarders the northern boundary of the valley. On the other hand, HFT separates the Siwaliks from the Indo-Gangetic alluvial plains (figure 3.6). The Siwalik group of rocks is mainly of fluviatile origin; comprising sandstones, shales and conglomerates. These fluvial deposits are termed as 'Dun gravels' (Medlicott, 1864; Karunakaran and Rao, 1979; Rao, 1986; Raiverman et al. 1983, 1990). Donga, Dehradun and Bhogpur alluvial deposits located within the valley are major alluvial fans within the valley.

The Delhi Haridwar basement ridge which acts as the present day drainange divide between the Indus and Ganges rivers (Yin 2006). The Delhi Haridwar basement ridge, running transverse to the Himalayan front, is a lithospheric-scale feature possibly marking the contact between the Rajasthan and Bundelkhand cratons at depth. Delhi-Haridwar basement ridge is bounded by the Shimla and Dehradun (Godin et al 2018).

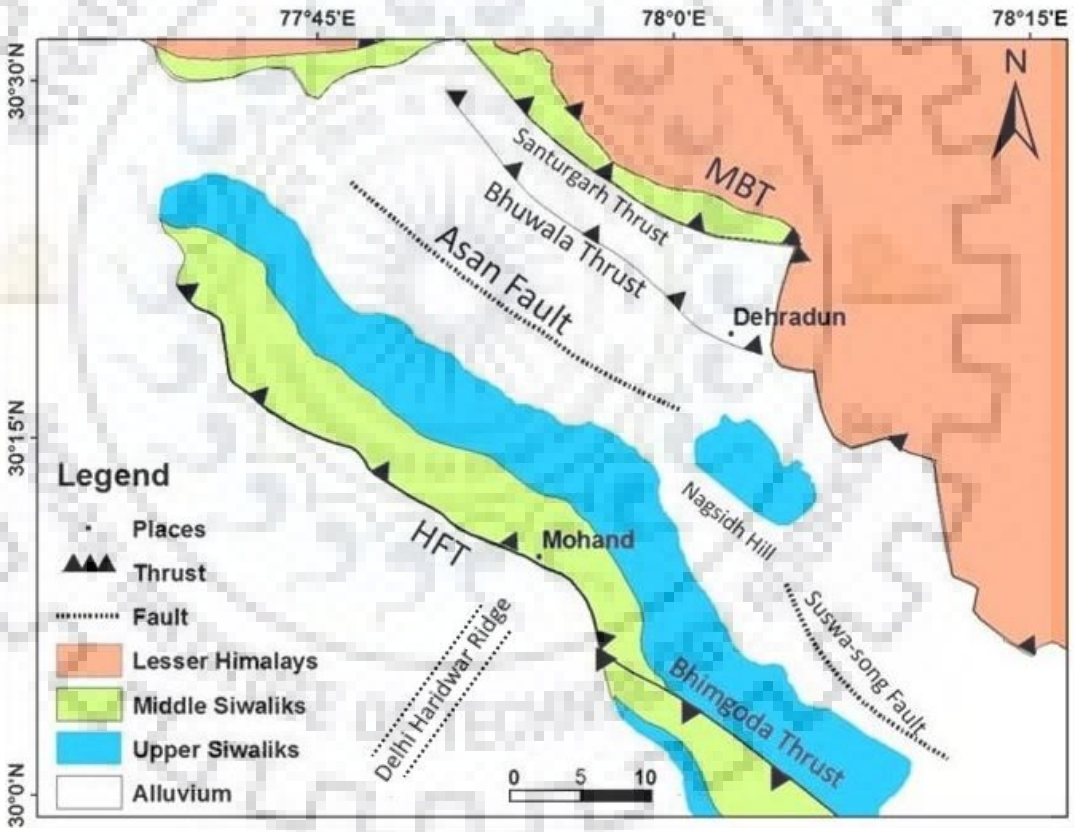

Figure 3.6. Tectonic and Geological set up of Mohand anticline and Dehradun region (after Raiverman et al., 1990 and Thakur et al., 2006).

3. 7. Earthquakes along plate Boundary:

Earthquakes magnitude equal/exceeding M8 are clustered near the eastern syntaxes of the Himalaya range (figure 3.7). The eastern Himalayan syntaxes are complex tectonic zones of multiple-plate interaction. The Himalaya and the Tibetan thrust zones and Burmese Arc have

converged at those locations. It has been observed that multiple plate junctions are more vulnerable to large earthquakes, as those junctions provide geometries capable of large stress build-up requisite for generation of great earthquakes (Gupta and Gahalaut, 2012). The Eastern Himalayan syntaxes have so far experienced many major earthquakes, for example 1950 Assam earthquake (M8.7), 1897 Shillong Earthquake (M8.0) etc.

3. 8. Seismic scenario:

It is well known that the Himalayan tectonic belt represents one of the most seismically action regions of the world. In general, the seismicity is concentrated in the area north of MBT except at a few regions across the MCT. In order to understand the nature of earthquake occurrence of the study area an area bounded by longitudes 75°E to 79°E and latitudes 29.5°N to 33.0°N are considered (figure 3.7). These earthquake events belong to the period 1809 to 2017 with magnitude and depth ranges1.2 to 8.0 and 1 to 225 respectively. The reported epicentre of great 1905 Kangra earthquake (longitude 76.25°E and latitude 32.3°N) is shown by red largest circle in figure 3.7.

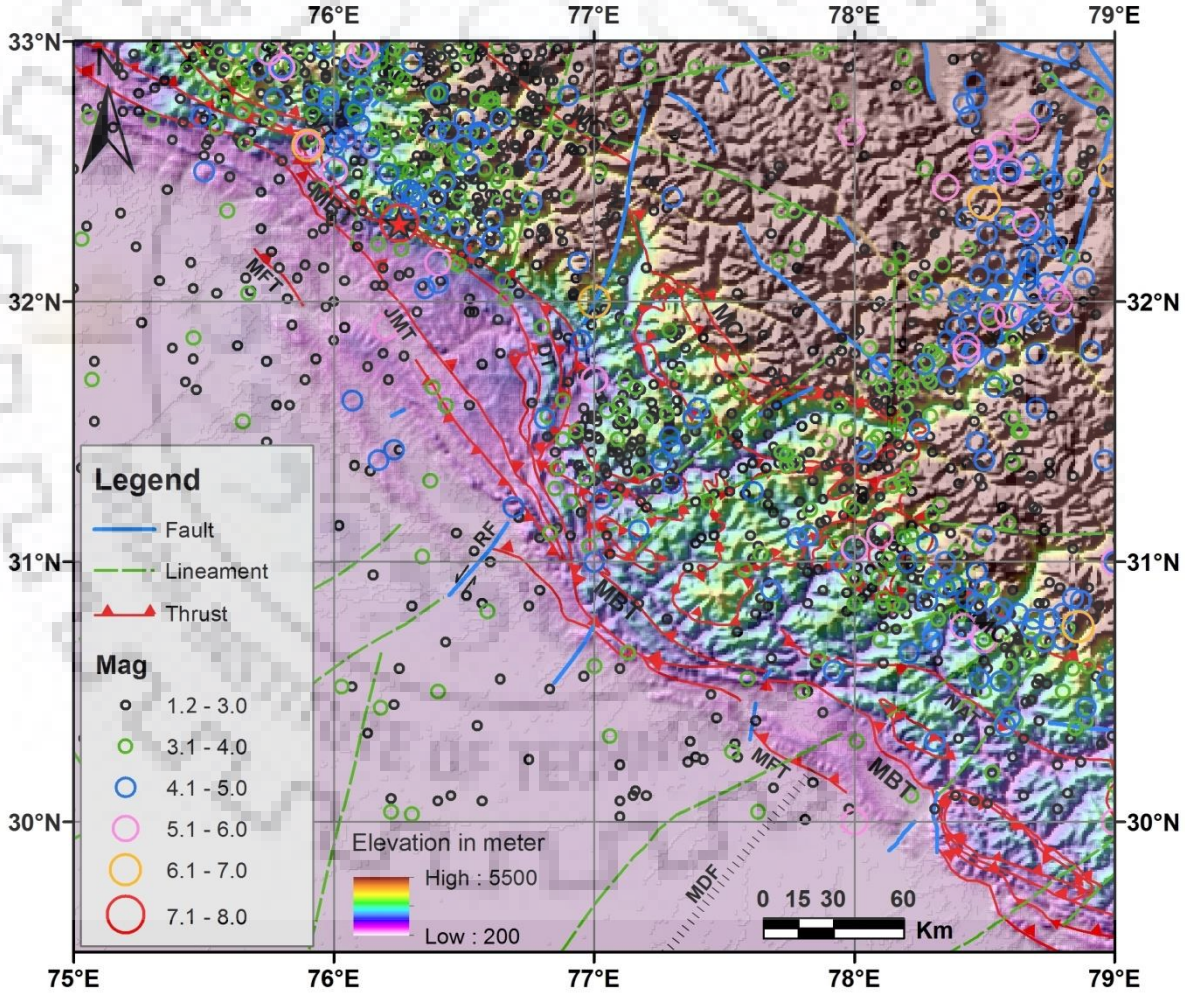

Figure 3.7. Seismotectonic set up of the Kangra-Nahan-Dehradun area (study area). KFS-Kaurik Fault System, SNF-Sundernagar Fault, MCT-Main Central Thrust, NAT-North Almora Thrust, VT-Vaikrita Thrust, DT-Drang Thrust, MBT-Main Boundary Thrust, JMT-Jwalamukhi Thrust, RF-Ropar Fault, MFT-Main Frontal Thrust, MDF-Mahendragarh Dehradun Fault (Seismotectonic Atlas of Indian and its Environs, 2000). Kangra earthquake of 1905 is shown by red circle and star.

Among the several earthquakes in the study area, the most prominent event is the Kangra earthquake of 1905 and in fact it is the major one in whole northwest Himalayan region. This earthquake was one of the most devastating earthquakes of the 20th Century. The Kangra earthquake was felt over an area of 416,000 km^2 and about 20,000 people were killed in the epicentral region (Ambraseys and Bilham, 2000). About 100,000 buildings were destroyed by the earthquake. The intensity close to the epicentre of the earthquake was X on the Modified Mercalli Intensity (MMI) scale and the main epicentral tract extended from Kangra in the south-easterly direction. A secondary tract along which damage was not so severe was near Dehradun (Ambraseys and Bilham, 2000). Gutenberg and Richter (1954) reported a magnitude of Ms=8 for the 1905 Kangra earthquake. Different magnitude estimates for this event are M=8.6 (Duda, 1965) to Ms = 7.5 (Abe and Noguchi, 1983).

Ground shaking intensity distribution indicates two different regions separated by about 200 km, one around Dehra Dun and another around Kangra. Maximum intensities assigned were of VIII and X on the Rossi–Forel (RF) scale, respectively based on detailed damage reports of Middlemiss (1905, 1910).

Seeber and Armbruster, 1981 interpret that the earthquake has ruptured a 280×100 km^2 area. According to Ambraseys and Bilham (2000), rupture area required for a Ms = 7.8 lies in the range 100×120 km^2 to 80×50 km^2 with 3–8 m of average slip and the rupture dimension is 80–100 km between the southern Tibetan plateau edge and main frontal thrust for the Himalayan earthquake with slip normal to the arc. Therefore, it may be inferred that that the main fault rupture responsible for 1905 Kangra earthquake did not have extension from Kangra region to the region near Dehradun. Wallace et al. (2005) suggested that the earthquake rupture occurred on a shallow-dipping fault lying at a depth of 15 km under the northern Himalaya. The rupture is parallel to the Himalayan structural trends in the region. Hence the 1905 Kangra earthquake is resulted due to rupturing of low angle thrust i.e. the main Himalayan detachment surface or decollement fault. Ambraseys and Bilham (2000) suggest no horizontal displacements due to the 1905 Kangra earthquake on the basis of re-evaluated coseismic levelling and triangulation data. According to Hough et al. (2005) the Kangra earthquake could possible triggered a M7.0 aftershock near Dehradun. However, Burrard (1910a, 1910b) found 15 cm of uplift in the Dehradun region which is 250 km southeast from the epicentre with assigned RF intensity VIII. Studies carried out by the researchers postulate that the southwest edge of the 1905 Kangra earthquake rupture

coincides with Jwalamukhi Thrust (Powers et al., 1998) and the north-eastern edge lies beneath the Greater Himalaya (Wallace et al., 2005).

Rupturing along the thrust/faults in the Himalayan belt is essentially due to the active convergence between the Indian and Eurasian tectonic plate and the convergence continued un-interruptedly. The convergence rate in the Kangra region is 14 ± 4 mm/yr (Powers et al., 1998; Wesnousky et al., 1999; Banerjee and Burgmann, 2002. Hence, the geological and morphological feature of this region has been experiencing modification from time to time.

Table 3.2. Some major earthquake in Indian region of Western Himalaya (Source: USGS).

Location	Date	Time	Latitude	Longitude	Magnitude
Kinnaur, Himachal Pradesh	19-Jan-1975	13:32 IST	32.46°N	78.43°E	6.8
Uttarkashi, Uttarakhand	20-Oct-1991	02:53 IST	30.73°N	78.45°E	6.8
Chamoli Uttarakhand	29-Mar-1999	00:35 IST	30.408°N	79.416°E	6.8
Kangara, Himachal Pradesh	4-Apr-1905	01:19 IST	32.01°N	76.03°E	7.8
Kashmir, Jammu and Kashmir	8-Oct-2005	08:50 IST	34.493°N	73.629°E	7.6
Kashmir, Jammu and Kashmir	1-May-2013	12:27 IST	33.1°N	75.8°E	5.8
Kangra, Himachal Pradesh	21-Aug-2014	13:41 IST	33.1°N	76.4°E	5

Chapter 4

Morphotectonic Study – A Review

Morphotectonic integrates topography and tectonic activity to describe landforms generally at continental, sub-continental and even at local scales. It includes the study of mountains, drainage patterns, erosion surfaces and sediments on land and offshore. Remote sensing and GIS tools have been used extensively for such studies since the last few decades. Further, with the help of geochronological tools for dating quaternary materials enhanced the ability to answer the questions associated with active tectonics and Earth's surface processes. Recently, studies on Neotectonics and landscape evolution have been emphasised to increasing the understandings of Earth's surface processes.

The morphometric studies have now been combined by studies of the relationship between global tectonics and geomorphic evolution. Oilier (1981) has proposed the term 'evolutionary geomorphology' for this portion of earth-science. In recent years, in the field of remote sensing and GIS, researchers stress primarily on the deformed landforms for morphotectonics. With the availability of digital elevation models, high resolution satellite data and topographical maps it has become possible to extract even little variations.

4. 1. Remote Sensing and GIS based approach in morphotectonic analysis:

Geomorphology and landform characteristics can be well understood from remote sensing images of high and coarse resolution. Spatial information obtained from aerial photographs, satellite data, topographic maps along with morphotectonic indices can well describe tectonic history of a region (Keller, 1986). Significant development in resolution of satellite data and advancement in GIS resources has enabled researchers to carry out quantifiable and more precise analysis of various landforms. Verrios *et al*. (2004) carried out morphotectonic study for Eliki fault zone to correlate active tectonics with erosional processes using topographic maps and aerial photographs. Cuong and Zuchiewicz (2001) studied the morphotectonic characteristics of Lo River fault near the Tam Dao in North Vietnam. Jain and Verma (2006) applied integrated remote sensing and GIS technique to identify geomorphology, slope, and vegetation index to assess neo-tectonic potential in Bundi-Indergarh sector of Rajasthan. Morphotectonics of Anandpur Sahib area of

Rupnagar district (Punjab) was studied by Bhatt et al. (2007) using remote sensing and GIS approach. Using Remote Sensing data products, Dalati (1994) has studied the tectonic of EI-Rouge Depression, NW of Syrian Arab Republics. Ramasamy (2006) and Ramasamy et al. (2011) studied mega drainage characteristics, tectonic, hydrological and geomorphic anomalies based on satellite images for whole peninsular India. Morphological analysis of topographic features, like minor faults and lineaments, has long been applied in structural and tectonic studies (Hobbs, 1912; Frisch, 1997). Satellite images show great ability as a tool for mapping and correlation of alluvial geomorphic surfaces (Gillespie et al., 1984; Kahle et al., 1984; Anderson and Beratan, 1993, 1994; Chaudhary et al., 1996).

4. 2. DEM based morphometric studies:

Morphometric analysis is the quantitative assessment of form features of the earth surface and any landform unit. It can also be defined as the quantitative measurement of landscape shape. Landforms can be characterized in terms of their elevation, size and slope. The geomorphologists can compare different landforms and can calculate less straightforward parameters which are useful for identifying a particular characteristic of an area such as level of tectonic activity (Keller and Pinter, 1996). Morphometric analysis includes quantitative study of the various components such as hypsometric analyses, sinuosity, SL indices, basin shape indices, drainage basin asymmetry, etc., which indicates the nature of development of the basin. These are used as parameter of active tectonics (Keller and Pinter, 1996).

DEMs derived from microwave (SAR Images) and optical images have several applications in various fields. The potential of DEMs for solving a wide spectrum of applied and theoretical problems has long been known (Evans, 1972). Its simple data structure and widespread accessibility have made it a popular tool for land characterization. DEMs derived from the ASTER (Advanced Spaceborne Thermal Emission and Reflection Radiometer) stereo data (GDEM), Shuttle Radar Topographic Mission (SRTM) and ALOS-PALSAR (Advance Land observing satellite with Phased Array type L-band Synthetic Aperture Radar) geo-corrected is now freely available for whole world with resolutions of 90m, 30m and 12.5m. These products can be very useful for research purposes as well as to supply basic topographic mapping data for poorly mapped areas (Rabus et al., 2003). SRTM-DEM's accuracy assessment is carried out by

various workers using different approaches (Sun *et al*., 2003; Miliaresis *et al*., 2005; Kocak *et al*., 2005; Sharma *et al*., 2010; Baral *et al*., 2016). DEM has a vital role in morphotectonic analysis as they are most widely used for representing topography. Moreover, DEM also displays the tectonically affected topography in better way. Most of the morphometric studies applying DEM use shaded relief models jumbled with remotely sensed data products over a wide region (Florinsky, 1998; Chorowicz *et al*., 1999). For better understanding three dimensional perspective views with image drape (Le Turdu *et al*., 1995) has been used by researchers. Chorowicz *et al*. (1991) used DEM to calculate dip and strike from geological maps. Koike *et al*. (1998) calculated fault plane geometries from DEMs. Florinsky (1998) studied the connection between fault type and landform followed by use of curvature maps to recognize and characterize fault line. Onorati *et al*., (1992) used aspect and slope calculations in a regional morphotectonic investigation. Jordan *et al*. (2005) suggest a technique for the reliable application of digital terrain analysis technique to classify tectonic phenomenon from geomorphological parameters in Hungary and NW Greece. Zizioli (2008) studied the DEM-based morphotectonics analysis of Western Ligurian Alps exhibiting a typical drainage network related to the geological events. They have used advance GIS based approach to extract the morphotectonic lineaments, drainage characteristics and neotectonics of the Lingurian Alps.

4. 3. Geomorphic marker and associated deformation:

Geomorphic markers are identifiable landforms, surfaces or linear features that provide a reference frame for deformational history. According to Marshall and Anderson (1995) they can be easily compared with their modern counterparts for variation in morphological parameters. Reconstruction of deformed markers is essential for reliable results.

To document upliftment, faulting and folding, river terraces are commonly used as geomorphic markers (Molnar *et al*., 1994; Rockwell *et al*., 1984). River terraces are very useful in evaluating the vertical as well as horizontal deformation. Alpine glaciation fluvial terraces have been used to compare with moraines associated with glacial advances still stand for years (Penck and Bruckner, 1909). The terrace crossing the San Andreas Fault in California near Cajon pass potentially illustrates the complex nature of terrace formation (Weldon, 1986). The comparison between terrace surface and the modern day stream gradient reveals that warping occurred more than 30m, although it is not physically

dislocated along fault. Dating of sediments indicates that both the initiation of aggradation and incision are diachronous. River terraces which are same as alluvial fans are not caused by immediately or uniformly changes in controlling parameters like sediment supply, discharge, rock uplift rate and base level lowering (Humphrey and Heller, 1995). Surface processes may tend to transform the appearance of alluvial fans (McFadden *et al*., 1982; Ritter *et al*., 1993). Whipple and Dunne (1992) observed that many arid alluvial fans are dominated by deposition from debris flows. Even surfaces with considerable roughness, can be used as effective markers, because in spite of its irregularities the average surface gradient can be defined (Avouac and Peltzer, 1993), and offset of the gradient by faulting can be readily predictable. Lava flows, landslides, debris flows, and erosional surfaces can provide excellent markers (Weldon, 1986; Small and Anderson, 1998). In central Asia, Tien Shan is regionally extensive erosion surface which was bevelled across Paleozoic rocks and suppressed by Cenozoic sedimentary rocks (Chediya, 1986; Sadybakasov, 1990). It offers an exceptional sign for recording faulting and folding of ranges that grows above the surrounding terrain (Burbank *et al*., 1999). A location for standardizing the amount of erosion is not only the erosion surface but itself the uncomfortable surfaces that has encountered beneath it (Small and Anderson, 1998). The displacement along ridge crests across strike-slip faults and through courses of river can evidently record lateral offsets (Beanland and Clark, 1994).

4. 4. Hypsometric analysis:

Hypsometry of a river basin describes cumulative distribution of elevations with respect to area. Hypsometric curves can reveal significant information on geomorphic condition of a catchment. Sediment yield and maturity of a river basin can be directly interpreted from hypsometric curve of the basin. Hypsometric curves for different catchments of the study area have been derived from ASTER-GDEM data. It should be noted that, only hilly regions of the catchments have been considered for this analysis. ArcGIS software has been used to extract the river basins of the study area to generate hypsometric curves. Hypsometric tool developed by ESRI has been used to delineate hypsometric curves of the selected basins.

Hypsometric curve: For a drainage basin, the hypsometric curve represents the relative proportion of the watershed area below (or above) a given height (Strahler, 1952; Pike and Wilson, 1971). Under similar hydrological conditions, a relative understanding into the past

soil movement of basins can be inferred by comparing the shape of the hypsometric curve for different drainage basins. Thus, the shape of the hypsometric curves is very useful in explaining the temporal changes in the slope of the original basin and in turn, provides information about the tectonic activities shaping out that basin.

Frequent variation is observed in the shape of the hypsometric curve during the early geomorphic stages of development which is followed by minimal variation after the watershed attains a stabilized or mature stage (Figure 4.1). Where (A) sum of area between each pair of adjacent contour lines and (a) is surface area within the basin. In the present study the hypsometric curves for the drainage basins of each location have been generated from ASTER GDEM using the watershed and hypsometric tools in ArcGIS.

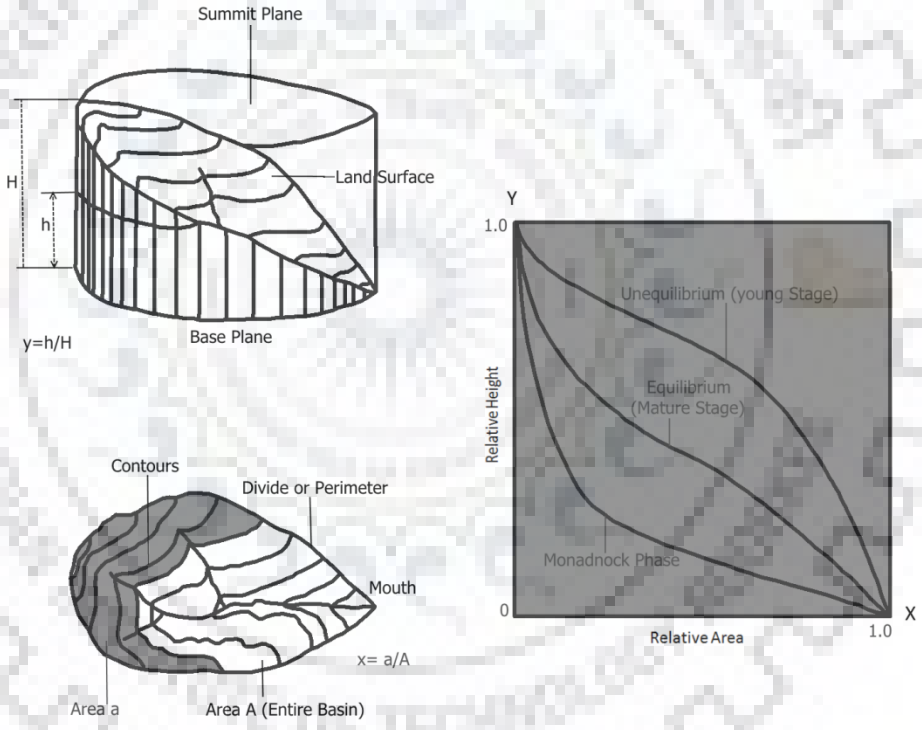

Figure 4.1. Typical hypsometric curves (HC) (Ritter *et al*., 2002 and Strahler, 1952).

4. 5. Stream-Length gradient index:

The stream-length gradient index reflects the relationship among rock resistance stream power, and tectonics (Hack, 1973). It is an important parameter to interpret if change in stream slope is due to tectonic deformation or rock resistance, especially if it has a vertical component (Keller and Pinter, 2002).

The stream gradient index is denoted by Hack (1973) as follows:

$$SL = (dH/dL)*L$$

Where, SL is the stream gradient index, dH/dL is the local gradient of the stream reach where the index is computed, dH is the drop in the elevation, dL is the length of the reach and L is the total length of the of the channel from the water divide to the centre of the reach measured along the channel (figure 4.2).

The SL values are high in areas where: (a) active tectonics has resulted or, (b) rocks are particularly resistant. Therefore, high SL indices in rocks of low to uniform resistance are a possible indicator of active tectonics (Keller, 1986). An area of soft rocks having higher SL value represents recent tectonic activity, at the same time low SL values indicates movement along strike-slip faults (Keller and Pinter, 2002). In this study, SL index was calculated along a number of sections of streams and rivers of the different locations, where faults were recognized, using SRTM DEM and GIS and its standardized average value for the segments of each basin was calculated.

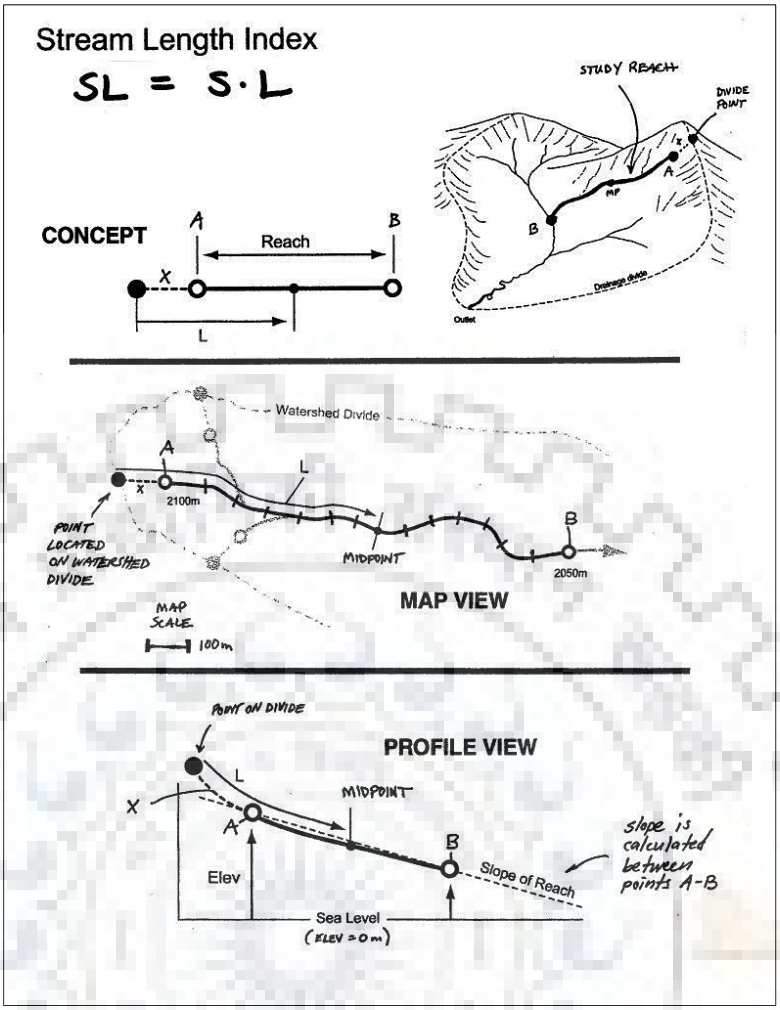

Figure 4.2. SL mechanism (Mahmood and Gloaguen, 2012).

4. 6. Sinuosity:

Sinuosity deals with the arrangements of channel of a drainage basin. Sinuosity is defined as the ratio of channel length to channel valley length (Figure 4.3). Its value ranges from 1 to 4 or more. Rivers which have a sinuosity of 1.5 are called sinuous, and above 1.5 are called meandering (Leopold *et al*., 1964). It is a significant quantitative index for interpreting the significance of streams in the evolution of landscapes. It is a useful parameter for the rivers located in tectonically active areas (Gomez and Marron, 1991). The secondary effect of uplift can be measured by increasing or decreasing channel sinuosity. It is measured as:

Sinuosity= Channel length/Channel Valley length= C/V.

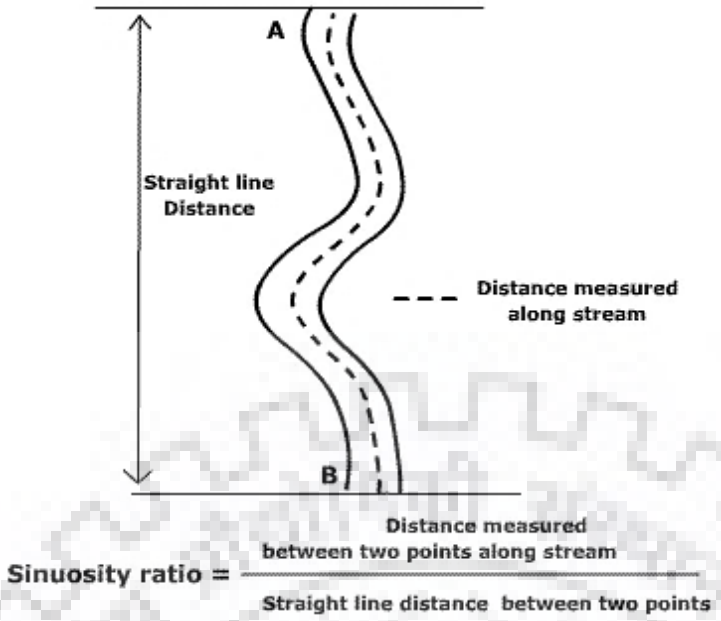

Figure 4.3. Sinuosity measurements (Michael and Ritter, 2016).

In this study, the drainage channels along the river are first digitized from world map base layer provided by ESRI online satellite image and then sinuosity of these drainage channels are calculated in ArcGIS.

4. 7. Drainage Basin Asymmetry:

The asymmetry factor (AF) was developed to identify tectonic tilting transverse to stream at drainage basin on larger scales (Hare and Gardner, 1985; Keller and Pinter, 2002).

The asymmetry factor is determined by the formula:

$$AF=100\ (A_r/A_t)$$

Where, A_r is the area of the basin to the right of the trunk stream that is facing downstream and A_t is the total area of the drainage basin (figure 4.4).

Asymmetry Factor (AF), greater or smaller than 50, shows effect of active tectonics, differential erosion or lithologic control (Hamdouni *et al*., 2008). Asymmetry Factor close to 50 is seen when there is no or little tilting perpendicular to the direction of the trunk channel.

The landforms are characterized by mountainous sides, relatively steep and flat floors in tectonically active topography. These steep sides are formed by displacement on faults such that the valley floor moves down relative to the surrounding margins or the boundaries move up relative to the floor. Then the consequence is basin sloping, causing the river to migrate and deviate from the basin midline (Cox, 1994). The drainage basin asymmetry factor is calculated from the watershed generated for each drainage basin in ArcGIS.

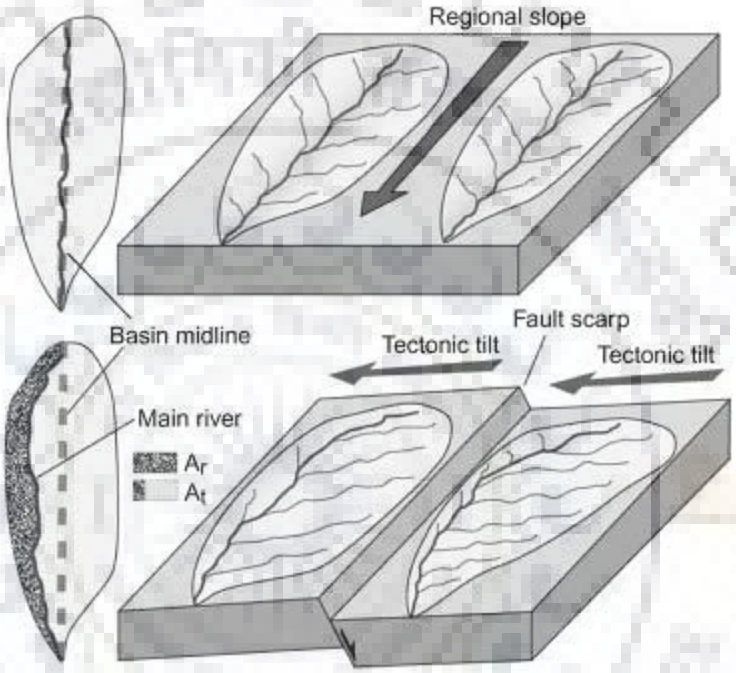

Figure 4.4. Drainage response to uplift along a fault by migrating laterally in a down-tilt direction, A_r is the area of the basin to the right (looking downstream) of the trunk stream and A_t is the total area of the drainage basin (Keller and Pinter, 2002).

4. 8. Basin shape index:

In tectonically active areas, young drainage basins tend to be elongated shape parallel to the topographic slope of a mountain. These elongated shapes become circular shapes with time due to less tectonic activities and continued topographic evolution (Bull and McFadden, 1977). In tectonically active areas, the drainage basin widths are narrower near the mountain front than upstream from the mountain front. This is due to the energy of the stream near the mountain front concentrated primarily to down-cutting compared to the lack of continuing rapid uplift in the upstream which permits broadening of the basins.

The elongation ratio is expressed as:

$$B_s = B_l / B_w$$

Where, B_l is the length of a basin measured from the headwaters point to the mouth, and

B_w is the width of a basin measured at its widest point (Figure 4.5).

High values of B_s are related with elongated basins which in turn are linked with relatively higher tectonic activity. On the other hand, low values of B_s indicate a more circular shaped basin, related with low tectonic activity. Hence, B_s reflects the rate of active tectonics. The basin shape index is calculated from the watershed generated for each drainage basin in ArcGIS.

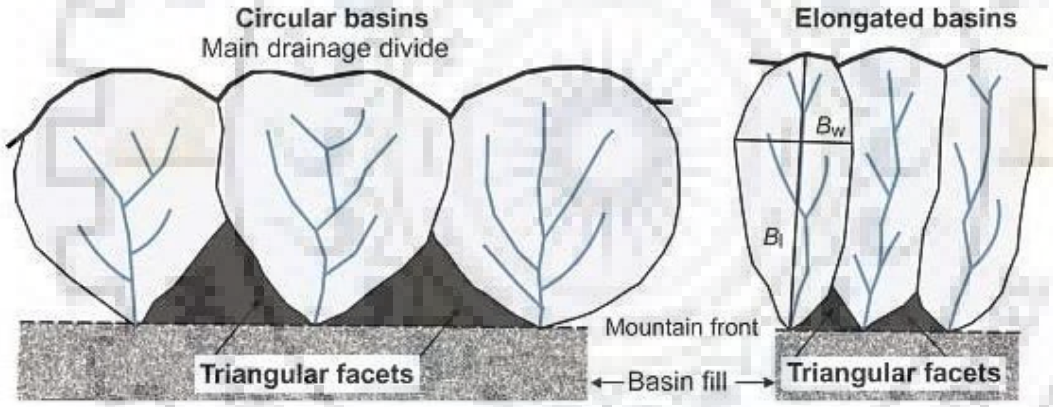

Figure 4.5. Basin shape index (B_s) calculation (Mahmood and Gloaguen, 2012).

4. 9. River response to active tectonics:

Fluvial system is the most sensitive natural system to active tectonics. Active deformation results a channel response which gets superimposed over long-term tectonic effects. Different types of channels respond differently to active tectonics. Responses may be in the form of changing course, channel pattern, sinuosity index, deposition, flooding, incision etc. However, tectonic induced changes depend on prevailed channel properties and tectonic regime of a river system. Alluvial rivers are very sensitive to the variation of slope of a region. By the process of aggradation and degradation along fault line, streams respond to vertical displacement. Aggradation and degradation can be perceived on the upstream from the

horst and the downside part of the horst respectively (Cartier and Alt, 1982). Slow rates of upliftment can cause more channel adjustment by widening and meandering of the river course (Ouchi, 1985). It is observed that the river shape changes at critical values of gradient, stream power, and sediment load (Schumm and Khan, 1972). Hooke (1995) has studied the adjustment to meander cut-offs on the River Bollin and River Dane, NW England. Some frequently observed influences of active tectonics on river channels have been discussed below.

4. 9. 1. Drainages and stream networks anomalies:

Drainage network anomalies are one most effective geomorphic marker for active tectonic studies. Drainage network is the most sensitive surficial features to valley slope. Any changes in the valley slope necessarily bring changes into the stream network (Cox, 1994). Therefore drainage anomalies are very good indicators of active tectonics (Jackson and Leeder, 1994). Active tectonics may bring changes in channel morphology, sediment load, sediment particle size, sinuosity, flooding, incision, or in combination of all parameters of a river system.

Local scale variation in regional slope can cause anomalous drainage pattern. Experimental studies showed that parallel drainage pattern form on the slopes greater than 2.5 percent, whereas dendritic pattern forms on the gentler slopes (Philips and Schumm, 1987). Changes of entire drainage network, with the effect of sloping, are described by Sparling (1967). Topography and drainage system in regions of active deformation results in aspects of faults growth (Cracknell & Hayes, 1991; Medwedeff, 1992; Mueller and Tailing, 1997; Delcaillau et al., 1998; Tate et al., 2002; Burbank and Anderson, 2001; Husson and Mugnier, 2003; Delcaillau, 2004; Gupta and Ellis, 2004). Morphometric indices are the proxy indicator of dynamic tectonic prevailing in the regions where the changes are gradual and drainage anomalies are not prominent (Pedrera et al., 2009). Some geomorphic markers are very effective to identify tectonic deformations. For example, hypsometric integral, hypsometric curve, stream sinuosity, drainage basin asymmetry, stream-gradient index, slope gradient index, elongation ratio etc. (Keller and Pinter, 1996). Sinuosity index (Muller, 1968) of an alluvial river is very sensitive to valley floor changes (Susan, 1993). Generally meandering channels responds by changing sinuosity.

In the present study few types of drainage anomalies have been identified which indicate towards the sub-surface faulting/activities or abrupt changes in bedrock or topography. Linear arrangement of lakes, sinkholes or drainage line indicates the presence of fault, fracture or less resistant linear rock outcrop as the stream tends to flow along weak path. Anomalous curves or turns of the streams indicates the presence of surface or near-surface structures across the path of the stream viz., acute or obtuse elbow turn indicates fault, round turn around an area indicates sub-surface high (e.g., dome structure) (Burbank and Anderson, 2012). Abrupt and localised meanders in streams represents interruption in normal pattern related to subtle upstream reduction in stream gradient and indicates the occurrence of a dome-like feature along the course of the stream which may be an active zone of uplift. Several meanders of a stream are squeezed; compressed and incised that may be due to the occurrence of a fault, fold or dome structure across the course of the stream or a plunging fold with plunge towards upstream direction. Long, rectilinear segment of streams are observed when the regional drainage pattern is other than rectangular, trellis or angulate which indicates that the stream is flowing along a fault, fracture or easily erodible vein or dike.

4. 9. 2. Longitudinal tilting affects:

Changes in river valley: In fluvial geomorphology the most cited example of deformation is the upwarping and/or subsidence of river valley. When there has been uplift or subsidence within a river valley, the river reacts accordingly. Upliftment of a river valley makes the river incise into its own valley abandoning its existing floodplain (figure 4.6). Under such condition paired terraces can be formed. Considerable lateral erosion may result unpaired terraces. The geometry of unpaired terraces is hard to reconstruct throughout the channel. Dating is necessary to correlate such terrace remnants. On the other hand, river incision into its bedrocks results strath terrace. Such bedrock terraces are found normally within or immediately adjacent to mountains. Under equilibrium condition valley widening may occur after down cutting. On the other hand, antecedent rivers maintain their course more or less unaffected in spite of active tectonics. However, deep gorges and canyons may develop. Some Himalayan rivers like Indus, Brahmaputra, Sutlej, Kosi and Subansiri are of antecedent type, which have originated from Tibetan Plateau on the northern side of the Himalaya and flows to south through deep gorges. Local base level fall of a river channel may also result incision by increasing the channel gradient. Therefore, base level related causes should be eliminated before correlating channel incision with tectonic deformations.

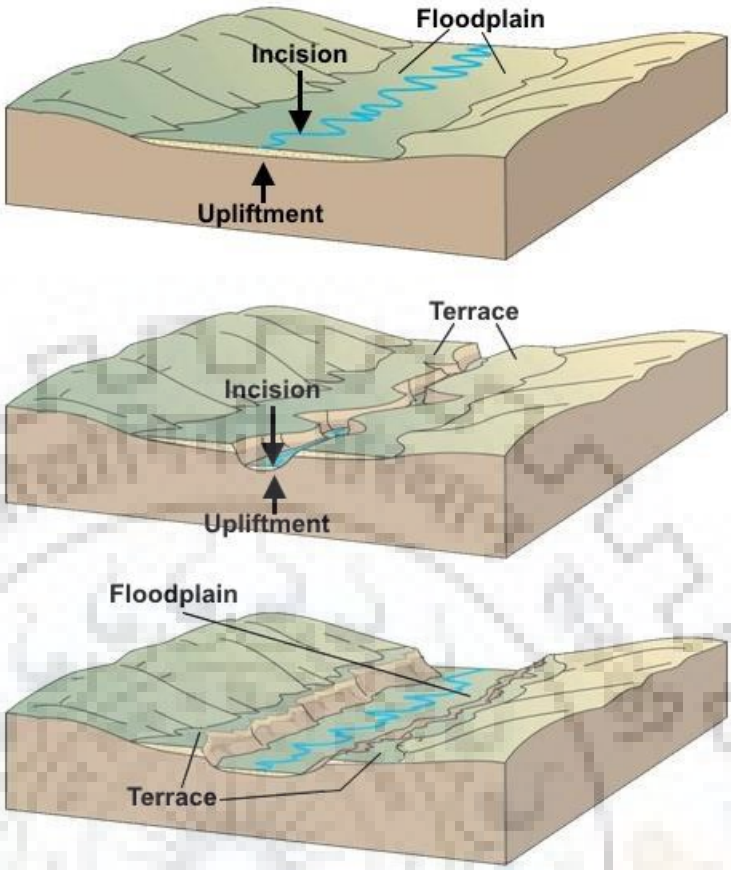

Figure 4.6: Schematic representation of terrace development triggered by tectonic uplift and river incision. Upliftment of a river valley makes the river incise into its own valley abandoning its existing floodplain. The older floodplain remains as river terraces (Borgohain, 2018).

In case of alluvial rivers, it is difficult to identify the small changes in river valley brought about by tectonics. However, valley-floor deformation can be indicated by depth of bedrock. The thickness of alluvial cover will be more over subsided/down-faulted zones and uplifted regions will have thinner alluvial cover (Kowalski and Radzikowska, 1968). Progressive changes of thalweg or water surface elevation can provide information on vertical changes of a channel. When the water surface and river bottom rise through time, either very rapid uplift or a decrease of channel capacity by aggradation can be the cause (Volkov et al., 1967). Correlation of longitudinal profile with adjacent valley shoulder profile can also reflect the influence of active tectonics (Sharma et al., 2011).

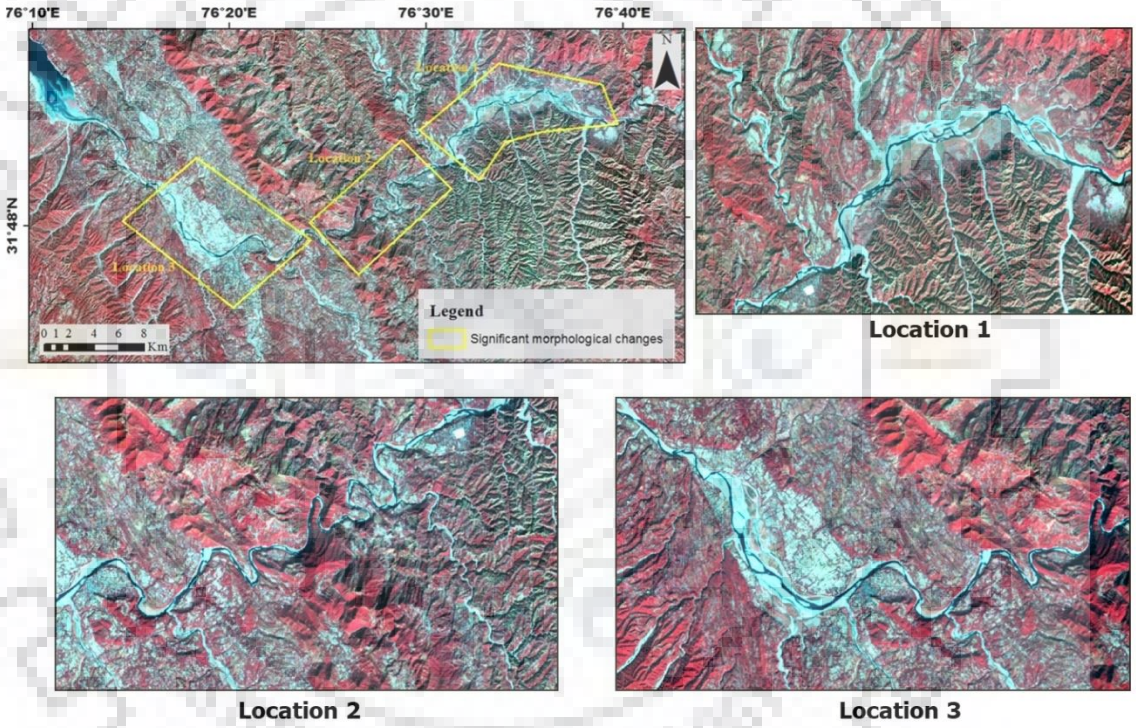

Figure 4.7. It is clearly visible that the river becomes braided within the Kangra valley after entering Jaisingpur (L1). There is increase in the sinuosity of the Beas river after crossing Sujanpur Tira (L2). River takes north-westward turn after crossing HFT near Nadaun (L3).

Deflection: Deflection of a river channel is one of the most readily observable effects of deformation. Rivers tend to deflect by surficial warping (Zernitz, 1932; Howard, 1967; Goodrich, 1898; Holbrook and Schumm, 1999). Deflection of the river around an uplift or into a zone of subsidence will be manifest as an abrupt shift in the river course coincident with the deformed zone. Streams naturally tend to gravitate toward the subsided zone, if the zone is proximal to the river and there are no topographic barriers between the river and the subsided region. Upliftment/subsidence affects the longitudinal profile and the river will either traverse the zone of deformation or will deflect (Holbrook and Schumm, 1999). Deflection is manifested as abrupt shift in the river course or change in the direction of river course (figure 4.7) L1, L2, and L3. Low gradient rivers are extremely sensitive to active tectonics. A slight deformation can change the course of a major river. For example, coseismic subsidence of Nazira region in Upper Assam resulted course change of the Dikhow river (Borgohain et al., 2017). It is also to be noted that sharp deflection of river channel might not necessarily be the result of tectonics. Lithology, fracture, joints, fault-planes etc. can also control a river channel.

Changes in sinuosity and braiding: Sinuosity and braiding are the most sensitive parameters of alluvial rivers. Any deformation activity that influences the slope of an alluvial river valley would bring changes to the sinuosity and/or braiding of the river. A river that is being steepened by a downstream tilt will increase its sinuosity to maintain a constant gradient, whereas reduction of valley slope will lead to a reduction of sinuosity (Adams, 1980; Russ,1982; Ouchi, 1985; Schumm et al., 1994) (figures 4.8 and 4.9). Similarly, a river may exhibit higher sinuosity along the upstream part of a subsided region or tectonic low. On the other hand, sinuosity may decrease along the downstream part of the subsidence due to lowering of valley slope. Opposite phenomena can be noticed over a tectonic up-warping. However, a slight upliftment or subsidence of a part of river channel can change sinuosity/braiding throughout the channel. An experimental study by Ouchi (1985) demonstrated that meandering channel responded to uplift by increasing the thalweg sinuosity where slope was increased. But the reaches where slope was decreased, water flooded over the point bars, thalweg became indistinct and clay deposition took place. Normally, lateral change may be preferred by streams to adjust changes in channel slope. And where lateral change occurs as increase in sinuosity, change in braiding or flooding, there might not be vertical changes, i.e., incision. However, sinuosity change is not only controlled by slope changes, but also by fluctuation in discharge, fluctuation in sediment supply, nature of bank materials etc. Bank erodibility/stability plays important role in changing channel morphology of river. Large

flood events may also bring changes in the morphology of a river channel as such events may supply huge amount of sediment into a river. Rise and/or fall of local base level of a river may also result similar changes in the channel. Because, rising of the local base level leads to a reduction in gradient of the channel and vice versa. For example, construction of a dam results in reduction of channel slope of upstream channels of the reservoir. Affect can be noticed as decrease in sinuosity of the channel and/or more deposition of fine grain sediments (figure 4.10). Therefore, these non-deformational causes should be eliminated first to correlate sinuosity changes of a river channel with active tectonics. While, braided channel responds to upliftment as incision and terrace formation in the uplifted area, deposition may take place in the upstream part of the uplifted region and aggradation may occur in the downstream part from uplift. Which may result multiple thalweg channel and mid channel bars in the upstream part and strong braiding in the downstream part of uplift (figure 4.11). However, these phenomena can be noticed over a region where the alluvial channel crosses an inselberg or isolated hard rock. On the other hand, subsidence will lead to aggradation in the subsided area, degradation in the upstream part of subsidence which supplied sediments to the subsided zone.

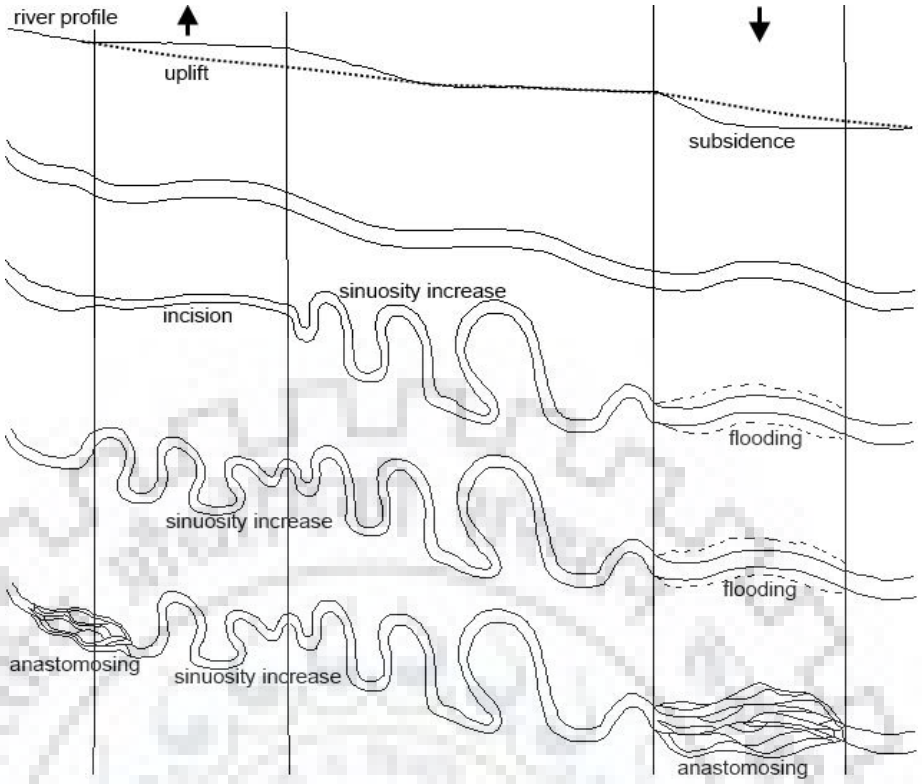

Figure 4.8. Generalized response of a straight channel to tectonic uplift and subsidence (Holbrook and Schumm, 1999). Incision may occur or sinuosity may increase along the uplifted region. On the other hand, flooding or anastomosing channel pattern may develop along the subsided region.

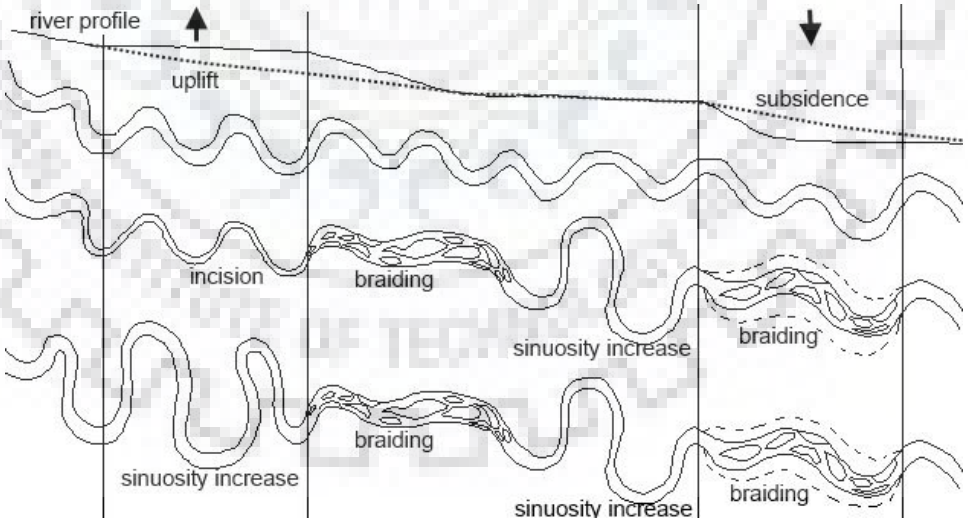

Figure 4.9. Generalized response of a meandering channel to tectonic uplift and subsidence (Holbrook and Schumm, 1999). Meandering channel responds to uplift by incision or by increasing the thalweg sinuosity where slope was increased. Whereas, subsidence may result braiding.

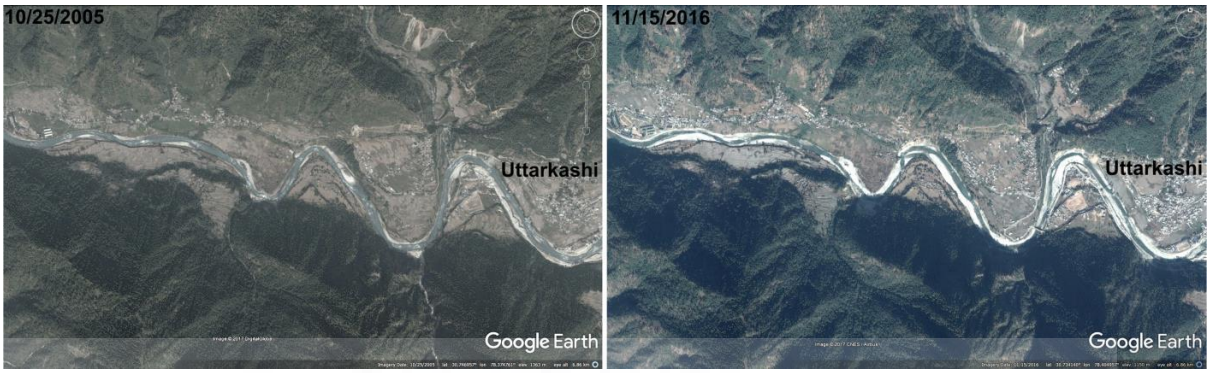

Figure 4.10. Google Earth images over a segment of Bhagirathi River showing increase in deposition along upstream part of the channel after construction of Tehri dam. The Tehri dam, present day local base level of Bhagirathi river have reduced the channel slope of the river. As a result deposition has increased along the upstream part (from the reservoir) of the channel.

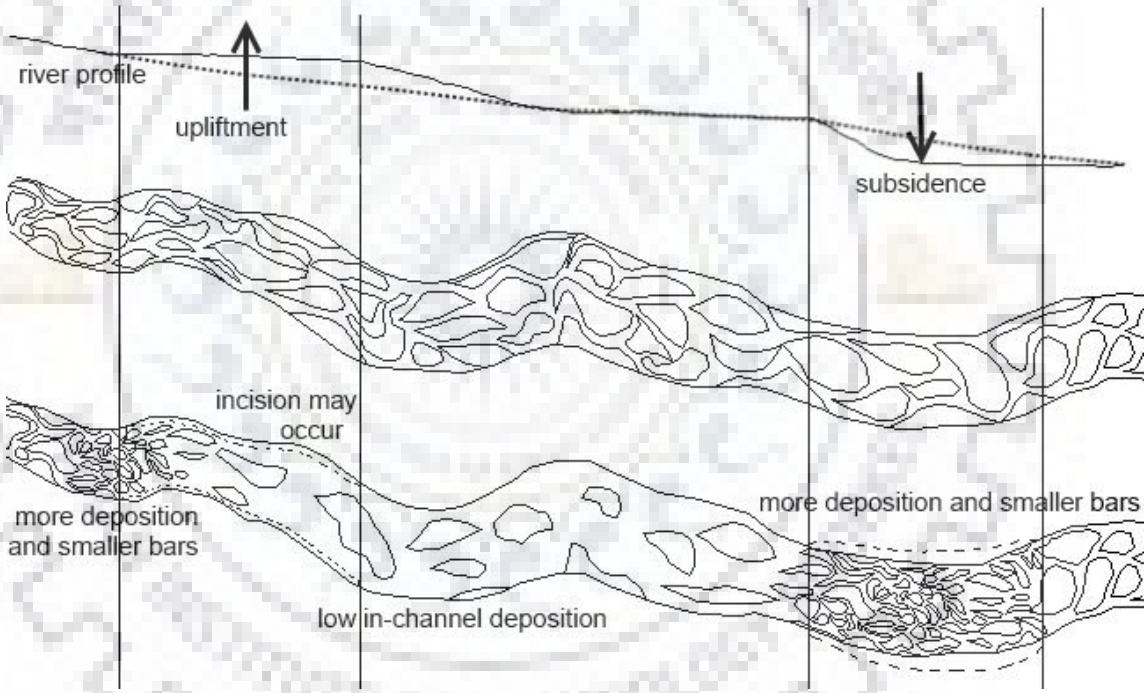

Figure 4.11. Generalized response of a braided channel to tectonic uplift and subsidence (after Holbrook and Schumm, 1999). Braided channel responds to upliftment as incision and terrace formation in the uplifted area. On the other hand, subsidence will lead to aggradation in the subsided area.

Longitudinal profile adjustment: Plot of channel thalweg or water surface elevation against channel length of a river is called the longitudinal profile. The longitudinal profile of a river provides useful information about deformation of the valley. Any deformation affecting the ground surface also affects a river crossing the site. For example, a large scale fault across a river can develop a waterfall, up-warping may result convexity of stream thalweg (figure 4.12), and concavity of thalweg may be the result of subsidence.

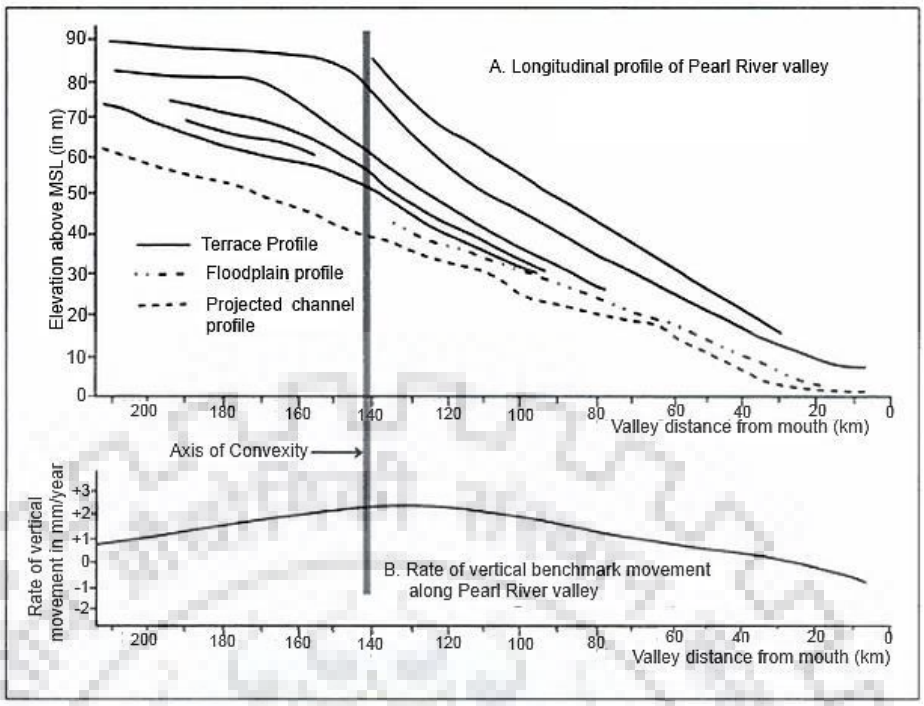

Figure 4.12. Longitudinal profile of Pearl River valley (A) compared to rate of vertical benchmark movement (B) (from Holbrook and Schumm, 1999).

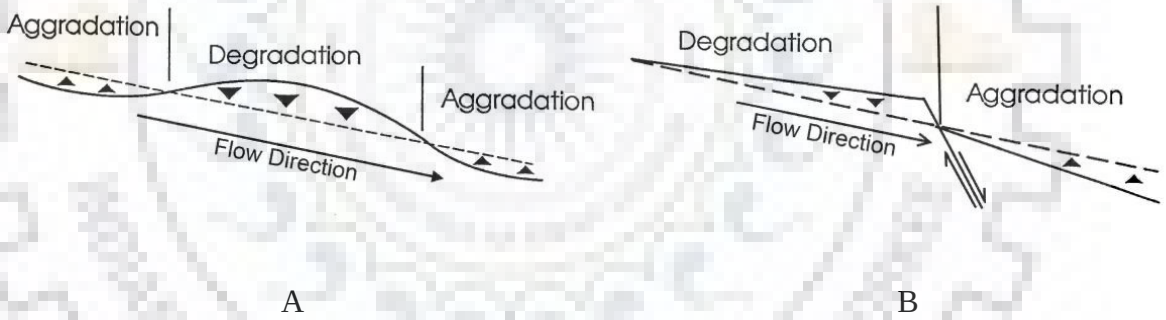

Figure 4.13. Aggradational and degradational response of a river crossing a dome (A) and a fault (B) (after Holbrook and Schumm, 1999).

Projected channel profile (plot of channel thalweg elevation against valley distance) also reveals deformation of the valley profile. The projected channel profile for Pearl river valley (figure 4.12) shows negligible convexity relative to average regional gradient. Aggradation and/or degradation are means of restoring a projected channel profile to a consistent grade after profile deformation (Maizels, 1979; Burnett, 1982). In ideal condition, a river restores a steady grade by aggradation over upstream and downstream part of an uplifted zone, and degradation over the uplifted zone (figure 4.13 A). While a river entering a subsided zone over steepened slope, aggradation occurs over the subsided region and degradation over the steepened slope (figure 4.13 B).

It is also important to notice that discharge fluctuation and sediment load may cause aggradation/degradation in a stream (Love, 1960). Which may manifest as abrupt change in channel size, geometry, morphology, and/or fill over the aggraded and degraded reach that are not explained by local gradient change. So, caution is necessary while using aggradation and degradation as indicators of tectonic deformation of channel profile. Knick point migration is another important aspect of profile adjustment to tectonics. A knick point may migrate up along a longitudinal profile in response to stream grade adjustment after local base level lowering. This can be triggered not only by tectonics, but also climatic change, sea level fall, river capture etc. Hence, a knick point may not coincide directly with site of deformation.

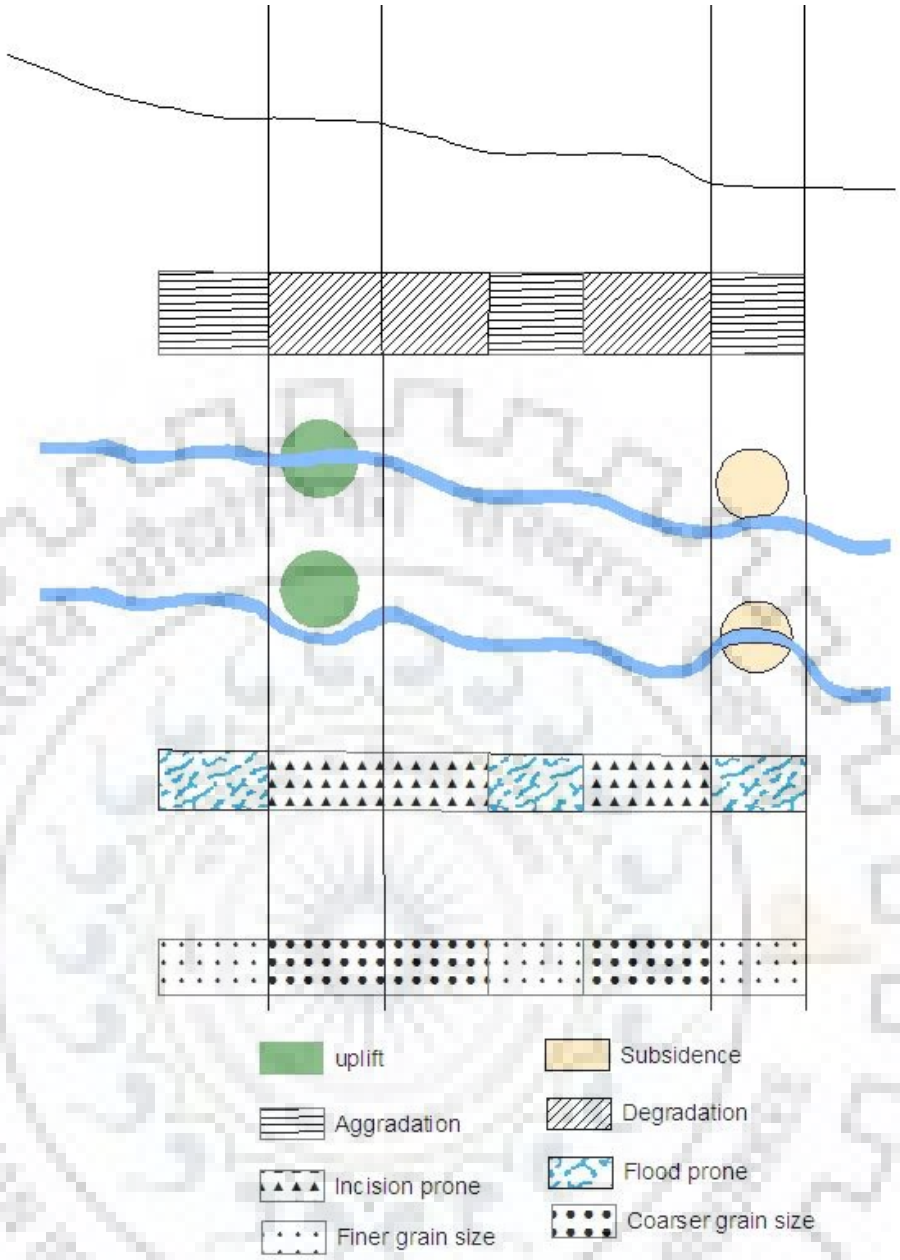

Figure 4.14. Generalized channel response to tectonic uplift and subsidence (after Holbrook and Schumm, 1999).

Grain size of sediments: Valley floor tilting leads to stream power variation which in turn affects the sediment carrying capacity of a river. Tectonically increased slope will be characterized by increased bedload grain size, and vice versa (Ouchi, 1985; Jorgensen, 1990; Holbrook and Schumm, 1999) (figure 4.14). However, it is not suggested to use grain size variation in determining tectonic tilting of a river valley. Grain size is not only controlled by stream power but also by availability and sediment source. Local increase in slope may also increase stream power and increase in grain size. A river crossing a resistant rock unit, bridge

or culvert may also show the same phenomena. So, extreme care should be taken while using grain size variation as indicator of active tectonics.

Width-depth ratio and channel capacity: Stream cross-sectional shape is always influenced by stream power. A river crossing a zone of uplift or subsidence, experiences changes in slope. Decreased slope result in decreased stream power, lower channel capacity, higher flood frequency and higher width/depth ratio. On the other hand, increased gradient leads to increase in stream power, increase in channel capacity, incision and lesser flood frequency (Burnett, 1982; Ouchi, 1985; Jorgensen, 1990). Width/depth ratio is more effective as indicator of modern deformation events than palaeo-deformation events. However, anomalies in width/depth ratio and channel capacity are not necessarily the result of tectonic deformation. They are highly dependent on discharge and sediment load and/or type too.

4. 9. 3. Lateral tilting affects:

Lateral tilting of a river valley makes a river to migrate laterally (figure 4.15). Abrupt avulsion of a stream towards down-tilt zone of the floodplain and combing, these two types of lateral channel migration can be seen (Todd and Went, 1991). Normally avulsion tends to produce isolated sand ribbons and immature channel belt, whereas combing results in wide channel belt (Alexander and Leeder, 1987). If a river combs, deformation must have generated sufficient gradient to cause preferential lateral tilting, but not enough for immediate avulsion.

Avulsion: Lateral tilting forces a river to avulse towards the down-tilt side of the floodplain. It is a common phenomenon associated with alluvial rivers (Bridge and Leeder, 1979). Evidence of avulsion towards down-tilted area is the asymmetric position of the channel in its valley, progressive unidirectional abandonment of channels in the down-tilt direction as evidenced by underfit streams on the up-tilted side. Lateral tilting of alluvial river causes channel belts to be clustered on the down-tilt side of the basin and reduces the effective floodplain width, but does not affect cross-section-averaged values of channel-belt deposition. Mack and James (1993) suggested that, compared to symmetrical basins, asymmetrical tilted basins have the following characteristics:

(a) Relatively narrower effective floodplain, here effective refers to areas of floodplain prone to channel occupation,
(b) A higher percentage of multistory channel sandstone bodies,

(c) A higher ratio of channel to floodplain deposits near the basin axis,

(d) Fewer paleosols and paleosols with a generally lower degree of maturity near the basin axis, and

(e) A lower proportion of sets of planar cross-beds.

Combing: When tilt rate is not very excessive, river may comb laterally in the down-tilt direction. Evidence of combing of modern stream exist as asymmetric mosaics of recently formed meander loops which are dominantly concave to the axis of maximum subsidence (Mike, 1975), as evidenced by oxbows and large meander scrolls (Fisk, 1944).

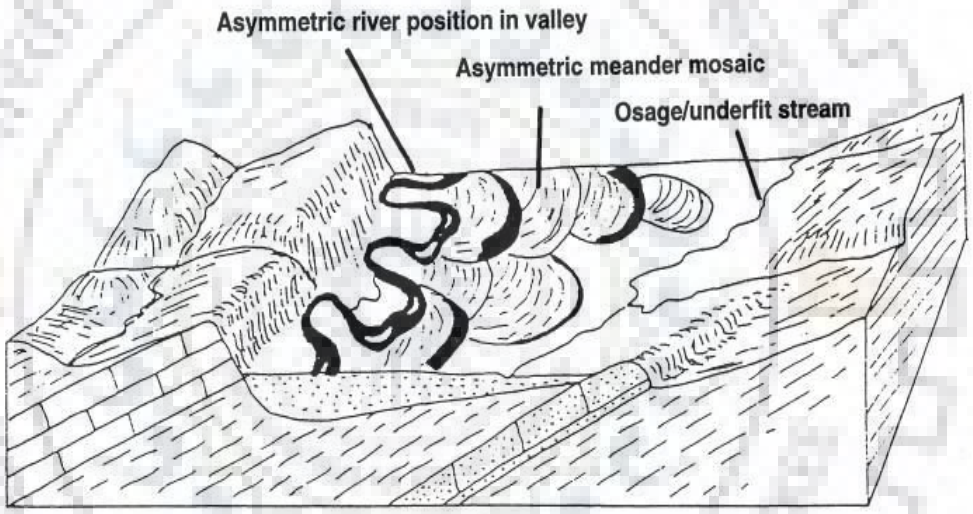

Figure 4.15. Lateral migration by unidirectional avulsion caused by lateral tilting of river valley (from Holbrook and Schumm, 1999).

Different types of rivers show different response to active tectonics. Simply a decrease in slope leads to lowering of stream power and increase leads to increase of the stream power. Aggradation/degradation, channel pattern adjustment, bed-load grain size variation, variation in width/depth ration, all this occur in association as response of a river to active tectonics. Where a river is improperly oriented to adjust to tectonic uplift/subsidence, it may tend to deflect. But it is also important that such effects may be generated by non-tectonic mechanisms too. Influence of such non-tectonic causes should be eliminated first to study the effects of active tectonics. Tectonic interpretations can be strengthened by studying their relationship with historically active structures. The tectonic effects discussed above should be viewed as a

collection of indicators. Like all other indicators, they also have caveats and alternative explanations. They have to be addressed before relating them with tectonic uplift or subsidence.

4. 10. Geomorphic constraints on the active tectonics:

In the last decades, the urge towards the development of quantitative geomorphology has shown the way from improved statistical and mathematical models to define different geomorphic processes (Scheidegger, 1961; Evans, 1972; Anhert, 1973; Mark, 1975). A varied range of work has outlined the utility of quantitative geomorphic estimations in interpreting morpho-evolutionary processes in the tectonically active regions (Avena *et al*., 1967; Buonasorte *et al*., 1991; Pike, 1993; Lupia Palmeiri *et al*., 1995, 1998, 2001; Centamore *et al*., 1996; Jasrotia *et al*., 2012; Maiti, 2013). Quantitative methodologies have shown their utility in detecting neotectonic effect on geomorphic processes through the application of statistical parameters (Keller *et al*., 1982; Ciccacci *et al*., 1986; Mayer, 1990; Cox, 1994; Merritts *et al*., 1994; Belisario *et al*., 1999; Currado and Fredi, 2000).

Study of interior tectonic forces that shape the topography of the earth surface is very difficult. Hence, most researchers have used digital topography to search for the symptom of active deformation preserved in the local geomorphology. The active tectonics and landscape evolution of the southern Taiwan on the basis of drainage anomalies and deviation of major river systems have been studied by Ramsay *et al*. (2007). Active normal faults evolution in Greece is revealed by geomorphology and drainage pattern (Goldsworthy and Jackson, 2000). Walker and Jackson (2002) have identified 3 km horizontal fault offset of Gawk fault, a major intra-continental strike slip system in SE Iran from well preserved geomorphology.

Chapter 5

Results and Discussion

5. 1. Kangra Re-entrant:

The Kangra Re-entrant is the largest recesses within major Himalayan thrust zones. The MBT curves towards the north-eastern direction from its general trend in this region. Figure 5.1 shows the shaded relief model of Kangra re-entrant. The Beas River flows across this re-entrant. Significant evidences of active tectonics within the Kangra re-entrant are discussed below.

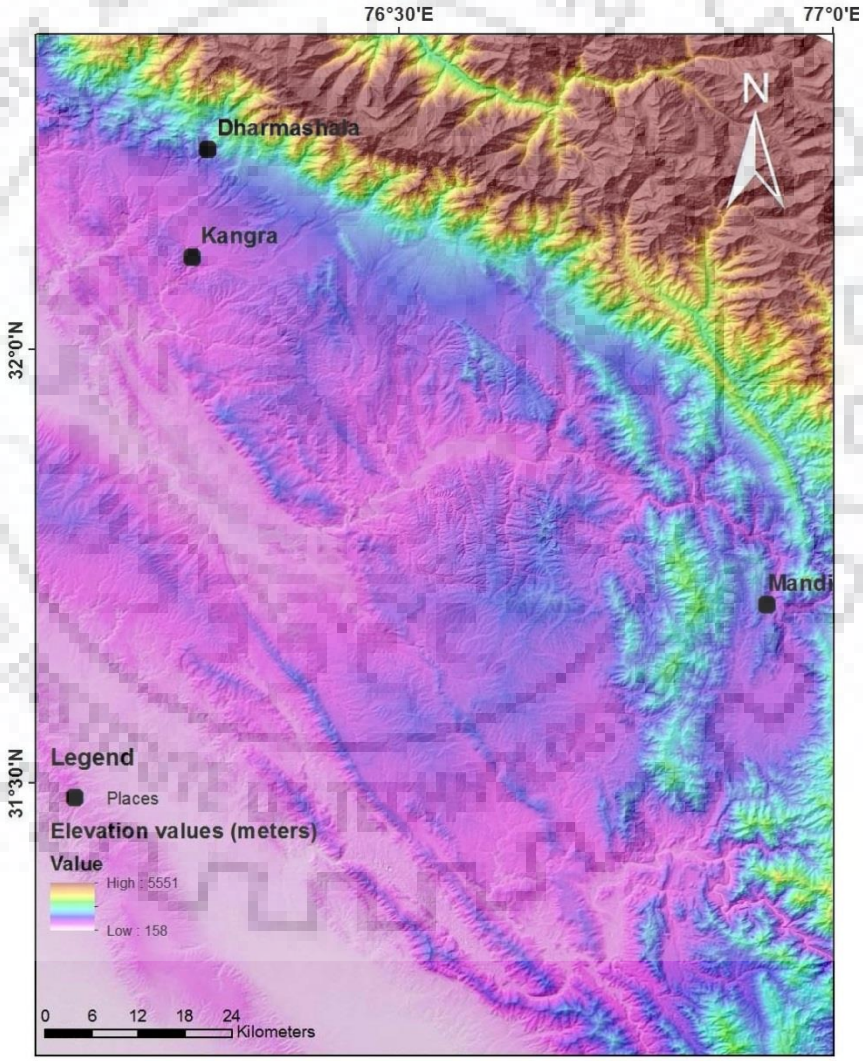

Figure 5.1. Shaded relief model of Kangra re-entrant showing NW trending ridges. Middle part of this Kangra re-entrant shows some parallel streams that is because of gentle slope towards NW direction.

5. 1. 1. Longitudinal Profile and Knick points:

Rivers are linear systems which show a gradient of characters along their length. Ideally the longitudinal profile of a river is concave with a steep upper portion near the source, giving way to reaches of progressively less gradient as the mouth is approached. A river always erodes away anything that reduces its efficiency.

Knick point is any break and slope in the river or stream. For example rapids or water falls figure (5.2). In the case of some rivers the breaks and slope that are probably not noticeable but they can be water fall, they can be held up by bedrocks and the thing about knick point is that the river does not like it and so it tries to erode it and usually erode by a plunge pool forming at the base and the under cutting it. Usually knick point is passing that is the most active part of the channel.

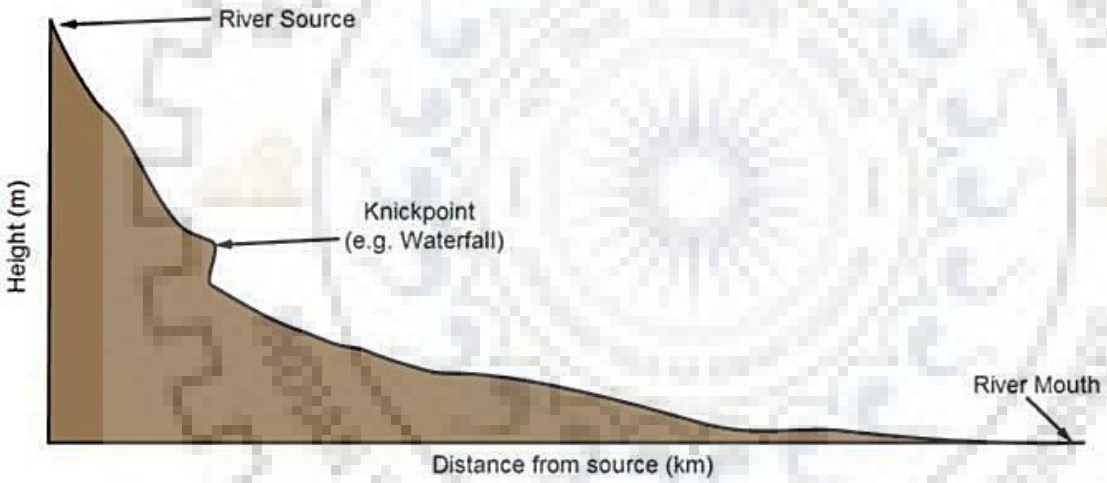

Figure 5.2. A typical longitudinal profile and Knick point of a river or stream in a tectonically active region. Most commonly knick points are associated with faults which results sudden drop in elevation of the river bed. However, sudden change in lithology across the river channel can also create knick points. Source: (Jackson A, 2014).

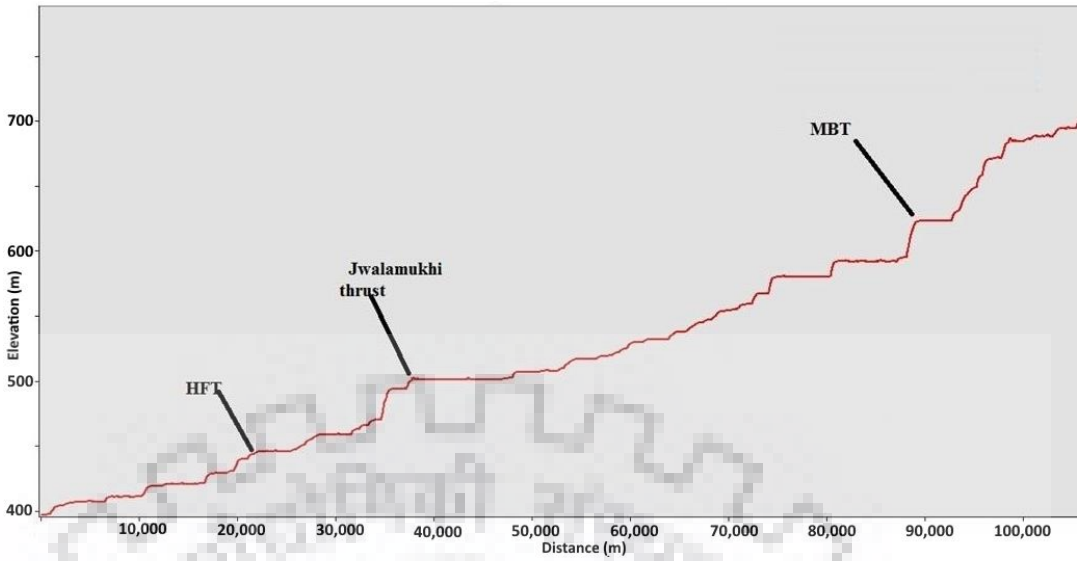

Figure 5.3. The longitudinal profile of the Beas River clearly reveals the effect of HFT, Jwalamukhi thrust and MBT. Among these, Jwalamukhi thrust and MBT are very prominent. On the other hand, the HFT is buried by alluvium and is not very prominent in the longitudinal profile of the river. These sharp mountain fronts indicate active tectonics in the area.

Longitudinal profiles of the major rivers within the study area are shown in figures 5.3 - 5.6. All the profiles have been extracted from ASTER Global DEM of the study area. At first stream lines were delineated using surface hydrologic modelling of the study area and those streams were used to draw longitudinal profiles of Beas, Sutlej, Yamuna and Ganga rivers. All these rivers within the study area show typical characters in their longitudinal profiles. The longitudinal profile of Beas River exhibits two prominent knick points. In both the knick points the elevation of the riverbed drops more than 50m within a distance of 50m of the river course (figure 5.3). Correlation of the locations of knick points with tectonic map of the study area revealed that those knick points coincide with MBT and Jwalamukhi thrusts (figure 5.7). Another minor knick point of Beas river channel can be noticed over the HFT. However, not very significant elevation drop of the river bed can be noticed in that region, as the HFT is buried under recent sediments within the study area.

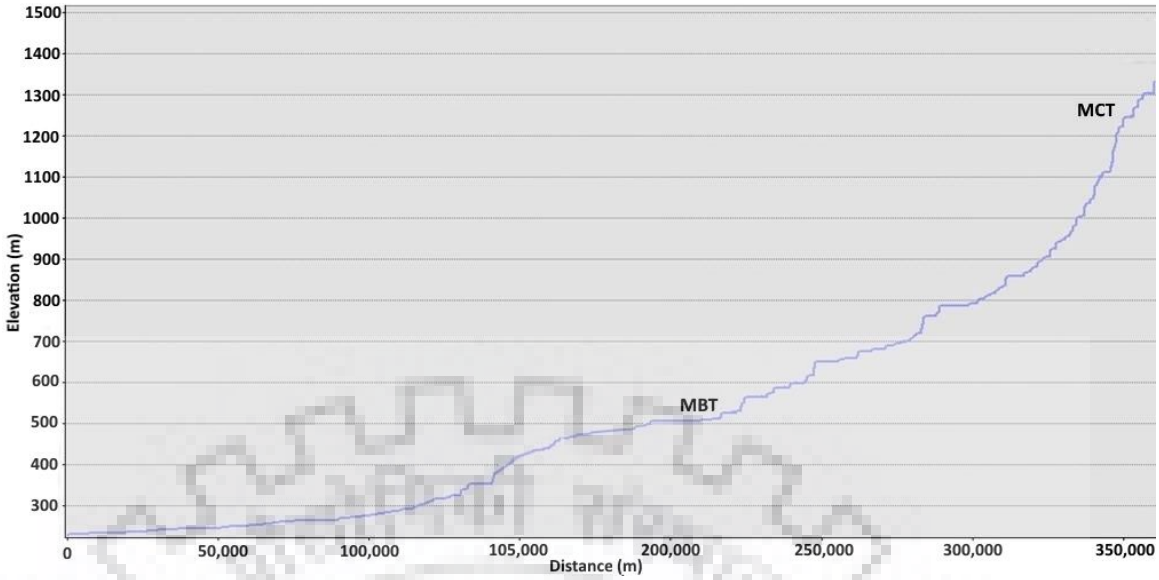

Figure 5.4. The longitudinal profile of the Sutlej River and its knick points. The elevation of the river bed drops suddenly from 1280m to 1200m, when the river crosses the MCT. Similarly elevation of the river bed drops from 530m to 500m when the river crosses MBT region. Both knick points are prominently visible in the longitudinal profile of the river.

Similarly the longitudinal profile of Sutlej River also shows two major knick points within the study area. In this case the elevation of the river bed of Sutlej River drops more than 150m within a distance of 30m of the river course (figure 5.4). Correlation of those knick points with tectonic map of the region shows that they overlap with the MCT and MBT. On the other hand, the Yamuna River does not exhibit major knick points over the major thrust zones (HFT, MBT) of Himalaya (figure 5.5). Only minor elevation drop of the river bed can be noticed as the Yamuna channel crosses major thrust zones of Himalaya. Similar characteristics of the Ganga River are also evident from its longitudinal profile (figure 5.6). Significant elevation drop of the river bed can be noticed as the river crosses the MBT and HFT.

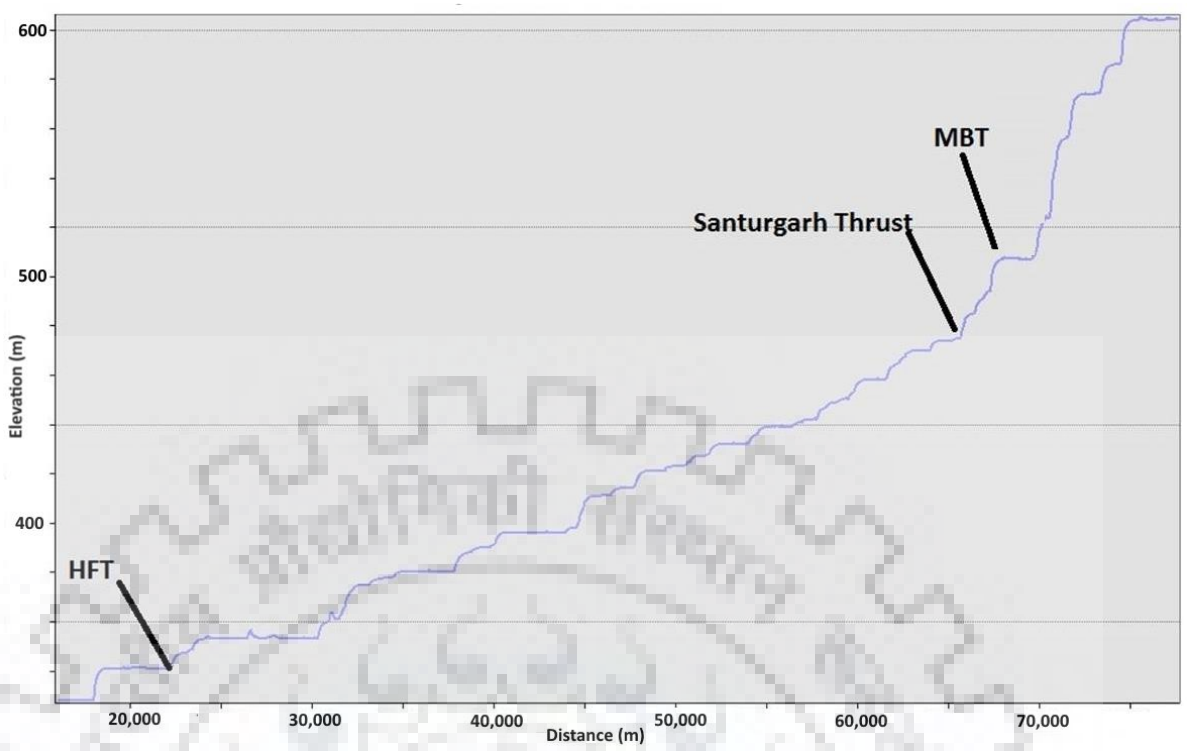

Figure 5.5. The longitudinal profile of the Yamuna River clearly shows the HFT, Santurgarh Thrust and MBT.

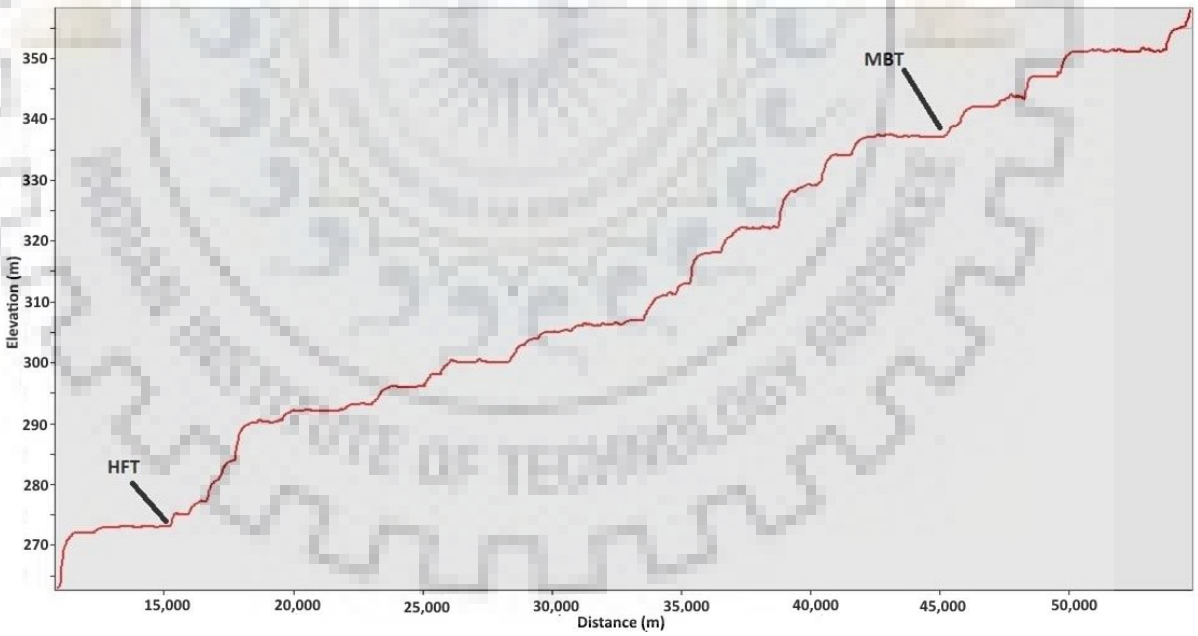

Figure 5.6. The longitudinal profile of the Ganga River clearly shows the HFT and MBT.

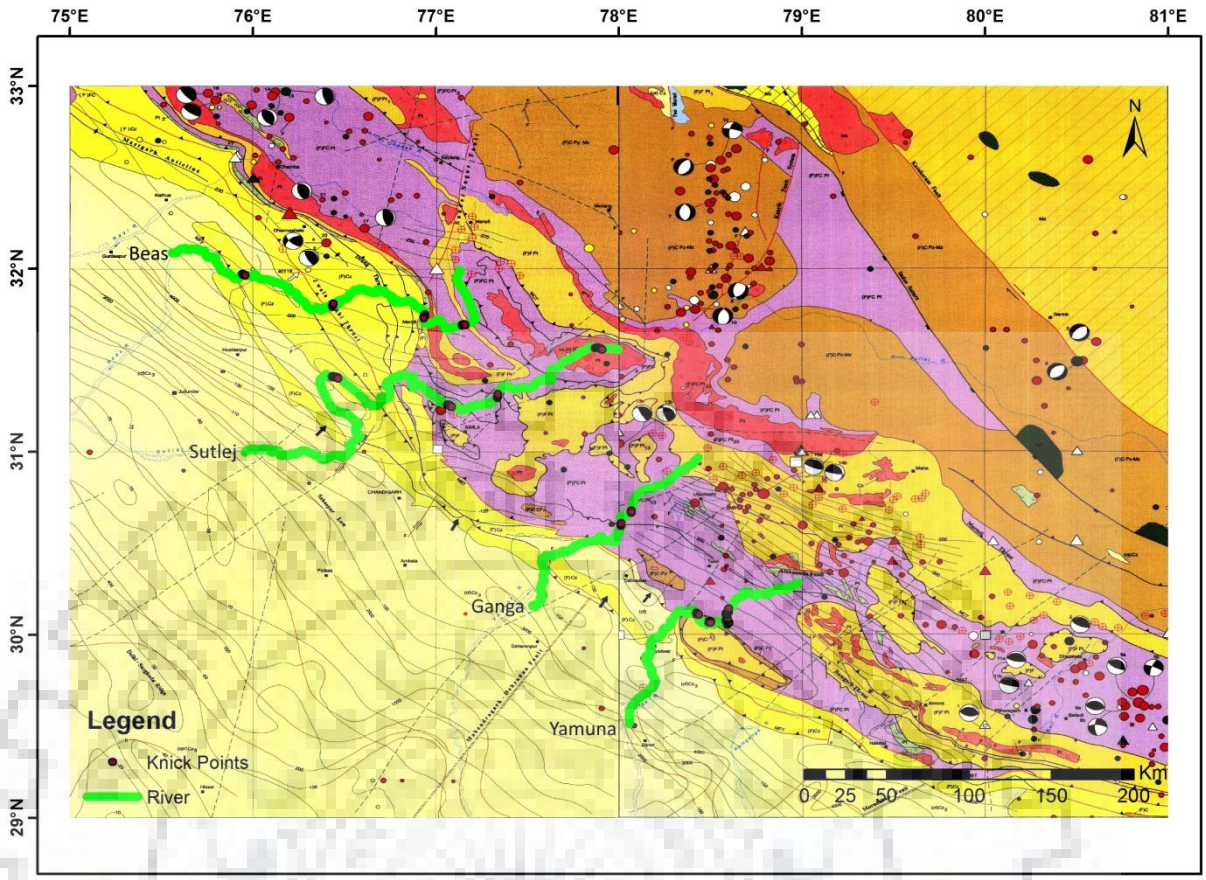

Figure 5.7. Major Rivers along with their knick points (marked by black circle) can be seen in this figure. In the background seismotectonic map is shown (Dasgupta et al, 2000). All knick points of Beas, Sutlej, Yamuna and Ganga are coinciding with major thrust and fault zones of the region.

5. 1. 2. Hypsometric Analysis:

Several sub-basins have been identified and delineated from the Beas, Sujlej, Yamuna and Ganga river basins for hypsometric analysis (figure 5.8).

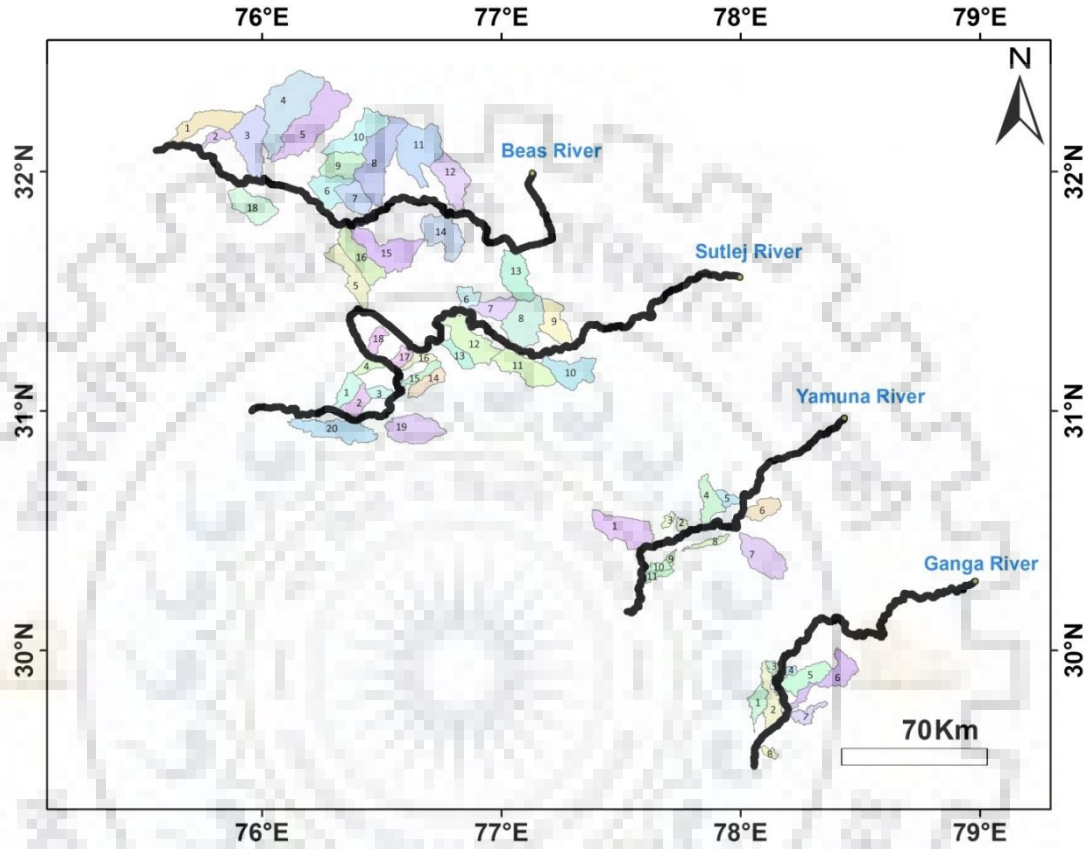

Figure 5.8. Basins of major rivers in the study area derived from ASTER GDEM for hypsometric analysis. 18, 20, 11 and 8 sub basins of Beas, Sutlej, Yamuna and Ganga Rivers respectively have been selected for hypsometric and basin asymmetry analysis. basins 3, 6, 7, 14 and 15 on Beas River, 4, 7, 9, 11 and 13 on Sutlej River, 3, 4, 7, 8 and 9 on Yamuna River shows different results from other sub basins

Hypsometric curves have been obtained for the different sub-basins 3, 6, 7, 14 and 15 on Beas River (figure 5.9); 4, 7, 9, 11 and 13 on Sutlej River (figure 5.10); 3, 4, 7, 8 and 9 on Yamuna River (figure 5.11); 4, 5, 7 and 8 on Ganga River (figure.5.12). In the first instance, the hypsometric curves dominantly show concave and similar shapes. However, in some parts along the curve in the graphs for some basins, distinct convex up tendency is observed. This is observed in case of basins shows anomalous curves with strong convexity. This convexity may be due to tectonic factors, which in turn, validates the presence of major faults/thrusts in these locations which have also been inferred from the satellite images. These faults might have uplifted the footwall where the catchments are located resulting in a continuous base level

lowering in the rivers and thus maintaining high downward erosion rates. Therefore, these convex portions have been suffering continuous rejuvenation process and preserving such convex profiles over time.

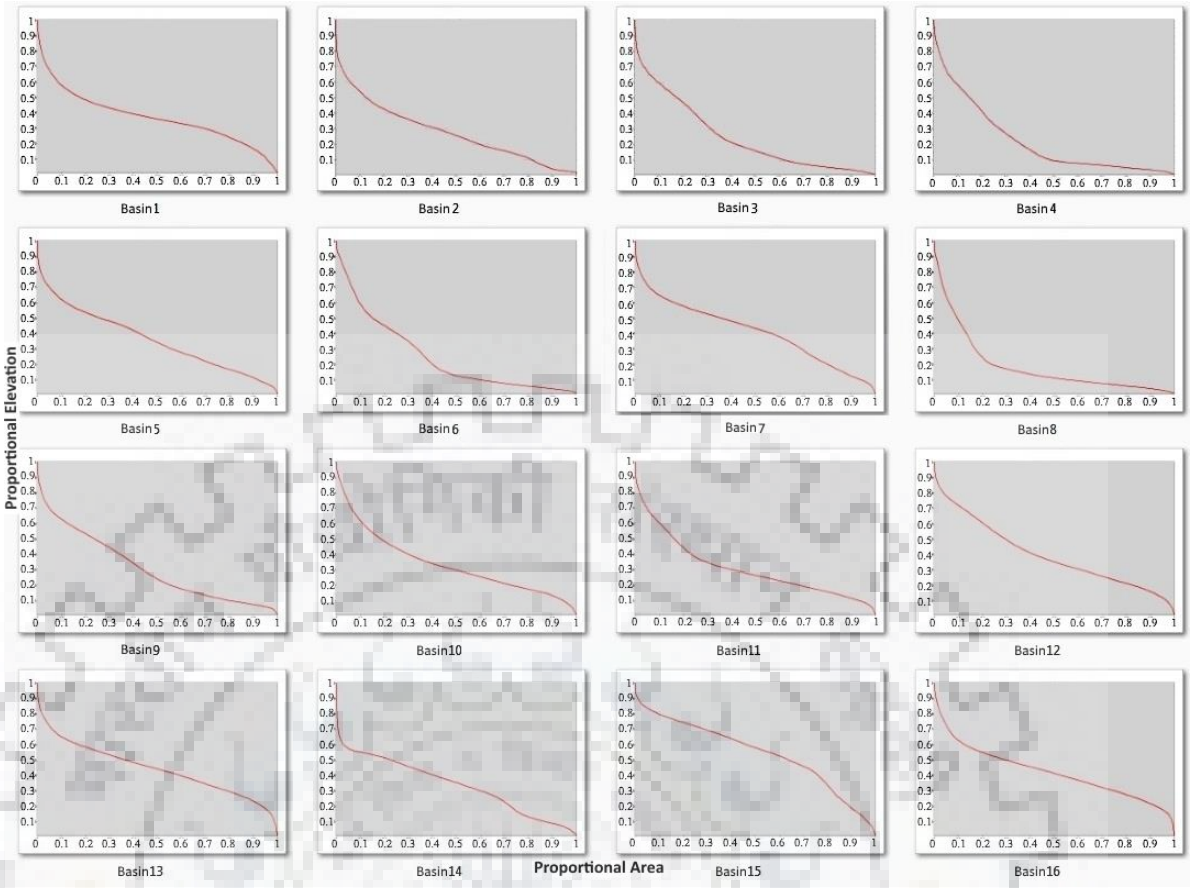

Figure 5.9. Hypsometric analysis of selected sub basins of Beas River indicates that basin 3, 6, 7, 14 and 15 have been subjected to tectonic perturbation. For example, in case of sub basin 6, the overall shape of the hypsometric curve is concave. However, the central part of the curve is partially convex shaped. This suggests that the basin 6 has been subjected to partial tectonic upliftment.

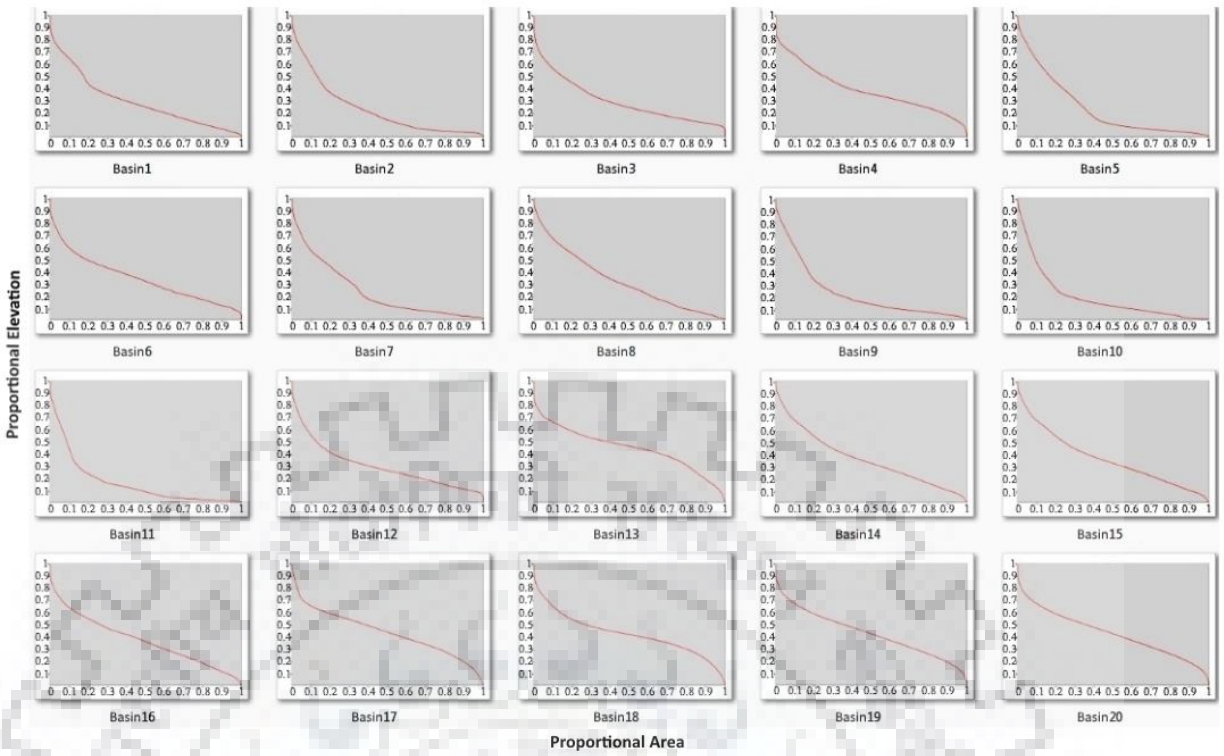

Figure 5.10. Hypsometric curves of Sutlej River indicate neotectonic activity along basin 4, 7, 9, 11 and 13 due to the presence of HFT.

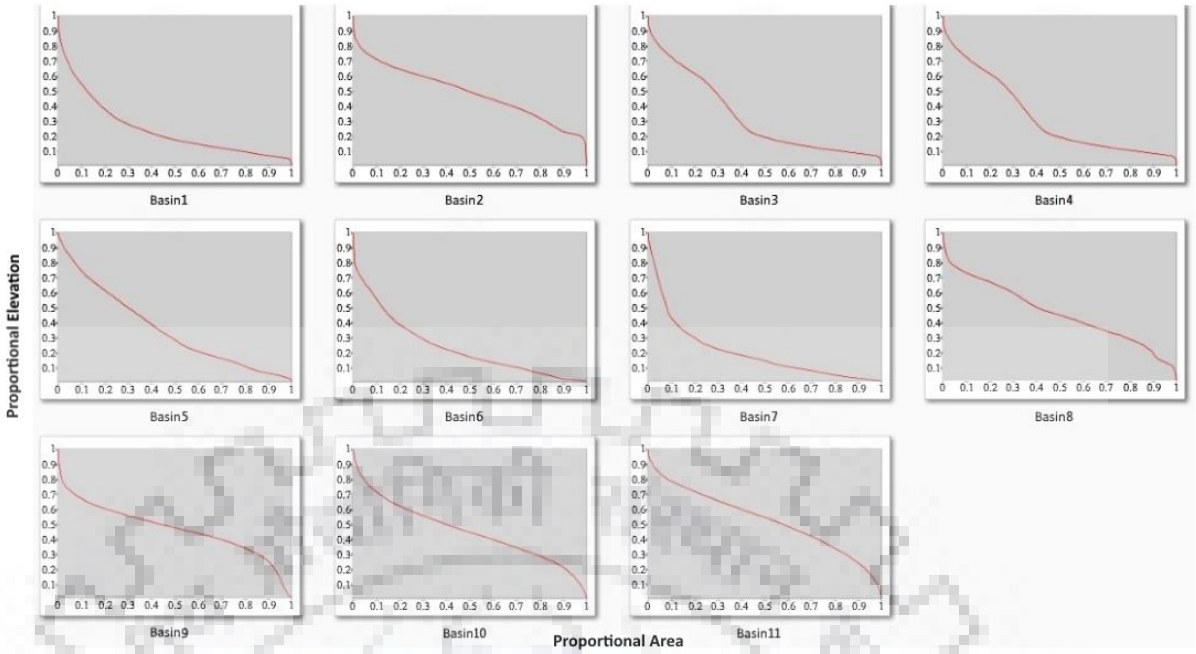

Figure 5.11. Hypsometric analysis of Yamuna River indicates that basin 3, 4, 7, 8 and 9 are subjected to tectonic uplift.

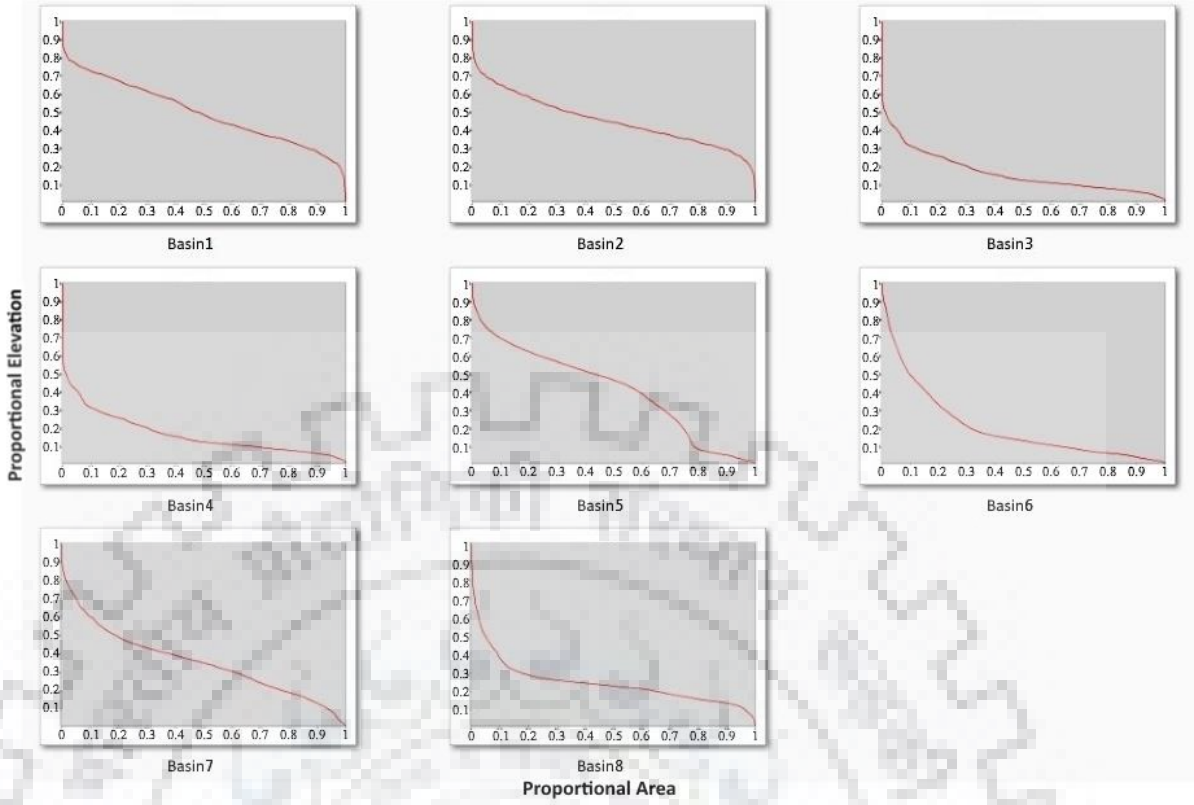

Figure 5.12. Hypsometric analysis of Ganga River indicates that almost all basins are subjected to tectonic uplift, especially 4, 5, 7 and 8.

Interpretation of hypsometric curves of the sub basins reveals that almost all major thrusts and faults within the study area have affected the river systems and their catchments. Hypsometric curves of sub-basins of Beas River 3, 6, 7, 14 and 15 (figure 5.9) exhibit prominent slope break. The overall shape of the hypsometric curves for those basins is concave upward. However, concave downward shape is prominent at the middle part of the curves. This clearly indicates that those basins have undergone tectonic uplift during their developmental phase. Similarly, in case of 4, 7, 9, 11 and 13, sub-basins of Sutlej River (figure 5.10) also exhibit similar characteristics in their hypsometric curves. Such typical hypsometric characteristics are also visible in some sub-basins of Ganga and Yamuna rivers. It should be noted that all those tributary basins of different rivers within the study area are located either over Jwalamukhi thrust zone or MBT thrust zone. This suggest that those catchments have experienced tectonic uplift occurred in Jwalamukhi and/or MBT thrust zones during their developmental phase.

5. 1. 3. Basin Asymmetry:

The AF values calculated for the basins of each location, around the faults/thrust are given in the table 5.1. There is a definite pattern in the AF values of the study area. It is observed from the table that basins no. 3, 14 and 15 of Beas, 9 of Sutlej, 7 and 9 of Yamuna and all basins of Ganga show greater than 50 AF values suggesting tilt direction towards west with respect to the thrust in these locations. In case Sutlej and Yamuna, all the basins show more or less low AF values, hence suggesting tilt towards east in case of Sutlej and west in case of Yamuna. Since in both the locations, the asymmetrical drainages are located, so the difference in their tilting and position with respect to the thrusts can only be explained due to the topography of the area.

Basin asymmetric factors have been calculated for sub basins of Ganga, Yamuna, Sutlej and Beas Rivers. Basin asymmetry values for some basins are highly deviated from 50 (table 5.1). This suggests that those basins have experienced lateral tilting during their developmental phase.

Table 5.1. Basin asymmetry values of selected sub basins of Beas, Sutlej, Yamuna and Ganga Rivers. Basin asymmetry of some sub basins of Beas, Yamuna and Ganga Rivers are showing significant deviations from 50, indicating influence of active tectonics in modification of the drainage system within the study area.

Location	Sub-Basins	Ar (Km Sq)	At (Km Sq)	AF= (Ar/At)*100
Beas	3	254.5	488.9	50.0
	6	56.6	228.8	24.7
	7	92.4	292.0	31.3
	14	144.0	229.0	62.7
	15	83.3	141.8	58.7
Sutlej	4	23.3	51.4	45.3
	7	54.6	125.4	43.5
	9	94.3	164.8	57.2
	11	98.5	228.4	43.1
	13	35.3	76.3	46.2
Yamuna	3	8.1	22.4	36.1
	4	54.6	132.1	41.3
	7	128.9	235.3	54.7
	8	18.3	40.2	45.5
	9	10.6	15.5	68.3
Ganga	4	13.4	19.0	70.5
	5	121.8	164.4	74.6
	7	49.7	64.9	76.5
	8	12.8	22.5	56.8

5. 1. 4. Sinuosity index:

All drainages in the study area, where the faults are inferred, show sinuous channels (sinuosity parameters of drainages from each basin are given in the table 5.2). The average sinuosity values of all the drainages of each location are around 1.2 to 1.5. The lower sinuosity is because of the fact that all rivers follow a straight deeply incised channel (faulted land) for a short distance as they emerge from the highland and flow onto the alluvial plain (Kar, et., al 2016). Owing to such values, it can be said that these drainages are fault modified. This is clear from the satellite images shown earlier as well where the drainages in vicinity of the faults or the drainages crosscutting the faults follow the fault trend near the faults and then resume their path as they emerge out of the fault. Sinuosity of the basins does not any significant value (table 5.2).

Table 5.2: Sinuosity of the selected sub basins of Beas, Sutlej, Yamuna and Ganga Rivers.

Location	Basin	Total Length (Km)	Shortest Path (km)	Sinuosity
Beas	3	29.3	24.4	1.2
	6	14.2	10.1	1.4
	7	14.5	11.1	1.3
	14	21.3	14.2	1.5
	15	26.6	16.6	1.6
Sutlej	4	10.9	9.0	1.2
	7	16.1	11.5	1.4
	9	20.4	18.5	1.4
	11	25.1	16.7	1.5
	13	15.9	12.3	1.2
Yamuna	3	6.9	5.3	1.3
	4	20.4	14.7	1.4
	7	19.4	12.9	1.5
	8	18.1	15.0	1.2
	9	9.2	7.0	1.3
Ganga	4	4.6	3.5	1.3
	5	18.4	15.3	1.2
	7	13.1	10.9	1.2
	8	5.9	5.3	1.1

5. 1. 5. River channel dynamics and topography:

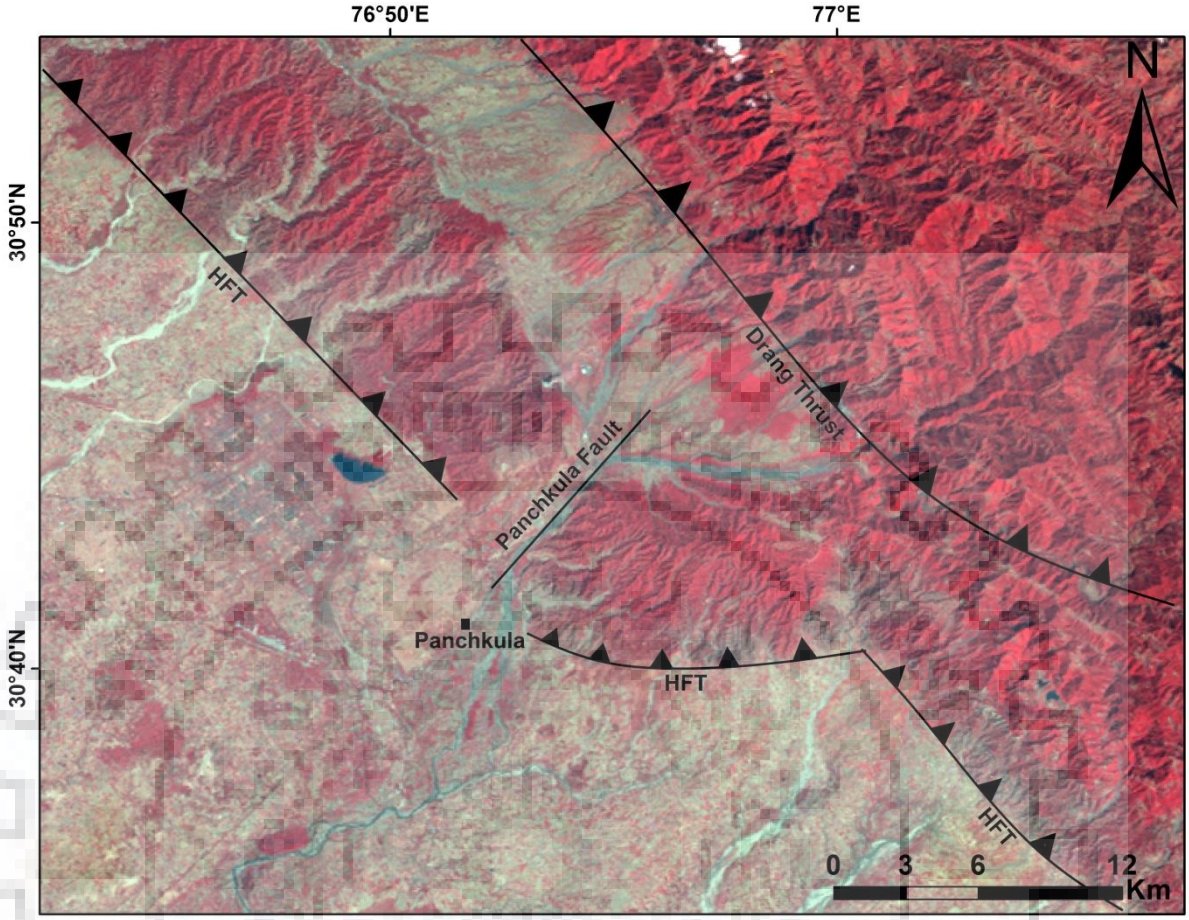

Figure 5.13: Image interpretations of FCC image shows that Panchkula fault has dissected the Chandigarh ridge. The Ghaggar River has flowed along the Panchkula fault. Major Thrust HFT and Drang Thrust can also be seen in the figure.

The Panchkula fault is a major structural feature within the Chandigarh ridge and Nahan Salient. The fault traverses across the Chandigarh ridge (figure 5.13). The Ghaggar River has occupied the Panchkula fault plane to cross the Chandigarh ridge. Some tributaries of the Ghaggar River show typical deflection towards the Ghaggar channel at this location.

Beas and Sutlej rivers flowing across the Kangra re-entrant have shown significant channel dynamics over the Himalayan foothills within the last few decades (figure 5.14). The thalweg of the Beas channel has migrated about 10km towards the mountain front within the period of 1975-2015. This might be controlled by active tectonics along the HFT within the region. On the other hand, the Sutlej channel has migrated about 15 km southward within the same period.

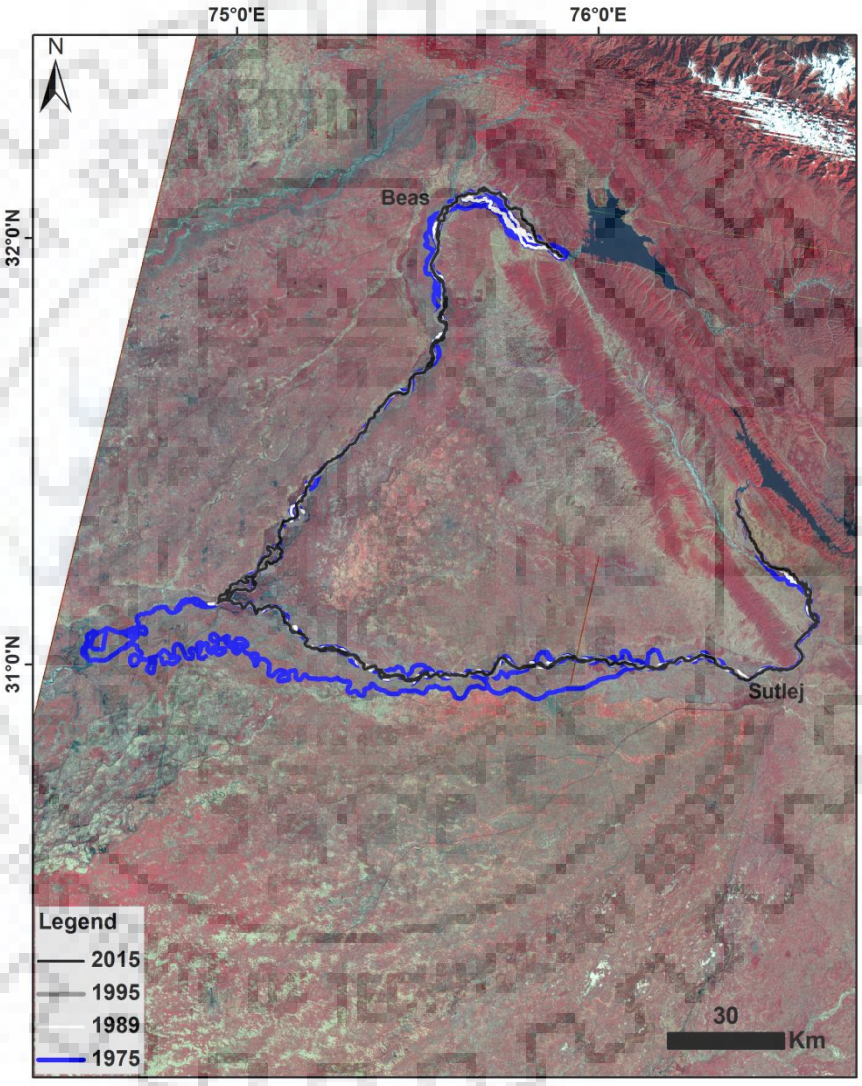

Figure 5.14. Channel dynamics of Beas and Sutlej Rivers with in the period of 1975-2015 including 1989 and 1995 years. The Beas channel has migrated about 5 km towards the foothills region during the last 40 years. On the other hand the Sutlej River has migrated about 13 km southward near its confluence point with Beas River.

Topographic sections delineated from different DEMs of Kangra re-entrant reveals typical topography of the region (figure 5.15). ASTER GDEM, SRTM DEM and ALOS PALSAR DEM have been used to delineate topographic sections of the region. Among all, the ALOS PALSAR DEM gives more details of topography of the region. However, ASTER-GDEM is good for highly rugged terrain (figure 5.16).

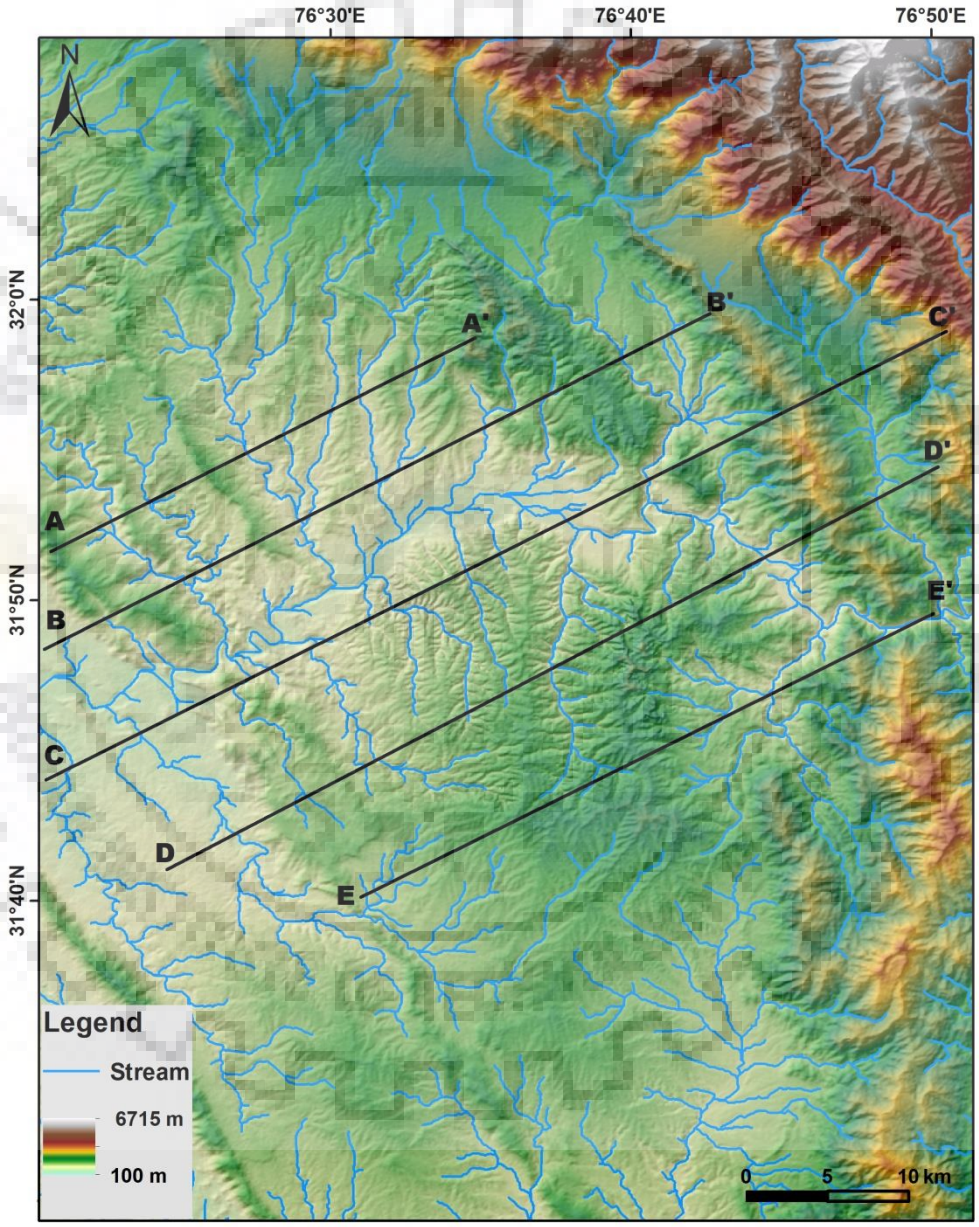

Figure 5.15: Topographic sections over Kangra Re-entrant. With the help of topographic profiles it has been analysed that Beas River is showing high density pattern in the middle of the area and because of gentle slope some streams in the western sides are in parallel.

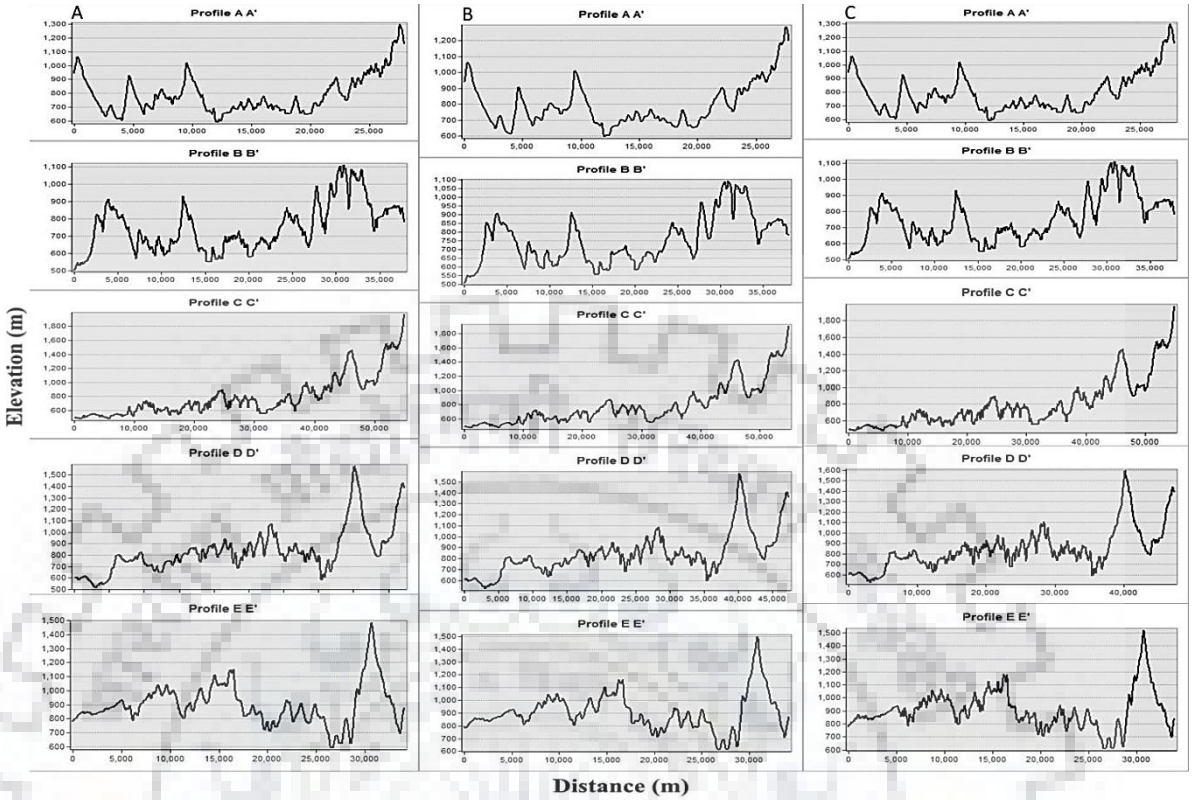

Figure 5.16: Showing all 3 DEM's topographic sections profile. A is from Aster GDEM, B is from SRTM and last C is from ALOS - PALSAR. Out of all DEM, ALOS - PALSAR profiles giving so much detail. This is because of better resolution compare to others.

5. 2. Dehradun Re-entrant:

The Dehradun re-entrant is one of the major re-entrant of the Himalayan thrust zones (figure 5.17). The Mohand anticline, Ganga tear fault and Yamuna tear fault are major structural features within the region. The Dehradun valley, alluvial filled basin lies between the Mohand anticline and MBT. The Ganga and Yamuna River flow along the Ganga tear fault and Yamuna tear fault respectively to cross the Mohand anticline. The Mohand hills of ~800 m elevation belonging to the frontal Siwalik range mark the southern limit of the Dun. This Siwalik range is separated from the adjoining alluvial plain towards its south by HFT, which is locally known as the Mohand thrust. The sudden elevation difference between the Middle Siwaliks and the Holocene sediments of alluvial plain demarcates the HFT in the region which dips moderately by an amount of ~30° due NE direction. Figure 5.18 shows the stream network of Mohand Anticline.

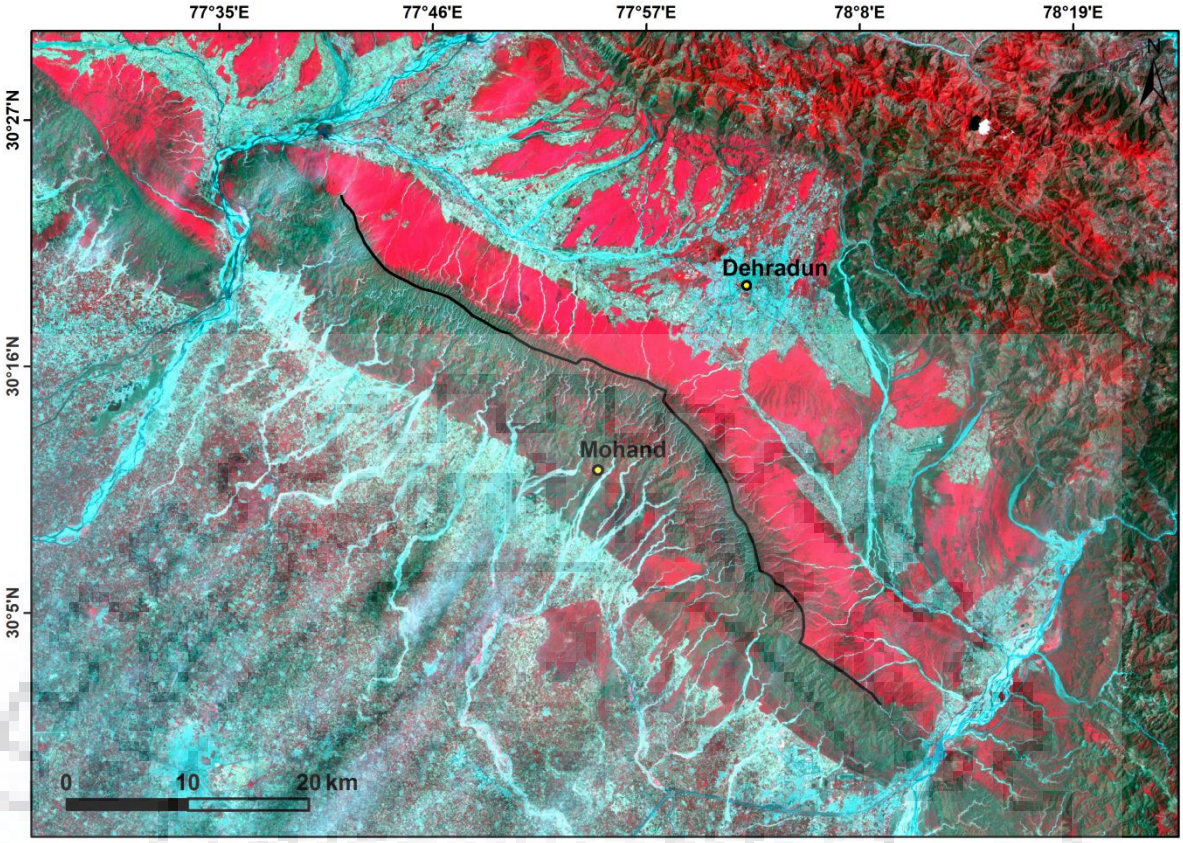

Figure 5.17. FCC of Landsat-8 images showing NW-SE trending Mohand ridge. The Mohand ridge is a folded anticline and comprises of Siwalik group rocks. The anticline extends for about 78 km with maximum width of 14 km.

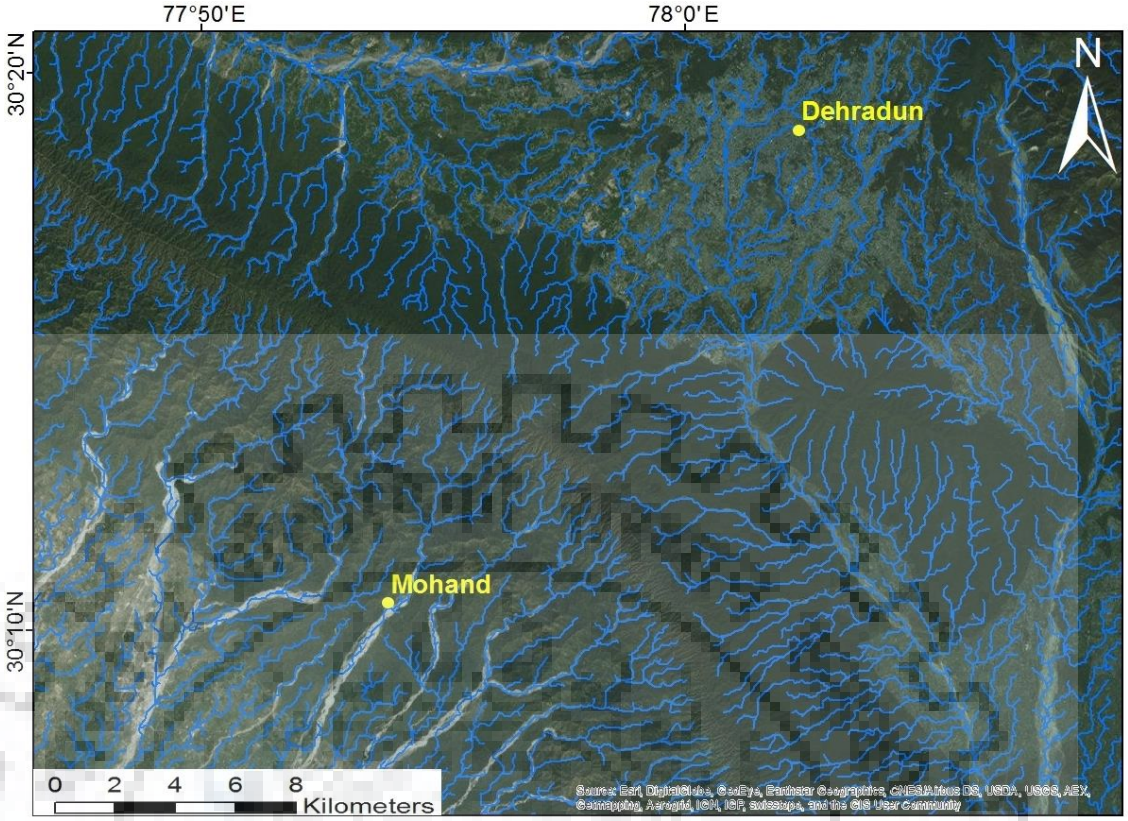

Figure 5.18. Stream network (derived from DEM) set up of Mohand anticline and Dehradun region.

5. 2. 1. Slope and Aspect analysis:

DEMs are storehouse of topographic information. DEMs denote terrain elevation as a function of geographic location (Burrough, 1986). They provide basic information required to characterize the topographic features of the terrain. Hence, to understand the Earth's surface in a better way, different viewing 3D ground elevation perceiving methods are used (Kaya, 2013). ASTER GDEM of 30m resolution has been used to derive slope, aspect, shaded relief model etc.

Slope: Slope measures the steepness of the surface at any particular place. The DEM data were processed in ArcGIS to extract slope map. Slope map (derived from Aster-GDEM) of the study area. The south-western part of the Mohand Anticline is highly dissected compared to northern part which is less dissected and having smooth or gentle slope (figure 5.19).

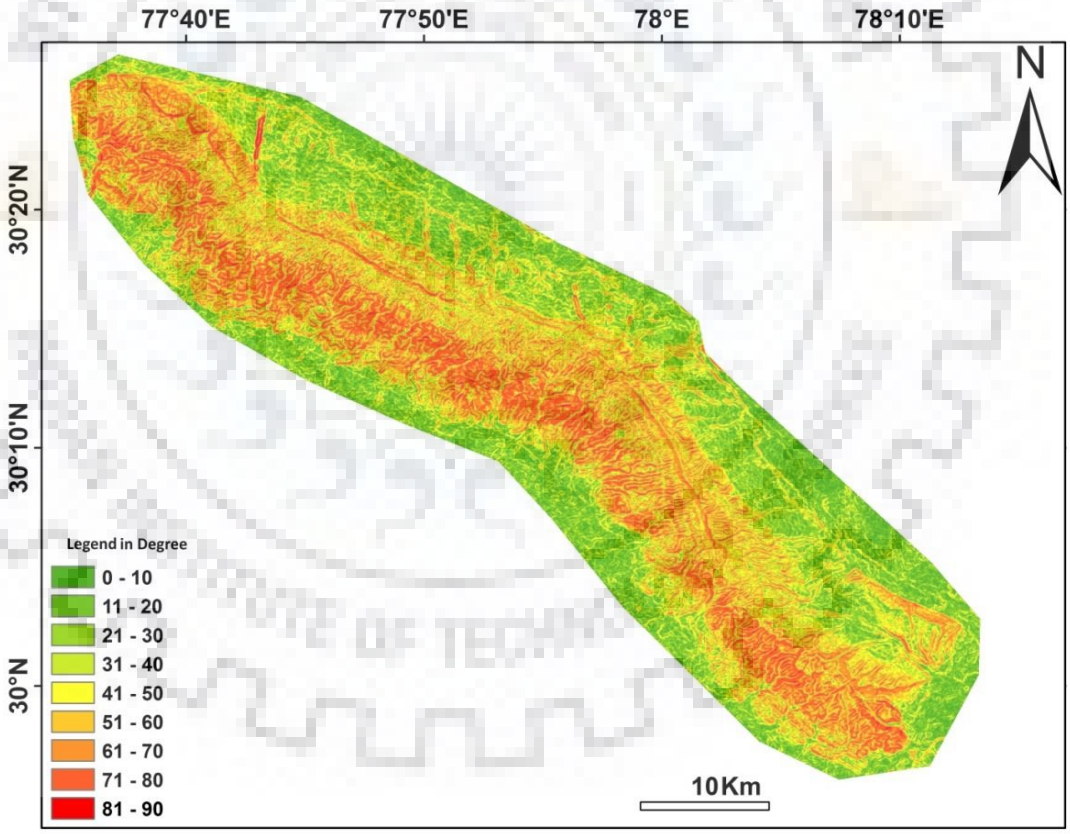

Figure 5.19. Slope map (derived from Aster-GDEM) of the study area. The south-western part of the Mohand Anticline is highly dissected compared to northern part which is less dissected and having smooth or gentle slope.

Aspect: Aspect measures the direction of steepest slope for a location on the surface. The DEM data were processed in ArcGIS to extract aspect map. The aspect map allows a visual support to determine if the direction of the slope is affecting the orientations observed in the streams and faults. Aspect map (derived from Aster-GDEM) of the Mohand anticline shows the different variations between northern part and the southern part of the Mohand Anticline (5.20). Aspects of northern faces of the anticline are mostly towards north-east direction. On the other hand most of the faces of southern side aspect towards south-west.

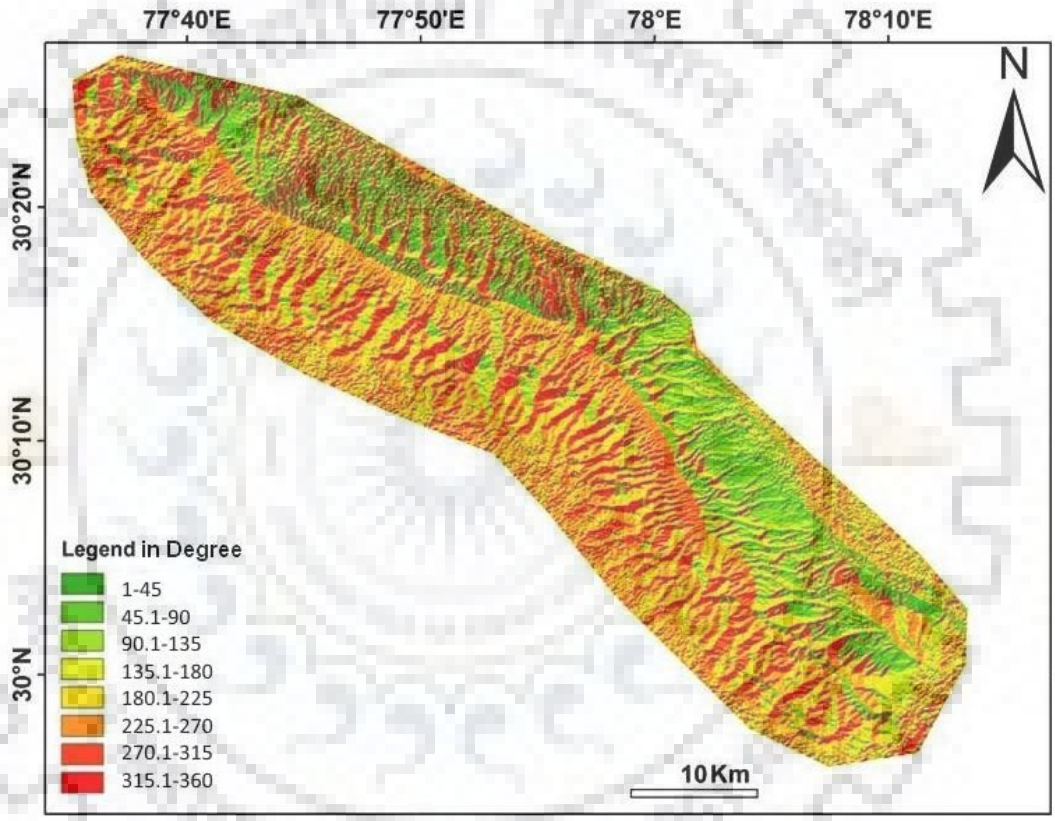

Figure 5.20. Aspect map (derived from Aster-GDEM) of the Mohand anticline shows the different variations between northern part and the southern part of the Mohand Anticline. Aspects of northern faces of the anticline are mostly towards north-east direction. On the other hand most of the faces of southern side aspect towards south-west.

5. 2. 2. Shaded relief model:

Hill shading illuminates the surface from a particular sun position. Surfaces which are inclined away from light are darker than average, whereas surfaces inclined toward the light are brighter. The DEM were processed in ArcGIS to extract a hillshade map. The controlling factors of hill shading are both light source elevation and azimuth. It is important to retain the elevation angles as low-elevation angles are noisy, highlighting streets as well as scarps; whereas high angles results in less contrast. Hence, for the present study a medium angle, such as 45°, proved useful (figure 5.21).

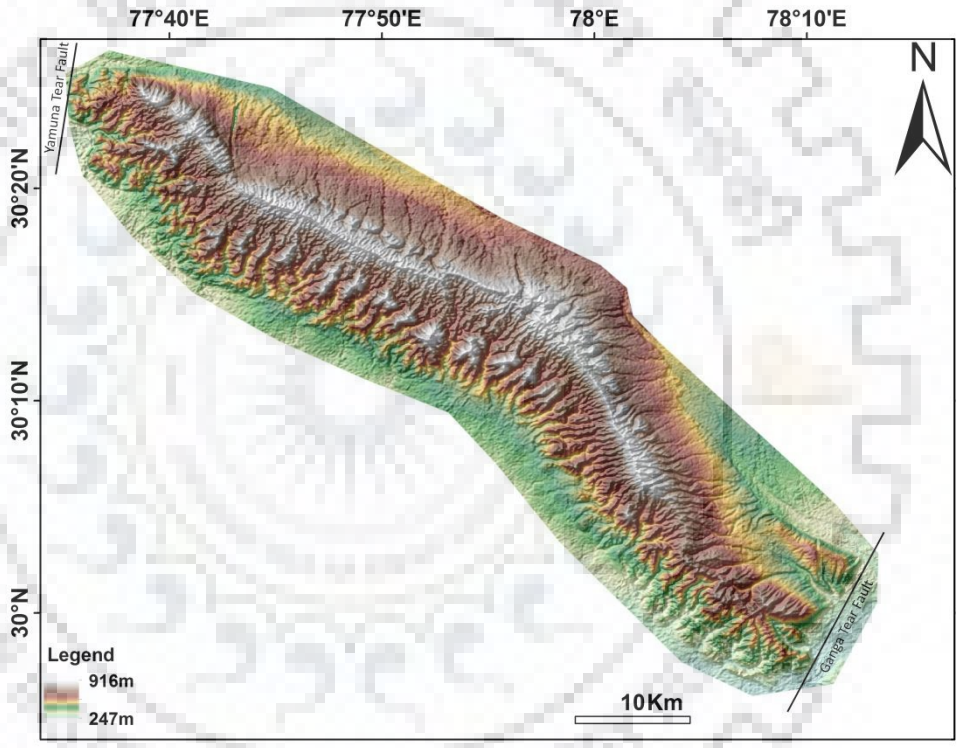

Figure 5.21. Shaded relief model of Mohand anticline southern-western part of Mohand anticline is highly dissected. This anticline forms a well-defined ridge bounded by Ganga and Yamuna tear faults at the southeast and northwest sides respectively.

Some tectonic features can be seen in the figure 5.22.These area have been delineated from satellite image and DEM for detailed study. First feature (L1) belongs to the north-western part of the Mohand anticline, the ridge axis gets displaces further along north. In this part the ridge has taken slightly northerly swing. Two distinct breaks within the Mohand ridge can be seen on both shaded relief model and satellite images. The middle part takes sharp bend forming south-westward concave ridge. Rocks of this part shows crushing effect and appear to have fractured

(L2). This bending might have caused due to longitudinal compressional forces from both the sides. This may suggest that in future there is a possibility of further bending or faulting. The location (L3) falls on the south eastern part of the anticline showing development of concave shaped valley initiating from the ridge. Figure 5.23 shows a 3D representative of the Mohand anticline derived from ASTER GDEM.

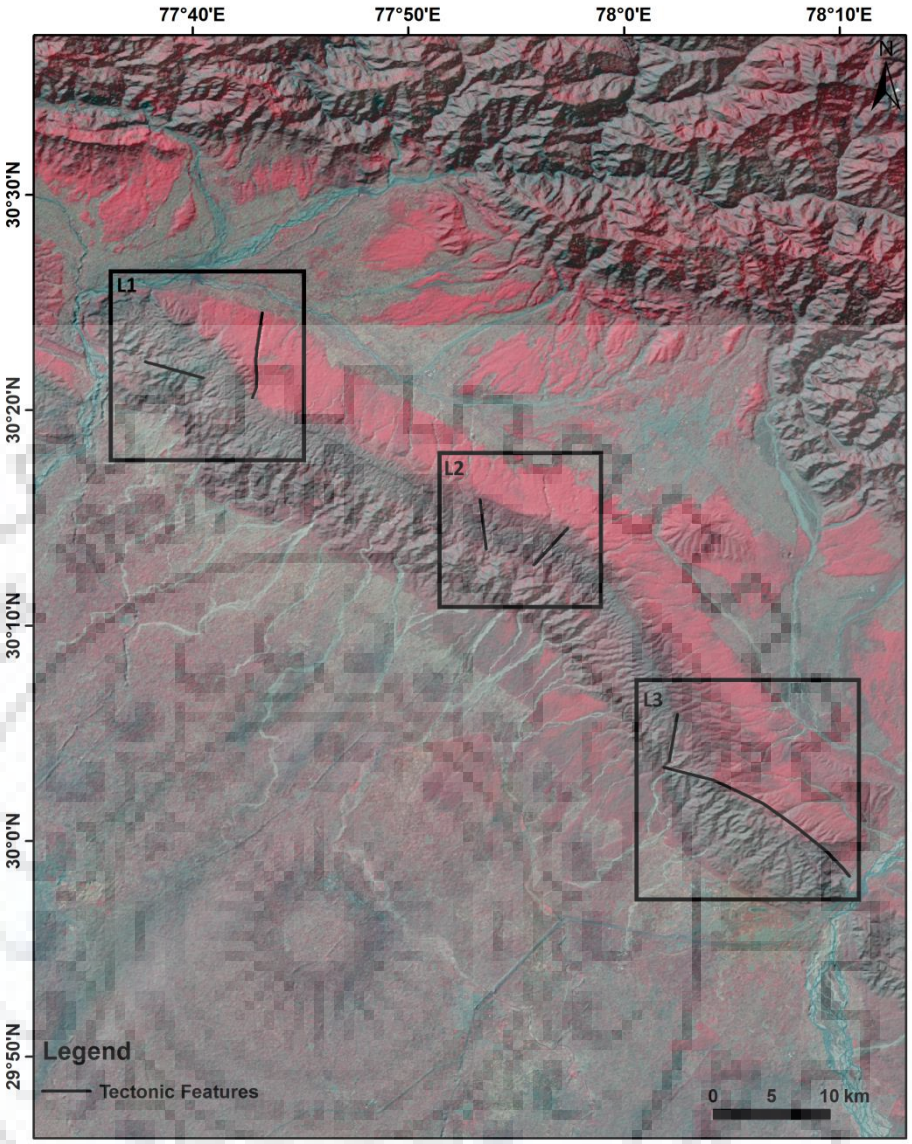

Figure 5.22. Location (L1, L2 and L3) shows tectonically modified surface features on Mohand anticline (hillshade model and FCC images). In these locations the continuity of the anticline changes drastically.

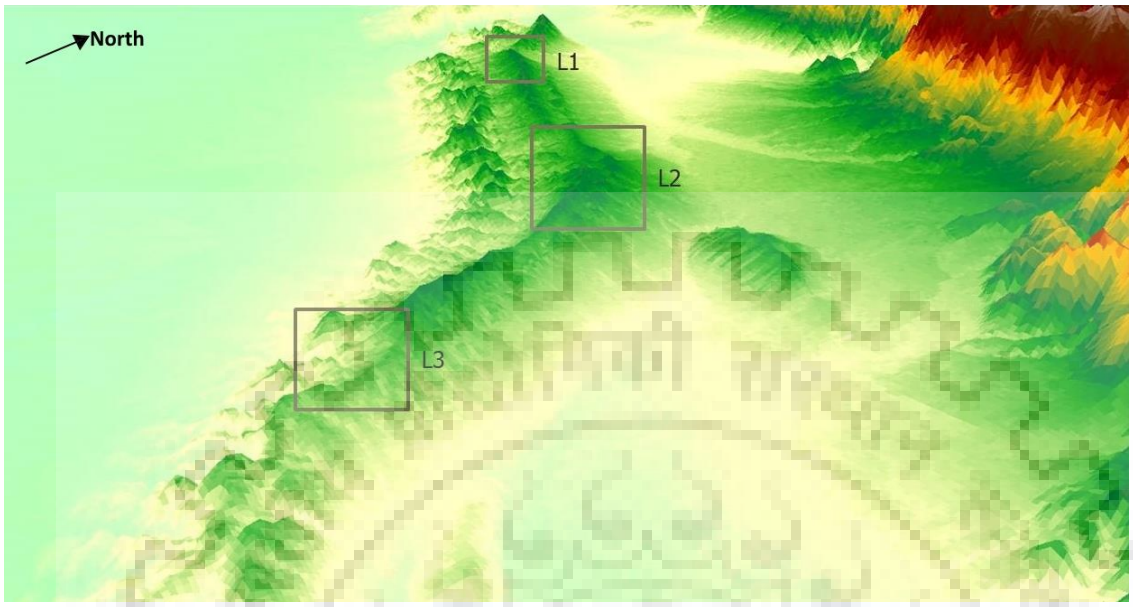

Figure 5.23. A 3D representation of Mohand Anticline along with locations of surface features modified by active tectonics.

5. 2. 3. River Anomalies:

Notable anomalies in courses of Ganga, Yamuna and their tributaries can be noticed within the study area (figure 5.24). Braiding of the Ganga River increases suddenly when it debouches onto the plains of Uttarakhand near Rishikesh (L1). Again in Haridwar, when the river flows along the Ganga Tear Fault, braiding of the river decreases suddenly (L2). Similarly braiding of the Yamuna River increases suddenly near Dakpathar (L3) and braiding decreases when the river crosses Yamuna Tear Fault near Ramdarbar (L4). Tributaries of Yamuna River at the location L5 suddenly changes their course as they encounter the MBT.

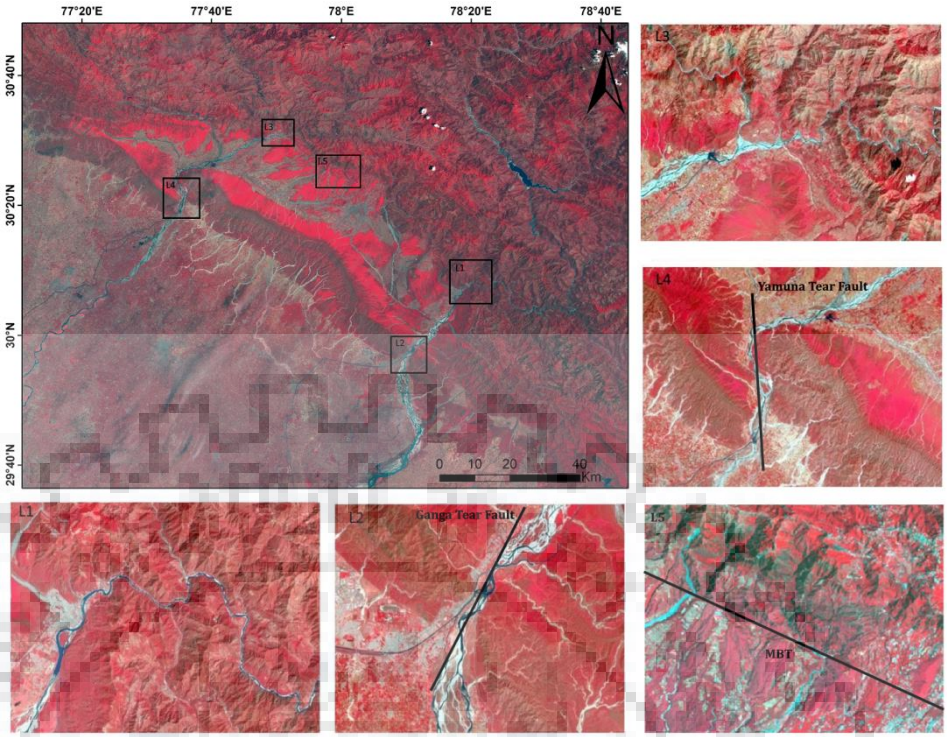

Figure 5.24. Response of Ganga, Yamuna and their tributaries within Dehradun re-entrant. The Ganga River has followed the Ganga tear fault within the Mohand anticline and the Yamuna River has followed the Yamuna tear fault. Channel morphology of both the rivers changes at certain locations, caused by prevailed structure and topography.

Studies of watersheds over the Mohand anticline suggest that the Khajnaur Rao and Mohan Rao Basins have been subjected to tectonic perturbation during their developmental phase (figure 5.25). Both basins have been shifted towards northeast relative to all other basins over the southwestern face of the Mohand anticline. Topographic section across Khajnaur Rao and Mohan Rao Basins shows that the streams within the basins have been subjected to deeper incision relative to other nearby basins (figure 5.25, 5.26). This suggests that both Khajnaur Rao and Mohan Rao Basins might have been subjected to tectonic uplift (figure 5.27).

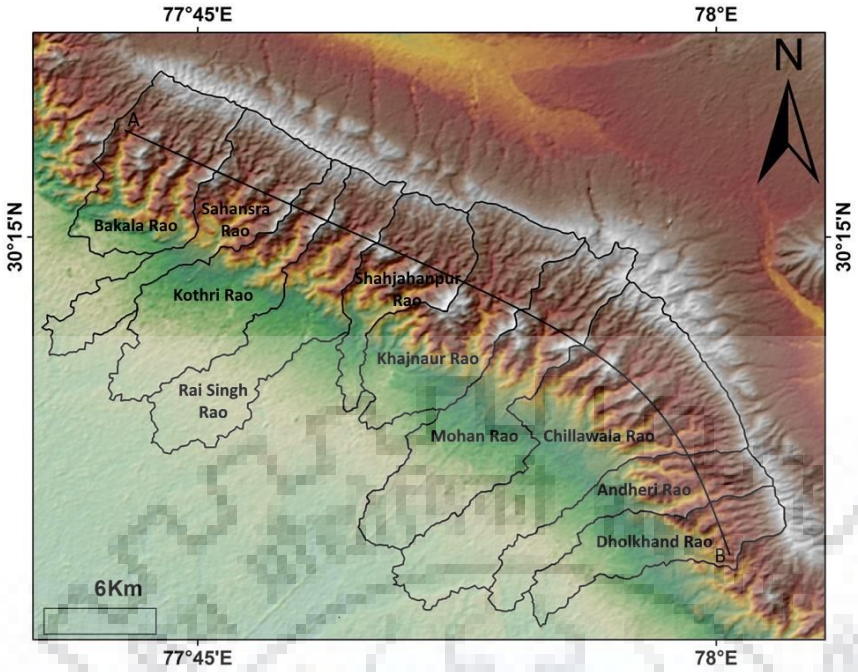

Figure 5.25. Watersheds of streams over south western face of Mohand Anticline. The Khajnaur Rao and Mohan Rao Basins have been subjected to tectonic upliftment as indicated by hypsometry analysis of the streams. The effects of active tectonics can be seen in the catchments of the streams. Both the catchments have been shifted north-eastward relative to other adjacent catchments. Topographic section has been obtained along AB (figure 5.26).

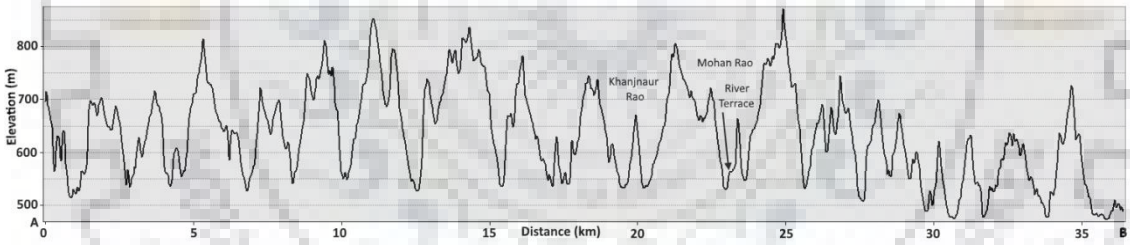

Figure 5.26. Cross section profile of Mohan Rao and Khajnaur Rao watersheds shows deeper incision of streams in both the catchments.

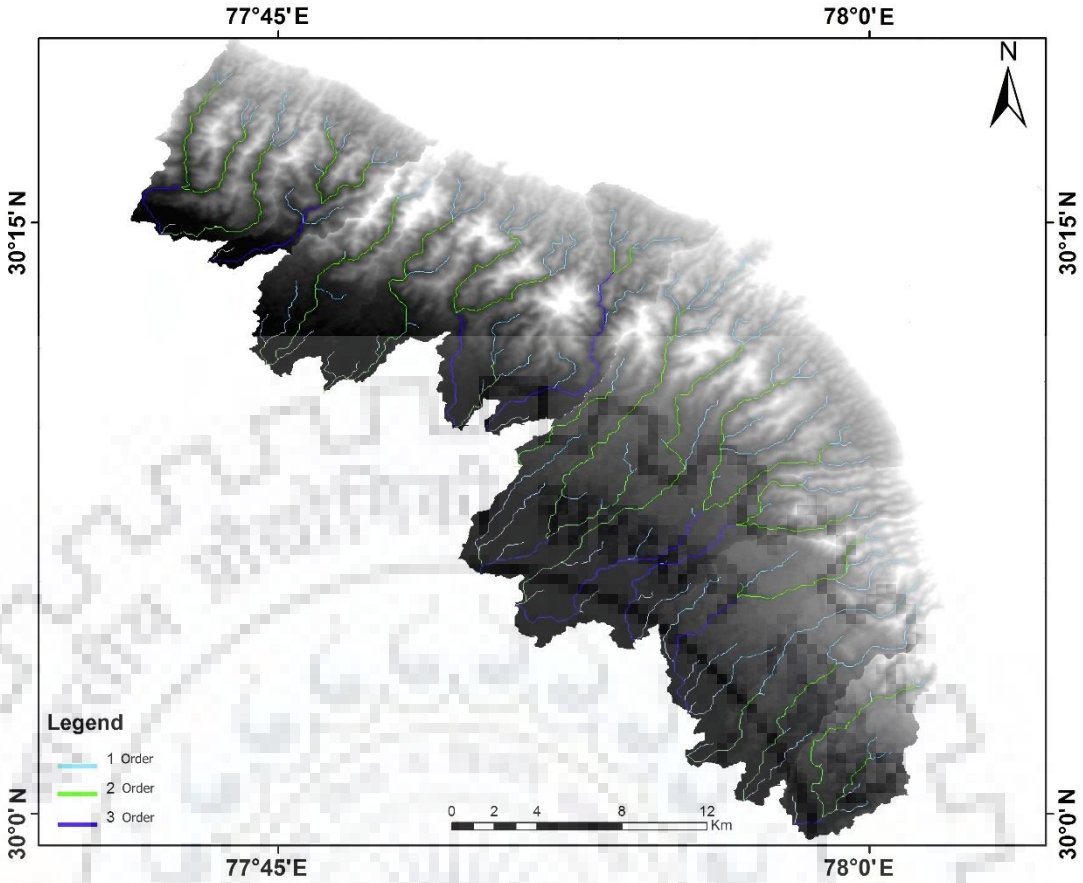

Figure 5.27. The order of streams for all basins derived from Aster GDEM while employing surface hydrological modelling technique in GIS. Stream orders of all basins show symmetrical signature of slope except Mohand Rao and Khajnaur basin which shows different signature comparison to rest of the basins of Mohand anticline. Second order stream on Mohand basin ends just after it started while in other basins it started and continues. This shows some anomaly between Mohand Rao, Khajnaur Rao and other basins of Mohand anticline.

5. 2. 4. Hypsometric Analysis:

Hypsometric Analysis of all catchments over south-western face of the Mohand Anticline also shows that both Khajnaur Rao and Mohan Rao catchments have been subjected to tectonic uplift during their developmental phase. Hypsometric curves of both the basins shows local concave downward nature, whereas the entire hypsometric curve is of concave upward nature (figure 5.28). All other catchments over the region are showing normal hypsometric curve.

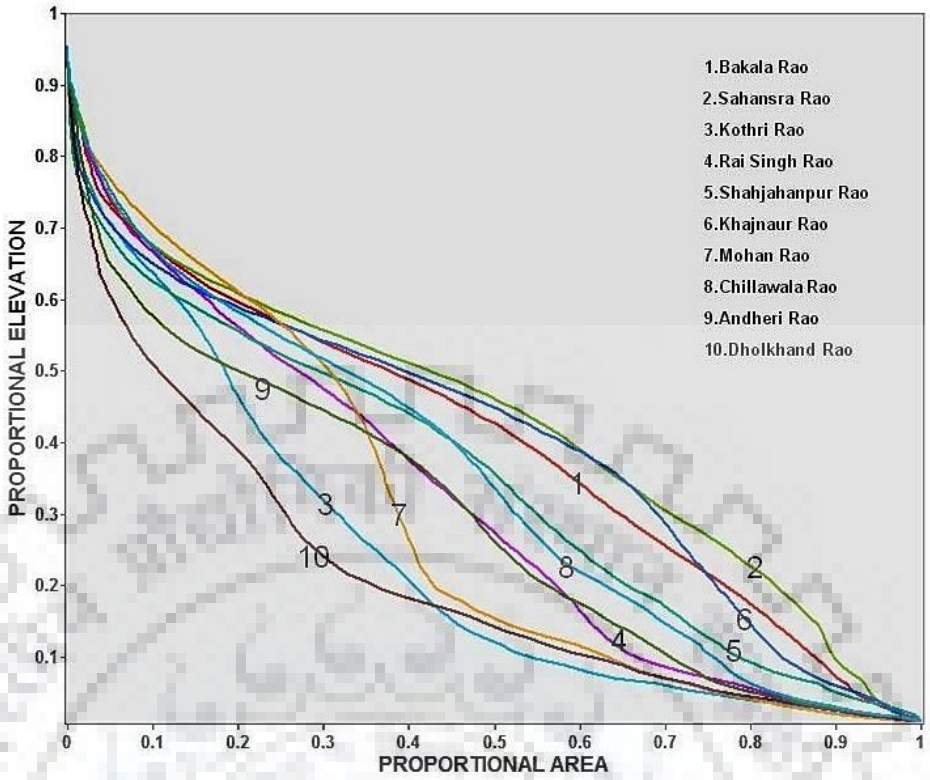

Figure 5.28. The result of hypsometric analysis for all basins. Hypsometric curves show low medium high hypsometric integral/elevation relief ratio indicating old, mature and youth stages. Out of all 10 hypsometric curves Khajnaur Rao and Mohan Rao curves also shows Late youth stage. On the other hand, all the other curves show monadnock and mature phase of the associated catchments.

This study deciphers the importance of Hypsometric analysis in observing the activity of the basins associated with the stream channels. According to study some basins show signatures of anomaly and it can be interpreted that the study area (Mohand anticline) are being subjected to tectonic activity (figure 5.30). Hypsometric analysis of the study area also shows significant changes in all basins Hypsometric analysis of watershed demonstrates the complexity of denudation processes and the rate of morphological changes. Therefore, it is useful to comprehend the erosion status of watersheds and prioritize them for undertaking soil and water conservation measures. With the hypsometric integral (elevation relief ratio) and hypsometric profile, we can identify and predict the geological stages of all watersheds (Pike and Wilson 1971). According to the hypsometric curves of watersheds, it is observed that Khajnaur Rao and Mohan Rao watersheds are having more influence of tectonic activity. According to hypsometric integral values of the watersheds lie on south-western face of the Mohand Anticline showing late youth geological stages (table 5.3). Hypsometric integral (HI) of Khajnaur Rao and Mohand Rao watersheds are having values 0.41 and 0.44 respectively

(Chorley and Morley 1959). This also indicates that Mohand Rao and Khajnaur Rao watershed are more prone to erosion in comparison to other watersheds adjacent to it (figure 5.29 a and 5.29 b). Some fault traces were also found near Mohand anticline along these two basins (5.31).

Table 5.3. Estimated Hypsometric integral values of all 10 watersheds. Out of these 10 basins Mohan Rao and Khajnaur Rao basins are showing high hypsometric integral.

Watersheds	**Area (Km^2)**	**Perimeter (Km)**	**Max. Elevation (m)**	**Min. Elevation(m)**	**Mean Elevation (m)**	**Total Relief (m)**	**HI**	**Geological Stage**
Bakala Rao	33.69	35.69	868	298	573	570	0.38	Late youth
Sahansra Rao	50.02	38.51	861	309	539	552	0.23	Late youth
Kothri Rao	32.93	38.51	834	302	441	532	0.33	Monadnock
Rai Singh Rao	41.10	46.79	890	305	460	585	0.38	Mature
Shahajahanpur Rao	47.43	44.44	870	308	596	562	0.27	Mature
Khajnaur Rao	46.12	31.77	883	343	558	540	0.45	Late youth
Mohan Rao	96.74	60.62	872	292	492	580	0.41	Late youth
Chillawala Rao	64.31	53.15	870	303	513	567	0.33	Mature
Andheri Rao	32.74	33.35	860	308	482	551	0.25	Monadnock
Dholkhand Rao	51.74	40.64	907	347	475	560	0.30	Monadnock

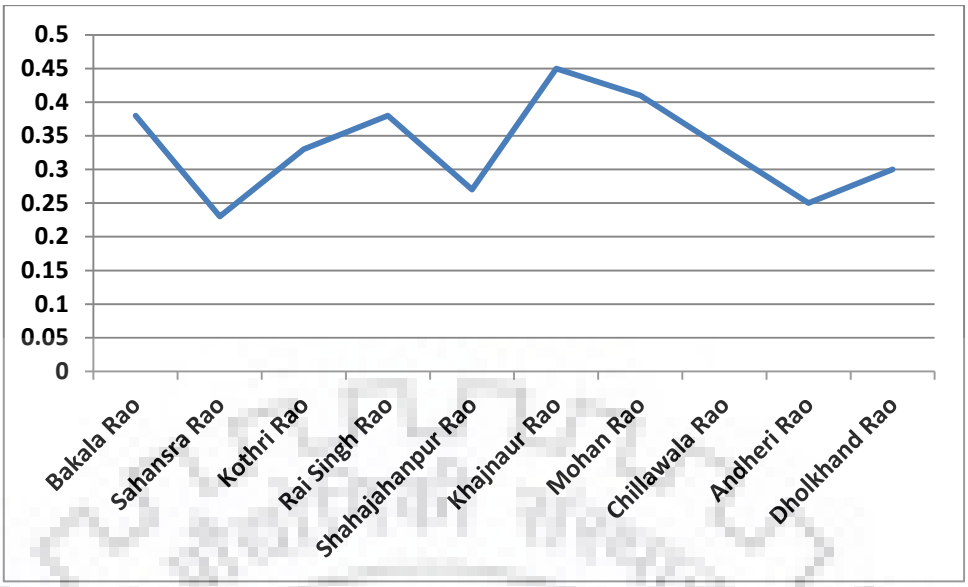

Figure 5.29.a Spatial Distribution of Basins based on Hypsometric Integral.

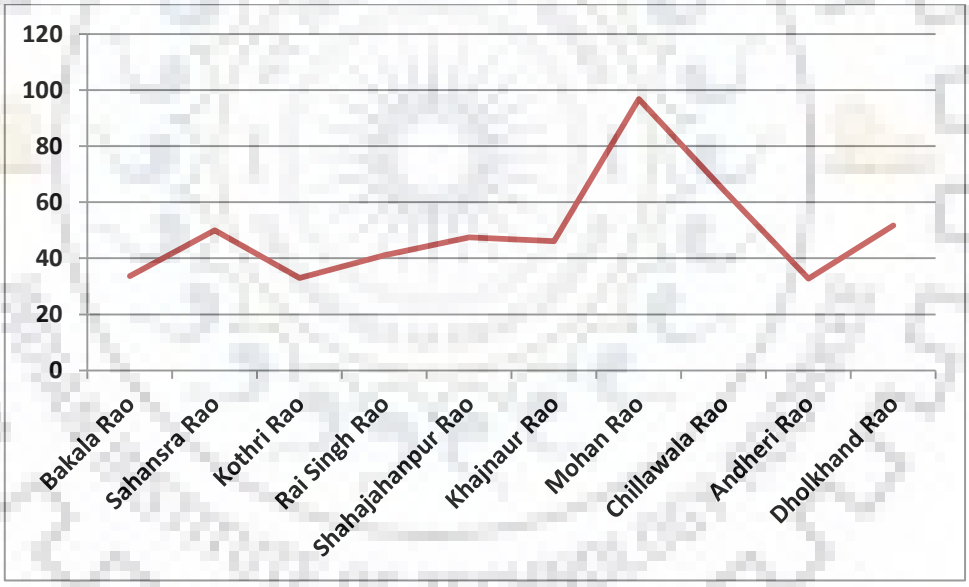

Figure 5.29.b. Spatial distribution of Basins based on Area.

Figure 5.30. Field photographs (1, 2) Rock exposers of faulted surface, erosion pattern and inclined bedding planes can be seen. River flows through a faulted line in this region also be shown in the photographs. Location map (a, b) also shown in the figure.

Figure 5.31. Fault trace on Mohand anticline along river section. Field photographs of the fault trace. (A-B, C-D and EF).

5.3 Deformation Model of Mohand Anticline

The Mohand anticline is a part of Dehradun re-entrant and hence the effect of Delhi Haridwar ridge on the Mohand anticline should be observed. A deformation model of the Mohan anticline has been conceived as shown in the figure number 5.32. Three stages have been shown wherein the stage first (A) represent a situation indicating the beginning of the formation of Mohand anticline over the Delhi Haridwar ridge. As the convergence in the Himalayan region continued the re-entrant structure began to form along with the deformation of the Mohand antcline in the form of north-eastward curvature. At the same time fractures also developed in the brittle rocks and subsequently the rock block displaced laterally along the conjugate strike slip faults. In the third stage (C) the compressional stress for the Mohan anticline due to the Delhi Haridwar ridge was at enhanced stage deforming the anticline more severely. Therefore, it is suggested that the Delhi Haridwar ridge remained responsible for the present arcuate shape of Mohand Anticline as well as conjugate strike slip faults affecting the Mohand anticline.

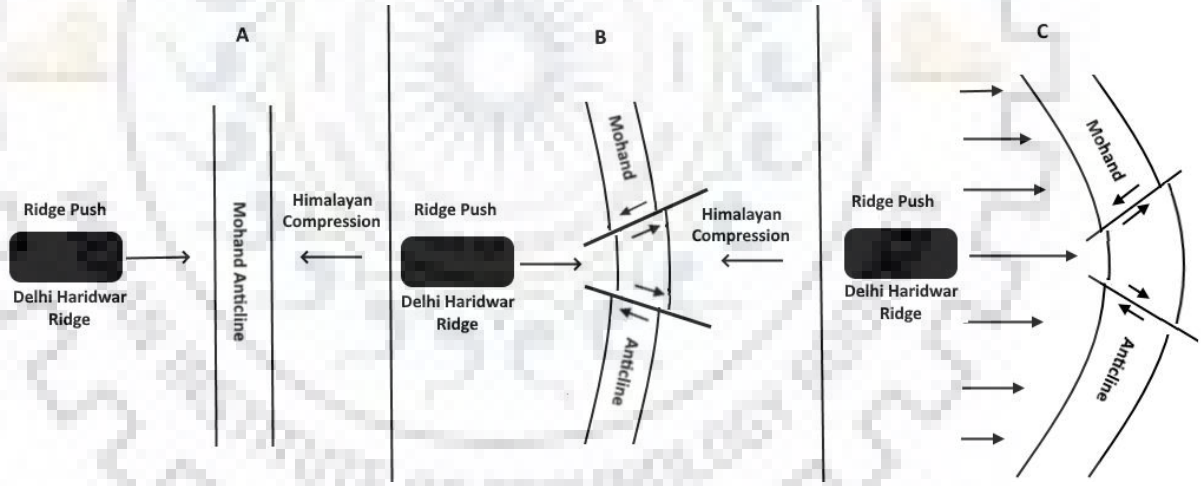

Figure 5.32. Sketches depicting stages of development of curvature in Mohand anticline and associated conjugate strike slip faults.

Chapter 6

Conclusion

Significant and unique tectonic feature depicting re-entrant and salient have formed in the northwest-southeast trending frontal Himalayan region. The re-entrants are Kangra and Dehradun which are bounded by the frontal most linear ridges which formed later under the influence of prevailed convergent tectonics. The folded rocks forming linear ridges are the result of fault propagation operated in these regions. The present topography comprising curved as well as linear ridges exhibit effect of extensive erosion carving out several erosional features in the area. These ridges also reveal effect of faulting through dislocations at many places. The nature of folded rocks in the re-entrant areas indicates the areas were subjected to slow and low intensity deformation.

The wide valleys of these re-entrants are bounded on the north-eastern side by the higher ridges and MBT allowing development of extensive river network. Many rivers have crossed NW-SE trending ridges at several places. The Beas river become braided within the Kangra valley after entering Jaisingpur indicating rapid flow of the water river controlled by tectonic activity. After Sujanpur Tira (N 31.83°, E 76.48°) the sinuosity of the river increases (fig. 4.7) and it crosses the Jwalamukhi thrust at a location near Har Dehri (N 31.78°, E 76.39°). The Beas River is an antecedent river. Near Jwalamukhi thrust the sinuosity of the river increases and the river valley has become deeper before the thrust. The river develops prominent knick point on the Jwalamukhi thrust. The river crosses HFT near Nadaun (N 31.78°, E 76.33°) and after crossing HFT, river takes a north-westward turn and becomes braided, finally debouches into Maharana Pratap Sagar. River takes north-westward turn after crossing HFT near Nadaun, Himachal Pradesh (N 31.78°, E 76.33°) (Location 3 of figure 4.7).

High density drainage developed in the central part of the re-entrant (near Jaisingpur) and overall drainage follow valleys. As the river flows along a strike of the valley, smaller tributaries feed into it from the steep slopes on the sides of mountains. These tributaries enter the main river at approximately 90 degree angle, causing a trellis-like appearance of the drainage system. This type of drainage is characteristic of folded mountains. Frontal ridge can be seen marked by two small scale faults at north-western end and south-eastern end (Ropar fault). And also rivers can be seen flowing through these faulted area.

Some tectonic features can be seen in the figure 5.22.These area have been delineated from satellite image and DEM for detailed study. First feature (L1) belongs to the north-western part

of the Mohand anticline, the ridge axis gets displaces further along north. In this part the ridge has taken slightly northerly swing. Two distinct breaks within the Mohand ridge can be seen on both shaded relief model and satellite images. The middle part takes sharp bend forming south-westward concave ridge. Rocks of this part shows crushing effect and appear to have fractured (L2). This bending might have caused due to longitudinal compressional forces from both the sides. This may suggest that in future there is a possibility of further bending or faulting. The location (L3) falls on the south eastern part of the anticline showing development of concave shaped valley initiating from the ridge. Figure 5.23 shows a 3D representative of the Mohand anticline derived from ASTER GDEM.

Notable anomalies in courses of Ganga, Yamuna and their tributaries can be noticed within the study area (figure 5.24). Braiding of the Ganga River increases suddenly when it debouches onto the plains of Uttarakhand near Rishikesh (L1). Again in Haridwar, when the river flows along the Ganga Tear Fault, braiding of the river decreases suddenly (L2). Similarly braiding of the Yamuna River increases suddenly near Dakpathar (L3) and braiding decreases when the river crosses Yamuna Tear Fault near Ramdarbar (L4). Tributaries of Yamuna River at the location L5 suddenly changes their course as they encounter the MBT.

Geomorphic features indicate that there are strike slip fault which are cutting the Mohand anticline.

Here we have tried to figure out the possible cause for the formation of the strike slip faults on Mohand anticline.

As the convergence in the Himalayan region continued the re-entrant structure began to form along with the deformation of the Mohand antcline in the form of north-eastward curvature. At the same time fractures also developed in the brittle rocks and subsequently the rock block displaced laterally along the conjugate strike slip faults

Some significant outcomes of the present study are:

1. Most of the rivers within the study area have followed fault traces to cross the topographic highs (ridges/anticlines).
2. The longitudinal profile of the Beas River clearly shows the Jwalamukhi thrust and MBT. Among these, Jwalamukhi thrust and MBT are very prominent. The river develops prominent knick point on the Jwalamukhi thrust. The HFT is buried by alluvium and is not very prominent in the longitudinal profile of the river.
3. Hypsometric analysis of Mohand anticline reveals that the Mohan Rao and Khajnaur Rao basin have been subjected to tectonic uplift relative to other nearby basins.
4. The Mohan Rao and Khajnaur Rao basins have shifted towards north-east (relative to other nearby basins) under the tectonic affect/longitudinal compressional forces from both the sides. This may suggest that in future there is a possibility of further bending or faulting of the Mohand anticline.
5. Kangra and Dehradun re-entrants are still under tectonic influence of major thrust in the region.
6. Sinuosity and Asymmetry analysis also shows the significant deviation indicating influence of active tectonics in modification of the drainage system within the study area.
7. Drainage pattern and streams orders are very helpful to correlate morphotectonic features in the region.
8. Knick points and longitudinal profiles analysis also suggests that river are tectonically affected in this region.

Bibliography:

1. Abdullah, A., Akhir, J. M. and Abdullah, I., 2010, Automatic Mapping of Lineaments Using Shaded Relief Images Derived from Digital Elevation Model (DEMs) in the Maran-Sungi Lembing Area, Malaysia, The Electronic Journal of Geotechnical Engineering, 15, 949–957.
2. Abe, K. and Noguchi S., 1983, Revision of magnitudes of large shallow earthquakes, 1897-1912. Phys. Earth Planet. Inter., 33, 1–11.
3. Ambraseys, N. and Bilham, R., 2000, A note on the Kangra Ms=7.8 earthquake of 4 April 1905. Current Science, 79, 45-50.
4. Anderson, R. C. and Beratan, K. K., 1993, Identification of geomorphic surfaces from Landsat data, Whipple Mountains, South-eastern California, Geological society of America Abstracts with Programs, 25, A-106.
5. Anderson, R. C. and Beratan, K. K., 1994, Identify characteristics of geomorphologic surfaces, Whipple Mountains, South-eastern California, Geological society of America Abstracts with Programs, 26, 34-35.
6. Anhert, F., 1973, COSLOPE 2- A comprehensive model program for simulating slope profile development, Geocommunication Programs, 8, 99-119, London.
7. Avena, G. C., Giuliano, G. and Lupia Palmieri, E., 1967, On the quantitative assessment of hierarchy and evolution of river networks, Bulletin of the Italian Geological Society, 86, 781 -796.
8. Avouac, J. P. and Peltzer, G., 1993, Active tectonics and southern Xinjiang, China: analysis of terrace riser and normal fault scarp degradation along the Hotan-Qira fault system, Journal of Geophysical Research, 98, 21773-21807.
9. Baghdadi, N. and Zribi, M., 2016, Microwave remote sensing of land surfaces. In Techniques and methods, ISTE/Elsevier Press p448.
10. Bamler, R. and Hartl, P., 1998, Synthetic aperture radar interferometry, Inverse Problems, 14, R1-R54.
11. Banerjee, P., and R. Burgmann., 2002, Convergence across the northwest Himalaya from GPS measurements, Geophys. Res. Lett., 29 (13), 1652.
12. Baral, S. S., Das, J., Saraf, A. K., Borgohain, S. and Singh, G., 2016, Comparison of Cartosat, ASTER and SRTM DEMs of Different Terrains, Asian Journal of Geoinformatics, 16 (1), 1-7.

13. Baral, S. S., Sharma, K., Saraf, A. K., Das, J., Singh, G., Borogohain, S. and Kar, E., 2016, Thermal anomaly from NOAA for Nepal Earthquake, Current Science, 110, 02: 150-153.
14. Bayuaji, L., Sumantyo, J.T.S. and Kuze, H., 2010, ALOS PALSAR DInSAR For land subsidence mapping in Jakarta, Indonesia, Canadian Journal of Remote Sensing, 36(1),1-8.
15. Beanland, S. and Clark, M.M., 1994, The Owens Valley fault zone, eastern California, and surface faulting associated with the1872 earthquake. U.S., Geological Survey Bulletin, 1982, 29.
16. Belisario, F., Del Monte, M., Fredi, P., Funiciello, R., Lupia Palmieri, E. and Salvini, F., 1999, Azimuthal analysis of stream orientations to define regional tectonic lines, Zeitschrift für Geomorphologie N. F., Supplement-Band, 118, 41-63.
17. Bhattacharya, A. and Agarwal, K., 2008, Some Observations on the Thrust Geometry of the Siwalik Rocks of the Outer Himalaya, India. Earthscienceindia.Info, I(Ii), 58–65.
18. Brookfield, M. E., 1998, The evolution of the great river systems of Southern Asia during the Cenozoic India- Asia Collision Rivers draining southwards, Geomorphology, 22, 285-312.
19. Brozovic N. and Burbank, D. W., 2000. Dynamic fluvial systems and gravel progradation in the Himalayan foreland. Geological Society of America Bulletin; v. 112; no. 3; P 394-412.
20. Bull, W. B. and McFadden, L. D., 1977, Tectonic geomorphology north and south of the Garlock fault, California D.O. Doehring (Ed.), Geomorphology in Arid Regions, Proceedings of the Eighth Annual Geomorphology Symposium, State University of New York, Binghamton, 115-138.
21. Buonasorte, G., Ciccacci S., De Rita, D., Fredi P. and Lupia Palmieri, E., 1991, Some relations between morphological characteristics and geological structure in the Vulsini Volcani Complex (North Latium, Italy), Zeitschrift für Geomorphologie N. F, Supplement-Band, 82, 59-71.
22. Burbank, D. W. and Anderson, R. S., 2001, Tectonic Geomorphology, Blackwell Science, Cambridge, 274.
23. Burbank, D. W. and Pinter, N., 1999, Landscape evolution: The interaction between tectonics and surface processes, Basin Research, 11(1), 1-6.
24. Burrough, P. A., 1986, Principles of Geographical Information Systems for Land Resources Assessment (Oxford: Oxford University Press), 193.

25. Cartier, K. and Alt, D., 1982, The bewildering Bitterroot, the river that won't behave, Montana Magazine, 12, 52-53.
26. Castleman, K. R., 1996, Digital Image Processing. Prentice Hall, Englewood cliffs, NJ, USA.
27. Centamore, E., Ciccacci S., Del Monte M., Fredi P. and Lupia Palmieri, E., 1996, Morphological and morphometric approach to the study of the structural arrangement of North-Eastern Arbuzzo (Central Italy), Geomorphology, 16, 127-137.
28. Chakrabarti, B. K., 2016, Geology of the Himalayan Belt: Deformation, Metamorphism, Stratigraphy. Elsevier, Netherland, 264.
29. Chaudhary, B. S. and Aggarwal, S., 2009, Demarcation of paleochannels and integrated ground water resources mapping in parts of Hisar district, Haryana, Journal of Indian Society of Remote Sensing, 37, 251-260.
30. Chaudhary, B. S. and Toleti, B. V. M. Rao., 2006, Hydrogeomorphological Mapping and Delineation of Ground Water Potential Zones Using Satellite Data in Sonipat District, Haryana, Annals of Agri-Bio Research, 11(1), 7-14.
31. Chaudhary, B. S., Kumar, M., Roy, A. K. and Ruhal, D. S., 1996, Applications of remote sensing and geographical information system in ground water investigations in Sohna Block, Gurgaon District, Haryana, India, Archives of International Society Photogrammetry and Remote Sensing, 34(B-6), 18-23.
32. Chediya, O. K., 1986, Morphostructures and neo-tectonics of the Tien Shan, Frunze, Academia Nauk Kyrgyz CCP, 313.
33. Chen, L. and Khan, S.D., 2009, Geomorphometric features and tectonic activities in sub-Himalayan thrust belt, Pakistan, from satellite data. Computers & Geosciences, 35(10), pp.2011-2019.
34. Chen, Y.C., Sung, Q.C. and Cheng, K.Y., 2003, Along-strike variations of morphotectonic features in the western foothills of Taiwan: tectonic implications based on stream gradient and hypsometric analysis, Geomorphology, 56, 109-137.
35. Chorley, R.J. and L.S.D Morley., 1959, a simplified Approximation for the Hypsometric Integral. J. Geology 67, 5, 566-571.
36. Ciccacci S., Fredi, P., Lupia Palmieri, E. and Salvini, F., 1986, An approach to the quantitative analysis of the relationship between drainage pattern and fracture trend, International Geomorphology, 2, 49-68.
37. Cotilla, M. O. and Cordoba, D., 2004, Morphotectonics of the Iberian Peninsula, Pure and Applied Geophysics, 161, 755-815.

38. Cotilla, M. O., Cordoba, D. and Calzadilla M., 2007, Morphotectonic Study of Hispaniola, Geotectonics, 41 (5), 368-391.
39. Cox, R.T., 1994, Analysis of drainage-basin symmetry as a rapid technique to identify areas of possible Quaternary tilt-block tectonics: an example from the Mississippi Embayment, Geological Society of America Bulletin, 106, 571-581.
40. Cracknell, A. P. and Hayes, L., 1991, Introduction to Remote Sensing, Taylor and Francis, London, p304.
41. Cracknell, A. P., 1997, Advanced Very High Resolution Radiometer AVHRR, Taylor and Francis Books Ltd., London, p968.
42. Cracknell, A. P., 1998, Synergy in remote sensing – what's in a pixel? International Journal of Remote Sensing, 19(11), 2025-2047.
43. Cuong, N. Q. and Zuchiewicz, W. A., 2001, Morphotectonic properties of the Lo River fault near Tam Dao in North Vietnam, Journal of Natural Hazards and Earth System Sciences, 1, 15-22.
44. Dalati, M., 1994, Application of Remote Sensing for Tectonic purposes in EI-Rouge Depression, North West of the Syrian Arab Republic. Proceedings of the International Symposium on Spectral Sensing Research, ISSSR, II, 859-867, San Diego, California, USA.
45. Dasgupta, S., Pande, P., Ganguly, D., Iqbal, Z, Sanyal, K, Venkatraman, N.V., Dasgupta, S., Sural, B., Harendranath, L., Mazumdar, K., Sanyal, S., Roy, K., Das, L.K., Misra, P.S. and Gupta, H., 2000, Seismotectonic Atlas of India and its Environs, Geological Survey of India.
46. Davis, D., Suppe, J., and Dahlen, F.A., 1983, Mechanics of fold-and-thrust belts and accretionary wedges. J. Geophys. Res., 88, 1153-1172.
47. Deffontaines, D. B., Chotin, D. P., Brahim, D. L. A. and Rozanov, D. M., 1992, Investigation of active faults in Morocco using morphometric methods and drainage pattern analysis, Geol Rundsch, 81(1), 199–210.
48. Delcaillau, B., 2004, Reliefs et Tectonique recente, In: Veubert (Ed.), p262.
49. Delcaillau, B., Deffontaines, B., Angelier, J., Deramond, J., Floissac, l., Souquet, P. and Chu, H. T., 1998, Morphotectonic evidence from lateral propagation of an active frontal fold: the Pakuashan anticline, foothills of Taiwan, Geomorphology, 24, 263-290.
50. Devi, R. K. M. and Singh, T., 2006, Morphotectonic setting of Ganga Lake, Itanagar Capital Complex, Arunachal Himalaya, Geomorphology, 76, 1-11.

51. Dubey, A. K., Bhakuni , S. S. and Selokar, A. D., 2004, Structural evolution of the Kangra recess, Himachal Himalaya: a model based on magnetic and petrofabric strains. Journal of Asian Earth Sciences, 24, 245–258.
52. Duda, S. J., 1965, Secular seismic energy release in the circum-Pacific belt, Tectonophysics, 2, 409–452.
53. Dumont, J. F., Santana, E., Vilema, W., Pedoja, K., Ordonez, M., Cruz, M., Jemenez, N. and Zambrano, I., 2005, Morphological and microtectonic analysis of Quaternary deformation from Puna and Santa Clara Island, Gulf of Guayaquil, Ecuador (South America), Tectonophysics, 339, 331-350.
54. Evans, I. S., 1972, General geomorphometry, derivative of altitude and descriptive statistics, In Spatial Analysis in Geomorphology, edited by R. J. Chorley (London: Methuen), 17-90.
55. Florinsky, I. V., 1998, Combined analysis of digital terrain models and remotely sensed data in landscape investigations, Progress in Physical Geography, 22 (1), 33-6
56. Formento – Trigilio, Merri L., Burbank, D. W., Nicol Andrew, Shulmeister J. and Reieser U., 2002. River response to an active fold-and-thrust belt in a convergent margin settling, North Island, New Zealand. Geomorphology 49, 125-152.
57. Frisch, W., 1997, Tectonic Geomorphology. In proceeding of the Fourth International Conference on Geomorphology, Zeitschrift für Geomorphologie N. F., Supplementary Band, 118.
58. Ganssar, A., 1964, Geology of Himalayas. Wiley Inter Science, New York, 289.
59. Garcia M. and Herail G., 2005. Fault-related folding, drainage network evolution and valley incision during the Neogene in the Andean Precordillera of Northern Chile. Geomorphology 65, 279-300.
60. Garcia-Melendez, E., Goy, J. L. and Zazo, C., 2003, Neotectonic and Plio-Quaternary landscape development within the easten Huercal-Overa basin (Betic Cordilleras Southeast Spain), Geomorphology, 50, 111-133.
61. Gillespie, A. R., Kahle, A. B. and Polluconi, F. D., 1984, Mapping alluvial fans in Death Valley, California using multi-channel thermal infra-red image, Geophysical Research Letters, 11, 1153-1156.
62. Godin, L., La Roche, R.S., Wafle, L. and Harris, L.B., 2918, Influence of inherited Indian basement faults on the evolution of the Himalayam Orogen. Geological Society, London, Special Publication, 481, SP481-4.

63. Goldsworthy, M. and Jackson, J., 2000, Active normal fault evolution in Greece revealed by geomorphology and drainage patterns, Journal of the Geological Society, London, 157, 967-981.
64. Guo, Z. and Wilson, M., 2012, The Himalayan leucogranites: Constraints on the nature of their crustal source region and geodynamic setting, Gondwana Research, 22(2), 360–376.
65. Gupta, S. and Ellis, M., 2004, Does the topography of actively ground folds mimic fold structures? The case of the Mohand Anticline, Frontal Himalaya, Geophysical Union, Annual meeting, April 2004.
66. Gutenberg, B. and Richter, C., 1954, Seismicity of the Earth and Associated Phenomena, Princeton Univ. Press, 2nd edn, 310.
67. Hack, J. T., 1973, Stream-profiles analysis and stream-gradient index, Journal of Research of the U.S. Geological Survey, 1, 421-429.
68. Hamdouni, E., Irigaray, C., Fernandez, T., Chacón, J. and Keller, E. A., 2008, Assessment of relative active tectonics, southwest border of Sierra Nevada (Southern Spain), Geomorphology, 96, 150-173.
69. Hobbs, W. H., 1912, Earth Features and their Meaning. McMillan Co., New York, p506.
70. Hooke, J. M., 1995, River channel adjustment to meander cut-offs on the River Bollin and River Dane, NW England, Geomorphology, 14, 235-253.
71. Humphrey, N. F. and Heller, P. L., 1995, Natural oscillations in coupled geomorphic systems: An alternative origin for cyclic sedimentation, Geology, 23, 499-502.
72. Husson, L. and Mugnier, J. L., 2003, Three Dimensional horizon reconstruction from outcrop structural data, restoration and strain field of the Baisahi anticline, western Nepal, Journal of Structural Geology, 25(1), 79-90.
73. Hough, S. E., Bilham, R., Ambraseys, N. and Feldl, N., 2005, Revisiting the 1897 Shillong and 1905 Kangra earthquakes in northern India: Site response, Moho reflections and a triggered earthquake. Current Science, 88, 1632-1638.
74. Jackson, A., 2014, Long and cross profile, Geography AS Notes.
75. Jackson, J. and Leeder, M., 1994, Drainage system and the development of normal faults- An example from Pleasant Valley, Nevada, Journal of Structural Geology, 16 (8), 1041-1059.
76. Jasrotia, A. S., 2007, Landslide Hazard Zonation along the NH-IA between Udhampur to Kud using remote sensing and GIS techniques, Natural Hazard, Special Vol. of Indian Geological Congress, 129-144.

77. Jasrotia, A. S., Kumar, A. and Bhat, A., 2012, Morphometric analysis and hydrogeomorphology for delineating groundwater potential zones of Western Doon Valley, Uttarakhand, International Journal of Geomatics and Geosciences, 2(4), 1078-1096.

78. Jasrotia, A. S., Kumar, R. and Saraf, A.K., 2007, Delineation of groundwater recharge sites using integrated remote sensing and GIS in Jammu district, India. International Journal of Remote Sensing, 28 (22), 5019-5036.

79. Jordan, G., Meijninger, B. M. L., van Hinsbergen, D. J. J., Meulenkamp, J. E. and van Dijk, P. M., 2005, Extraction of morphotectonic features from DEMs: Development and applications for study areas in Hungary and NW Greece, International Journal of Applied Earth Observation and GeoInformation, 7. 163-182.

80. Kar, E., Baral, S. S., Saraf, A. K., Das, J., Singh, G. and Borgohain, S., 2017, Remote Sensing and GIS Based Analysis of Geomorphic Evidences and Morphometry of Active Faults in Kachchh Area. Journal of the Indian Society of Remote Sensing, 45(1), 79-88.

81. Karunakaran, C. and Ranga, Rao, A, R., 1979, Status of exploration for hydrocarbon in the Himalayan region - contributions to stratigraphy and structure; Geol. Surv. India Misc. Pubn. 41, 1-66.

82. Keller, E. A. and Pinter, N., 2002, Active tectonics: Earthquakes Uplift and Landscapes, Second edition, Prentice Hall, New Jersey, p362.

83. Keller, E. A., Rockwell, T. K., Clark, M. N., Dembroff, G. R. and Johnson, D. L., 1982, Tectonic geomorphology of Ventura, Ojai, santa Paula areas, western Transverse Ranges, California. In: Cooper, J. D. (Ed.), Neotectonics in Southern California: Geologic Society of America Cordilleran Section Field Guidebook, 25-42.

84. Keller, E., 1986, Investigation of active tectonics: use of surfacial earth processes. In: Wallace, R. E. (eds). Active tectonics studies in geophysics, National Academy Press, Washington, D. C. 136-147.

85. Kobor, J. S. and Roering, J. J., 2004, Systematic variation of bedrock channels gradient in the central Oregon Coast Range: implication for rock uplift and shallow landsliding, Geomorphology, 62, 239-256.

86. Krishna, A. P. and Rai, L. K., 1996, GIS and remote sensing for natural resources management at watershed level in the mountain environment: a conceptual approach, Asian-Pacific Remote Sensing and GIS Journal, UN-ESCAP, Thailand, 9(1), 93-99.

87. Krishna, A. P., 1996, Land Cover Change Dynamics of a Himalayan Watershed Utilizing Indian Remote Sensing Satellite (IRS) Data, 0-7803-3068-4/96 IEEE, 221-223.

88. Krishna, A. P., 2005, Snow and glacier cover assessment in the high mountains of Sikkim Himalaya, Hydrological Processes, John Wiley and Sons Ltd Country of publication, Great Britain, ISSN0885-6087, 19 (12), 2375-2384.

89. Krishna, M. R., 1996, Isostatic response of the Central Indian Ridge (Western Indian Ocean) based on transfer function analysis of gravity and bathymetry data, Tectonophysics, 257(2), 137– 148.

90. Kumar, S. and Mahajan, A.K., 2001. Seismotectonics of the Kangra region, Northwest – Himalaya. Tectonophysics 331, 359-371.

91. Le Turdu, C., Coussement, C., Tiercelin, J. J., Renaut, R. W., Rolet, J., Richert, J. P., Xavier, J. P. and Coqulet, D., 1995, Rift basin structure and depositional patterns interpreted using 3-D remote sensing approach: The Barongo and Bogoria basins, Central Kenya rift, East Africa, Bulletin Centres Re'cherches, 19, 1-37.

92. Lifton, N. A. and Chase, C. G., 1992, Tectonic, climatic and lithologic influences on landscape fractal dimension and hypsometry: implication for landscape evolution in the San Gabriel Mountains, California, Geomorphology, 5, 77-114.

93. Luo, W. and Harlin, J.M., 2003, A Theoretical Travel Time Based On Watershed Hypsometry. Journal of the American Water Resources Association, 39(4), 785-792.

94. Lupia Palmieri, E., Ciccacci S., Civitelli, G., Corda, L., D 'Alessandro L., Del Monte M., Fredi P. and Pugliese, F., 1995, Quantitative geomorphology and morphodynamics of Abruzzo. I. II River basin Sinello, Physical Geography and Quaternary Dynamics, 18, 31-46.

95. Maiti, S. and Bhattacharya, A. K., 2011, A three-unit-based approach in coastal-change studies using Landsat images, International Journal of Remote Sensing, 32, 209-229.

96. Maiti, S. and Bhattacharya, A., 2009, Shoreline change analysis and its application to prediction: a remote sensing and statistics based approach, Marine Geology, 257, 11-23.

97. Maiti, S., 2013, Interpretation of coastal morphodynamics of Subarnarekha estuary using integrated cartographic and field techniques, Current Science, 104(12), 1709-1713.

98. Malik, J. N. and Mohanty, C., 2007, Active tectonic influence on the evolution of drainage and landscape: Geomorphic signatures from frontal and hinterland areas along the Northwestern Himalaya, India. Journal of Asian Earth Sciences 29, 604-618.

99. Malik, J. N. and Nakata T., 2003, Active faults and related Late Quaternary deformation along the Northwestern Himalayan Frontal Zone, India. Annals of Geophysics, vol.46, N.5.

100. Mansor, S., Cracknell, A. P., Shilin, B. V. and Gornyi, V. I., 1994, Monitoring of underground coal fires using thermal infrared data, International Journal of Remote Sensing, 15(8), 1675-1685.

101. Mansor, S., Pradhan, B., Daud, M., Khuzaimah, Z. and Lee, S., 2007, Utilization of optical Remote sensing data and GIS tools for regional landslide hazard analysis in Malaysia, Journal of Institution of Surveyors Malaysia (Peer Reviewed Journal), 51, 50-55.

102. Mark, D. M., 1975, Geomorphometric parameters- a review and evaluation, Geografiska Annaler, 57A, 165-77.

103. Marshall, J. S. and Anderson, R. S., 1995, Quaternary uplift and seismic cycle deformation, Peninsula de Nicoya, Costa Rica, Geological Society of America, 107, 463-473.

104. Mayer, L., 1990, Introduction to Quantitave Geomorphology, Prentice Hall, Englewood Cliffs, New Jersey, p380.

105. McFadden, L. D., Tinsley, J. C. and Bull, W. B., 1982, Late quaternary pedogenesis and alluvial chronologies of the Los Angeles basin and St. Gabriel mountain areas, southern California in Tinsley, J. C., and McFadden, L. D., eds., Late quaternary pedogenesis and alluvial chronologies of the Los Angeles basin and St. Gabriel mountain areas, southern California, and Holocene faulting and alluvial stratigraphy within the Cucamonga fault zone, Field Trip 12, Cordilleron Section of the Geological Society of America, 1-13.

106. Medwedeff, D. A., 1992, Geometry and Kinematics of an Active, Laterally Propagating Wedge Thrust, Wheeler Ridge, California. In: Mitra, S., Fisher, G. W., (Eds.) Structural Geology of Fold and Thrust Belts, John Hopkins Studies in Earth and Space Sciences, 5, 1-28.

107. Meigs, A. J., Burbank, D. W. and Beck, R. A., 1995, Middle- Late Miocene (>10 Ma) formation of the Main Boundary Thrust in the Western Himalaya. Geology; v.23; no. 5; P 423-426.

108. Merritts, D. J. and Vincet, K. R., 1989, Geomorphic responses of coastal streams to low, intermediate, high rates of uplift, Mendocino Triple Junction region, Northern California, Geological Society of America, 110, 1373-1388.

109. Merritts, D. J., Vincet, K. R. and Wohl, E. E., 1994, Long River profiles, tectonism and eustasy: a guide to interpreting fluvial terraces, Journal of Geophysical Research, 99 (B7), 14031-14050.

110. Middlemiss, C. S., 1905, Preliminary account of the Kangra earthquake of 4th April 1905, Rec. Geol. Surv. India, 32, 258– 294.

111. Middlemiss, C. S., 1910, The Kangra earthquake of 4th April 1905, Mem. Geol. Surv. India, 38, 405.

112. Miliaresis, G. C. and Paraschou, C. V. E., 2005, Vertical accuracy of the SRTM DTED level 1 of Crete, International Journal of Applied Earth Observation and Geoinformation, 7(1), 49-59.

113. Mohindra, R., Parkash, B. and Prasad, J., 1992, Historical geomorphology and pedology of the Gandak megafan, Middle Gangetic plains, India. Earth surface processes and landforms, 17, 643–662.

114. Molnar, P., Brown, E. T., Burchfiel, B. C., Deng, Q., Feng, X., Li, J., Raisbeck, G. M., Shi, J., Wu, Z., Yiou, F. and You, H., 1994, Quaternary climate change and the formation of river terrace across growing anticlines on the north flank of the Tien Shan China, Journal of Geology, 102, 583-602.

115. Mukherji, A. D. and Iyer, S. D., 1999, Synthesis of morphotectonics and volcanics of the central Indian Ocean Basin, Indian Journal of Marine Sciences, 19, 13-16.

116. Mukhopadhyay, D. K. and Mishra, P., 2004, The Main Frontal Thrust (MFT), NW Himalayas: thrust trajectory and hanging wall fold geometry from balanced cross sections. Journal of geological society of India, 64, 739–746.

117. Muller, J. E., 1968, An introduction to the hydraulic and topographic sinuosity indexes, Annual Association of American Geographers, 58, 371-385.

118. Nieto-Samaniego, A. F., 1999, Stress, strain and fault patterns, Journal of Structural Geology, 21(8), 1065–1070.

119. Nossin, J.J., 1971. Outline of the geomorphology of the Doon Valley, Northern U.P., India. Z. Goemorphologie N.F, 12,18–50.

120. Novak, I.D. and Soulakellis, N., 1999, Identifying geomorphic features using Landsat – 5/ TM data processing techniques on Lesvos, Greece. Geomorphology 34, 101-109.

121. Oilier, C. D., 1981, Tectonics and landforms, Longman Group Limited, Harlow, England, p324.

122. Onorati, G. and Poscolieri, M., Ventura R., Chiarini, V. and Crucilla, A., 1992, A digital elevation model of Italy for geomorphology and structural geology. Catena, 19, 147-178.

123. Singh, O., Sarangi, A. and Sharma, M.C., 2008. Hypsometric integral estimation methods and its relevance on erosion status of north-western lesser Himalayan watersheds. Water Resources Management, 22(11), 1545-1560.
124. Ouchi, S., 1985, Response of alluvial rivers to slow tectonic movement, Geological Society of America, 96, 504-515.
125. Panda, S. K., Choudhury, S., Saraf, A. K. and Das, J. D., 2007. MODIS land surface temperature data detects thermal anomaly preceding 8 October 2005 Kashmir earthquake. International Journal of Remote Sensing, 28(20), 4587-4596.
126. Pandey, A., Chowdhry, V. M. and Mal, B. C. 2004, Hypsometric analysis using Geographical Information System. J. Soil & Water Cons. India, 32, 123-127.
127. Pati, J. K., 2005, The Dhala Structure, Bhundelkhand Craton, Central India – A New Large Paleoproterozoic Impact Structure, Meteoritics and Planetary Sciences, Supplement, Proceedings of 68th Annual Meeting of the Meteoritical Society, between 12-16 September in Gatlinburg, Tennessee, 40, 5092.
128. Pati, J. K., Lal, J., Prakash, K. and Bhusan, R., 2008, Spatio-temporal shift of Western bank of the Ganga river Allahabad city and its implications, Journal of Indian Society of Remote sensing, 36, 289-297.
129. Pati, J. K., Malviya, V. P. and Prakash, K., 2006, Basement reactivation and its relation to neotectonic activity in and around Allahabad, Ganga plain, Journal of the Indian Society of Remote Sensing, 34 (1), 47-56.
130. Pedrera, A., Perez-Pena, J. V., Galindo- Zaldivar, J., Azanon, J. M. and Azor, A., 2009, Testing the sensitivity of geomorphic indices in areas of low rate active folding (Eastern Betic Cordillera, Spain), Geomorphology, 105, 218-231.
131. Penck, A. and Bruckner, E., 1909, The Alps in the Ice Age: Leipzing, Tauchnitz, p1199.
132. Philip, G., 2007. Remote sensing data analysis for mapping active faults in the northwestern part of Kangra Valley, NW Himalaya, India. International Journal of Remote Sensing Vol. 28, No. 21, 4745–4761.
133. Pike, R. J. and Wilson, S. E., 1971, Elevation-relief ratio, hypsometric integral and geomorphic area-altitude analysis, Geological Soc. Am. Bull., 82, 1079-1084.
134. Pike, R. J., 1993, A bibliography of geomorphometry, with a topical key to the literature and an introduction to the numerical characterization of topographic form, U.S. Geological Survey Open-file Report, 93-262-A, 132.
135. Pirasteh, S., Mahmoodzadeh, A. and Mahtab, A., 2008, Integration of Geoinformation Technology and Survey Analysis for Development in Mitigation Study against

Earthquake: A Case Study for Esfahan Iran, International Disaster Advances Journal, 1 (2), 20-26.

136. Pirasteh, S., Rizvi, S. M. A., Ayazi, M. H. and Mahmoodzadeh, A., 2010, Using Microwave Remote Sensing for Flood study in Bhuj Taluk, Kuchch District Gujarat, India, International Geoinformatics Research and Development Journal, 1 (1), 13-24.
137. Pirasteh, S., Woodbridge, K. and Rizvi, S. M., 2009, Geo-information technology (GiT) and tectonic signatures: the River Karun and Dez, Zagros Orogen in south-west Iran, International Journal of Remote Sensing, 30 (1-2), 389-404.
138. Powers, P. M., Lille, R. J., and Yeats, R. S., 1998, Structure and shortening of the Kangra and Dehra Dun reentrants, Sub-Himalaya, India. Geological society of America bulletin, 110, 1010–1027.
139. Prost, G. L., 1994, Remote Sensing for Geologists: A Guide to Image Interpretation, Gordon and Breach Science Publishers, p487.
140. Raiverman, V., 2002. Foreland sedimentation in Himalayan tectonic regime. A relook at the orogenic process. Bishen Singh Mahendra Pal Singh Publication, Dehradun. 371p.
141. Ramasamy, S. M., 2005, Remote sensing in Geomorphology, New India Phlishing Agency, New Delhi, p276.
142. Ramasamy, S. M., 2006, Remote Sensing and Active Tectonics of South India, International Journal of Remote Sensing, 27 (20), 4397-4431.
143. Ramasamy, S. M., Kumaran, C. J., Selvakumar, R. and Saravanavel, J., 2011, Remote sensing revealed drainage anomalies and related tectonics of South India, Tectonophysics, 501, 41-51.
144. Ramsay, L. A., Walker, R. T. and Jackson, J., 2007, Geomorphic constrains on the active tectonics of Southern Taiwan, Geophysical Journal International, 170, 1357-1372.
145. Ramsey, L. A., Walker, R. T. and Jackson, J., 2008, Fold evolution and drainage development in the Zagros mountains of Fars province, SE Iran, Basin Research, 20(1), 23–48.
146. Rhea, S., 1989, Evidence of uplift near Charleston, South Carolina, Geology, 17, 311-315.
147. Ritter, D. F., Kochel, R. C., and Miller, I. R., 2002, Process Geomorphology. McGraw Hill, Boston.
148. Rockwell, T. K., Keller, E. A., Clark, M. N. and Johnson, D. L., 1984, Chronology and rates of faulting of Ventura River terraces, California,. Geological Society of America Bulletin, 95, 1466-1474.

149. Sadybakasov, I., 1990, Neotectonics of High Asia: Moscow, Nauka, p176.
150. Sati, D. and Rautela, P., 1998. Neotectonic deformation in the Himalayan foreland fold-and-thrust belt exposed between the rivers Ganga and Yamuna. Himalayan Geol, 19, 21-28.
151. Schumm, S. A. and Khan, H. R., 1972, Experimental study of channel patterns, Geological Society of America, 83, 1755-1770.
152. Schumm, S. A., 1956, Evolution of drainage systems and slopes in bad-lands at Perth Amboy, New Jersey, Geol. Soc. Am. Bull., 67, 597–646.
153. Seeber, L., and Armbruster J. G., 1981, Great detachment earthquakes along the Himalayan arc and long-term forecasting, in Earthquake Prediction: An International Review, Maurice Ewing Ser., vol. 4, edited by D. W. Simpson and P. G. Richards, pp. 259–277, AGU, Washington, D. C.
154. Sharma, K., Saraf, A. K., Das, J. D., Rawat, V. and Shujat, Y. 2010, SRTM and ASTER DEM characteristics of two areas from Himalayan region, International Geoinformatics Research and Development Journal, 1 (3), 25-31.
155. Sharma, S. K. and Seth, N. K., 2010, Use of GeographicalInformation System (GIS) in assessing the erosion status of watersheds. Sci-fronts A journal of multiple science, 4, 77-82.
156. Singh, O. and Sarangi, A., 2008a, Hypsometric analysis of the lesser Himalayan watersheds using geographical information system. Indian J. Soil Cons. 36(3), 148-154.
157. Singh, O., Sarangi, A. and Sharma, M.C. 2008b, Hypsometric integral estimation methods and its relevance on erosion status of north-western Lesser Himalayan Watersheds, Water Res. Mgt., 22, 1545-1560.
158. Singh, S., 2019, Protracted zircon growth in migmatites and in situ melt of Higher Himalayan Crystallines: U–Pb ages from Bhagirathi Valley, NW Himalaya, India. Geoscience Frontiers, 10(3), 793-809.
159. Singh, T. and Jain, V., 2009, Tectonic constraints on watershed development on frontal ridges: Mohand Ridge, NW Himalaya, India. Geomorphology, 106(3-4), 231-241.
160. Singh, T., 2008, Hypsometric analysis of watersheds developed on actively deforming Mohand anticlinal ridge, NW Himalaya. Geocarto International, 23(6), 417-427.
161. Singh, T., Awasthi, A. K. and Caputo, R., 2012, The Sub-Himalayan fold- thrust belt in the 1905 Kangra earthquake zone: A critical taper model perspective for seismic hazard analysis. Tectonics, vol. 31(6), 1-18.

162. Singh, T., Sharma, U., Awasthi, A. K., Virdi, N. S. and Kumar, R, 2011, Geomorphic and structural evidences of neotectonic activity in the Sub-Himalayan belt of Nahan Slient, NW India. Journal of the Geological Society of India, 77(2), 175-182.
163. Sparling, D. R., 1967, Anomalous drainage pattern and crustal tilting in Ottawa country, Ohio. Ohio Journal of Science, 67, 378-381.
164. Strahler, A. N., 1952, Hypsometric (area–altitude) analysis of erosional topography, Geological Society of America Bulletin, 63, 1117-1142.
165. Susan, R., 1993, Geomorphic observations of rivers in the Oregon coast range from a regional reconnaissance perspective, Journal of Geomorphology, 6, 135-150.
166. Thakur, V. C. and Rawat, B. S., 1992, Geological Map of the Western Himalaya, Wadia Institute of Himalayan Geology, Dehradun.
167. Thakur, V. C., 2004, Active tectonics of Himalayan Frontal Thrust and Seismic Hazard to Ganga Plain. Current Science, Vol.86, No. 11.
168. Tripathi, N. K. and Singh, P., 2000, Integrated GIS and Remote Sensing Approach to Map Pollution in Upper Lake, Bhopal, India, Geocarto International, 15(4), 49-55.
169. Tripathi, N. K. and Soomro, A. S., 2007, A GIS Approach to Tsunami Disaster Risk Zonation, Krabi, Thailand, International journal of Geoinformatics, 3(3), 9-16.
170. Tripathi, N. K., Siddiqi, M. U. and Gokhale, K. V. G. K., 2000, Directional morphological image transforms for lineament extraction from remotely sensed images, International Journal of Remote Sensing, 21(17), 3281-3292.
171. Tronin, A. A., 1996, Satellite thermal survey-A new tool for the studies of seismoactive regions, International Journal of Remote Sensing, 17, 1439-1455.
172. Tronin, A. A., 2006, Remote sensing and earthquakes: A review, Physics and Chemistry of Earth, 31, 138-142.
173. Tronin, A. A., Hayakawa, M. and Molchanov, O. A., 2002, thermal IR satellite data application for earthquake research in Japan and China, Journal of Geodynamics, 33, 519-534.
174. Tsimi, C., Ganas, A., Soulakellis, N., Kairis, O. and Valmis S., 2007, Morphotectonics of the Psathopyrgos active fault, western Corinth Rift, Greece. International Conference of the Geological Society of Greece, Athens, 24-26.
175. Verrios, S., Zygouri, V. and Kokkalas, S., 2004, Morphotectonic analysis in the Eliki fault zone (Gulf of Cornith, Greece). Bulletin of the Geological society of Greece. V-XXXVI. Proc. 10th International Congress, Thessaloniki, 1706-1715.

176. Verstappen, H. Th., 1977, Remote Sensing in Geomorphology, Elseviers, Amersterdam, p214.
177. Walker, R. and Jackson, J., 2002, Offset and evolution of Gowk fault, SE Iran: a major intra continental strike-slip system, Journal of Structural Geology, 24, 1677-1698.
178. Weissel, J. K., Pratson, L. F. and Malinverno, A., 1994, The length-scaling properties of topography. Journal of Geophysical Research, 99, 13997-14012.
179. Wesnousky, S. G., Kumar, S., Mohindra, R. and Thakur, V. C., 1999, Uplift and convergence along the Himalayan Frontal Thrust of India. Tectonics, 18(6), 967-976.
180. Whipple, K. X. and Dunne, T., 1992, Debris flow fans in Owen Valley, California, Geological Society of America, 104, 39-43.
181. Woodhouse, L. H., 2017, Introduction to Microwave Remote Sensing, Taylor and Francis, New York, p400.
182. Wright, T., Fielding, E. and Parsons, B., 2001, Triggered slip: observations of the 17 August 1999 Izmit (Turkey) earthquake using radar interferometry, Geophysical Research Letter, 28, 1079-1082.
183. Yeats, R. S. and Thakur, V.C., 2008, Active faulting south of the Himalayan Front: Establishing a new plate Boundary. Tectonophysics 453, 63-73.
184. Yin, A. and Harrison, T.M., 2000. Geologic evolution of the Himalayan-Tibetan orogen. Annual review of earth and planetary sciences, 28(1), 211-280.
185. Yin, A., 2006. Cenozoic tectonic evolution of the Himalayan orogen as constrained by along-strike variation of structural geometry, exhumation history, and foreland sedimentation. Earth-Science Reviews, 76(1-2), 1-131.
186. Zizioli, D., 2008, DEM based morphotectonic analysis of Western Ligurian Alps., Scientifica Acta, 2(2), 44-47.

URL Links:

1. http://biodiversityinformatics.amnh.org/interactives/bandcombination.php
2. http://dwtkns.com/srtm/
3. http://earthexplorer.usgs.gov
4. http://earthnow.usgs.gov/earthnow_app.html?sessionId=0439f1ff7761e2cb0ccb941a50a90e1313558
5. http://geoawesomeness.com/top-11-maps-ultimately-explain-climate-change-impact/
6. http://gis4geomorphology.com/hypsometric-index-integral/
7. http://gis4geomorphology.com/roughness-topographic-position/
8. http://gisgeography.com/basic-gis-processing-tools/
9. http://glcfapp.glcf.umd.edu/
10. http://glcfapp.glcf.umd.edu:8080/esdi/
11. http://landsat.usgs.gov/L8_band_combos.php
12. http://landsat.usgs.gov/landsat8.php
13. http://landsatlook.usgs.gov/
14. http://maps.unomaha.edu/Peterson/gis/notes/RS2.htm
15. http://pubs.usgs.gov/gip/earthq1/where.html
16. http://reverb.echo.nasa.gov/reverb/#utf8=%E2%9C%93&spatial_map=satellite&spatial_type=rectangle
17. http://srtm.csi.cgiar.org/
18. http://transition.fcc.gov/mb/audio/bickel/DDDMMSS-decimal.html
19. http://www.astrium-geo.com/en/19-gallery

20. http://www.eorc.jaxa.jp/ALOS/en/aw3d30/data/index.htm

21. http://www.esri.com/arcview

22. http://www.gis-mysuni.blogspot.in/

23. http://www.globalchange.umich.edu/globalchange1/current/lectures/evolving_earth/evolving_earth.html

24. http://www.jspacesystems.or.jp/ersdac/GDEM/E/2.html

25. http://www.lib.utexas.edu/maps/ams/india/

26. http://www.mapsofindia.com/maps/india/majorearthquake.html

27. http://www.portal.gsi.gov.in/gismap/seismotectonicmap/default.aspx

28. http://www.usgs.gov/

29. http://www.xmswiki.com/xms/GSDA:GSDA

30. https://blogs.esri.com/esri/arcgis/2013/07/24/band-combinations-for-landsat-8/

31. https://earthengine.google.com/datasets/)

32. https://earthquake.usgs.gov/earthquakes/search/

33. https://eos.com/landviewer/?utm_source=Email&utm_medium=10_images&utm_campaign=LandViewer&lat=28.74840&lng=78.53027&z=6

34. https://maps-for-free.com/

35. https://www.mapsofindia.com/maps/rivers/ganges.html

List of Publications:

Paper published in journals:

1. Geospatial Technology in Hypsometric Analysis of Mohand Anticline, Uttarakhand, India. Asian Journal of Geoinformatics, 2018 (Accepted).
2. Comparison of Cartosat, ASTER and SRTM DEMs of different terrains. Suman Sourav Baral, Josodhir Das, Arun Kumar Saraf, Susanta Borgohain and Gaurav Singh. Asian Journal of Geoinformatics, 16, 1, 2016.
3. Morphodynamic changes of Lohit River, NE India: GIS-based study. Susanta Borgohain, Josodhir Das, Arun Kumar Saraf, Gaurav Singh and Suman Sourav Baral. Current Science, 110 (9), 1810-1816, 2016. doi: 10.18520/cs/v110/i9/1810-1816.
4. Remote Sensing and GIS Based Analysis of Geomorphic Evidences and Morphometry of Active Faults in Kachchh Area. Eirin Kar, Suman Sourav Baral, Arun Kumar Saraf, Josodhir Das, Gaurav Singh and Susanta Borgohain. Journal of the Indian Society of Remote Sensing, 44, 1-10, 2016. doi: 10.1007/s12524-016-0588-z
5. Structural controls on topography and river morphodynamics in Upper Assam Valley, India. S. Borgohain, J. Das, A.K. Saraf, G. Singh & S.S. Baral. Geodinamica Acta, 29, 62-69, 2017. DOI: 10.1080/09853111.2017.1313090.
6. Mapping and Change Detection Study of Nepal-2015 Earthquake Induced Landslides. Kanika Sharma, Arun Kumar Saraf, Josodhir Das, Suman Sourav Baral , Susanta Borgohain and Gaurav Singh. Journal of the Indian Society of Remote Sensing. , 1-11, 2017. https://doi.org/10.1007/s12524-017-0720-8.
7. Thermal anomaly from NOAA data for the Nepal earthquake, Suman Sourav Baral, Kanika Sharma, Arun Kumar Saraf, Josodhir Das, Gaurav Singh, Susanta Borgohain and Eirin Kar. Current Science, 110 (2), 2016.

Papers under review:

1. Geo-Informatics in identification of groundwater recharge structures in Bundelkhand Region" Paper Under review in "Journal of the Geological Society of India".
2. InSAR technique detects post-seismic ground deformations of Kathmandu valley, Natural Hazards.
3. Pseudo Colour Transformation Technique for Deforestation and Forest Degradation Studies, Journal of the Indian Society of Remote Sensing.

Papers in Conferences/Workshops:

1. Study of Kangra Re-entrant and associated morphotectonic features based on Remote sensing and GIS. AGU Fall Meeting 2018, 10-14 December 2018, Walter E. Washington Convention Center, 801 Mt. Vernon Place, NW, Washington, DC
2. Understanding the impact of regional climate condition and local features on glacial behavior around Satopanth and Bhagirath Glacier in Alaknanda valley, Uttarakhand, India. Proceedings of International Conference on Climate Change Mitigation and Technologies for Adaptation (IC3MTA-2016) 20th & 21st June, 2016 Synod College, Shillong, Meghalaya,India.
3. Hypsometric Analysis of Mohand Anticline, Uttarakhand, India Using Geospatial Technologies. National Geo-Research Scholars Meet 2016, 1-4 June, 2016 at Wadia Institute of Himalayan Geology, Dehradun.
4. Delineation of major seismotectonic boundaries in Sub-Himalayan region using geospatial technologies. Gaurav Singh, Josodhir Das, Arun Kumar Saraf, Suman Sourav Baral, Susanta Borgohain, Kanika Sharma. Himalayan-Karakorum-Tibet workshop, 2016, Aussois, France.
5. Morphometric and Morphodynamic analysis of Lohit River, Assam, India. Susanta Borgohain, Josodhir Das, Arun Kumar Saraf, Gaurav Singh and Suman Sourav Baral. National Seminar on Geology, Tectonics, Geo-Hazards & Natural Resources of North East India, 2014. Organized by Dept. of Geology, Pachhunga University College, Aizawl, Mizoram.
6. Flood induced changes in Kedarnath valley, Uttarakhand, India. Gaurav Singh, Josodhir Das, Arun Kumar Saraf, Susanta Borgohain and Suman Sourav Baral. National Seminar on Geology, Tectonics, Geo-Hazards & Natural Resources of North East India, 2014. Organized by Dept. of Geology, Pachhunga University College, Aizawl, Mizoram.
7. Participated National conference on "Earth Sciences in India: Challenges and Emerging Trends" has been organized by Department of Earth Sciences during 07-09th Nov. 2013.
8. Geospatial Technology in Hypsometric Analysis of Mohand Anticline, Uttarakhand, India. Asian Journal of Geoinformatics.